5-2012

Hydrology, Soil Erosion and Climate Interactions on Low Compaction Steep-Sloped Reclaimed Sites in the Southern Appalachian Coal Fields, Tennessee

Siavash Hoomehr
shoomehr@utk.edu

To the Graduate Council:

I am submitting herewith a dissertation written by Siavash Hoomehr entitled "Hydrology, Soil Erosion and Climate Interactions on Low Compaction Steep-Sloped Reclaimed Sites in the Southern Appalachian Coal Fields, Tennessee." I have examined the final electronic copy of this dissertation for form and content and recommend that it be accepted in partial fulfillment of the requirements for the degree of Doctor of Philosophy, with a major in Civil Engineering.

John S. Schwartz, Major Professor

We have read this dissertation and recommend its acceptance:

Daniel C. Yoder, Eric C. Drumm, Russell Zaretzki, Glenn Tootle

Accepted for the Council:
Dixie L. Thompson

Vice Provost and Dean of the Graduate School

(Original signatures are on file with official student records.)

Hydrology, Soil Erosion and Climate Interactions on Low Compaction Steep-Sloped Reclaimed Sites in the Southern Appalachian Coal Fields, Tennessee

A Dissertation
Presented for the
Doctor of Philosophy Degree
The University of Tennessee, Knoxville

Siavash Hoomehr
May 2012

DEDICATION

I dedicate this dissertation to my wonderful family. I dedicate it to my parents, Kazem and Morvarid, who have always given me their support throughout my life and encouraged me to pursue my goals in life. I would also like to dedicate this dissertation to my wife, Bahareh, for her understanding, support, and love during the past years. Her support and encouragement was in the end what made this dissertation possible.

ACKNOWLEDGEMENTS

I would like to express my deepest gratitude to my advisor, Dr. John S. Schwartz, for his support, patience, and encouragement throughout my graduate study. He provided me an excellent atmosphere for doing research. His technical and editorial advice was essential to the completion of this dissertation and has taught me innumerable lessons and insights on the workings of academic research in general.

My special thanks also go to the members of my dissertation committee, Dr. Daniel C. Yoder, Dr. Eric C. Drumm, Dr. Glenn Tootle and Dr. Russell Zaretzki. They challenged me throughout my graduate study and provided me with a better understanding of hydrology and water resources concepts. Their comments and suggestions have been invaluable and as a result added significant value to my dissertation.

I also want to express my gratitude to my friend Wesley C. Wright for his support during this research. I enjoyed his partnership and learned a lot from his suggestions and experience.

I want to thank the U.S. Department of Interior, Office of Surface Mining (OSM) Applied Science Program Grant CA No. S08AP12822 which helped fund my education and this study. OSM staff members David Lane and Victor Davis were particularly helpful obtaining permission to conduct field experiments on private coal mining property, and suggesting improvements on the study design. I greatly appreciate the support by the coal companies with the construction of the field plots and allowing access to their property during the study; they were: National Coal Corporation, Premium Coal Company, and Mountainside Coal Company

At last but not least, I want to thank all people helped me in this research. Field and laboratory assistance for data collection were aided by many University of Tennessee students, including Isaac Jeldes, Nathan Felosi, Sam Mathews, Chris Dixon, and Chris Drinnon.

Abstract

The use of loose spoil on steep slopes for surface coal mining reclamation sites has been promoted by the US Department of Interior, Office of Surface Mining for the establishment of native forest. Although low-compaction spoils improve tree survival and growth, the erodibility and hydrology of steep slopes may change due to this practice. The purpose of this study was to quantify the erodibility (K factor), and the Curve Number (CN) value for low compaction, steep-sloped (> 20%) reclaimed mine lands in the Appalachian region, USA. This study also investigated the performance of the SEDCAD model in estimating erosion and sediment delivery from these slopes, and tried to estimate the potential change in rainfall erosivity due to climate change in the study region.

Three active coal mining sites in the Appalachian region of East Tennessee were monitored for rainfall, runoff, and sediment yields. The estimated time-varying K factor ranged between 0.03 and 0.5 $t \cdot ha \cdot h \cdot ha^{-1} \cdot MJ^{-1} \cdot mm^{-1}$, with the highest values immediately following reclamation site construction. Rill development greatly influenced sediment yields. A fining of delivered sediment size was observed from the period of rill development to relatively stable rill morphology, with the D_{84} changed from 17.3 mm to 1.7 mm. Meanwhile, different methods were used to identify CN values of these new reclaimed surfaces as they are vital for design of runoff and sediment control structures. In contrast to previous studies, CN estimation methods utilized in this study propose a narrower, more practical CN value range of 58.5 ~ 60.0, based on standard asymptotic behavior, for low-compaction steep-sloped reclaimed surfaces.

This study also investigated the performance of SEDCAD in estimating erosion and sediment delivery. Model input parameters were assessed with respect their impacts on SEDCAD outputs. In general, SEDCAD appeared to overestimate sediment yield compared to

what was measured from study sites, and modeled sediment yields were found to be sensitive to CN selection. Finally, this study showed that for all future greenhouse gas emission scenarios the overall annual rainfall erosivity will increase in the study area, though the distribution of erosivity throughout the year will be similar to the present.

Table of Contents

List of Figures

List of Tables

Chapter 1

Introduction

1.1 Scope and Justification

Modern life depends on different sources of energy, with coal playing a vital role in energy generation worldwide. The US, as one of the biggest consumers of energy on the planet, to a great extent relies on coal for generating its energy, with coal used to create almost half of all electricity generated in the United States (IEA 2010). Coal mining, particularly surface mining, requires large areas of land to be temporarily disturbed. This raises a number of environmental issues, including soil erosion and sediment delivery, which can affect the aquatic resources, streams, and habitats. Reclamation has been used to reduce the environmental effects of the coal mining. Reclamation is defined as rehabilitation of disturbed areas resulting from surface or underground mining. The basic objective of surface mining reclamation is to reestablish vegetative cover, soil stability, and water quality conditions. A better understanding of the hydrology and erosional geomorphology of reclaimed areas is needed in order to assess the effectiveness of reclamation efforts.

The Appalachian Regional Reforestation Initiative (ARRI) is a cooperative effort between the Appalachian states and the Office of Surface Mining (OSM) (Angel et al. 2005). The ARRI goals are to plant more high quality hardwoods on reclaimed mine lands, increase their survival rates, and expedite the establishment of quality forest habitat, through the encouragement and promotion of the Forestry Reclamation Approach (FRA). One of the most critical aspects of the FRA is the use of low compaction grading techniques to assure that a zone of "loose" material remains at the surface to encourage tree survival and growth (Sweigard et al. 2007). OSM needs to understand the hydrology and erosional geomorphology of steep slopes

reclaimed after mining activity utilizing this new technique of low level of compaction, in order to be able to assess effectiveness of reclamation and quality of surface water that leaves these areas. Also, the hydrologic conditions and sediment delivery immediately following hillslope construction must be understood in order to engineer adequate runoff retention and erosion control structures. This new information will also support reforestation research efforts to improve native tree regeneration using the FRA.

This research will address these needs by: 1) estimating the erodibility (Universal Soil Loss Equation, USLE, K-factor) of low-compacted reclaimed material, which include a wide range of material size and texture, on steep slopes; 2) estimating the curve number value (CN) for steep-slope, loose spoil land surface in order to predict direct runoff from rainfall excess; 3) evaluating the performance of the SEDCAD model on reclaimed surfaces; and 4) estimating potential effects of future climate change on the rainfall erosivity (USLE R-factor) using the New River basin of East Tennessee as case study. Results from this study will support future efforts to evaluate effects of erosivity changes on watershed-scale water quality while implementing the estimated K and CN values obtained from the first two parts of this research.

1.2 Hydrology, Erosion and Climate Interactions on Reclaimed Surfaces

The Surface Mining Control and Reclamation Act of 1977 (SMCRA) is the federal law regulating the environmental effects of coal mining in the United States. It requires that after completion of active surface mining, all disturbed areas from the mining operation must be reclaimed (U.S. Dept. of Interior, 1977). It also mandates that hydrologic impacts from coal surface mining operations must be assessed and mitigated (Tolbert et al. 1994; Graves et al. 2000). Conventional reclamation of disturbed surfaces during mining activities, as practiced from 1970's until now, has been traditionally successful in reducing erosion, especially in areas

where the slopes are low to moderate. Establishment of forest cover in the reclaimed areas has been less successful, primarily due to construction techniques which focus on slope stability and erosion control using high levels of compaction and aggressive grass covers. Research has established that over-compaction of the reclaimed surface soils impedes the establishment of healthy fast-growing forests (Swiegard et al. 2007). Unfortunately, the mass stability of steep slopes is dependent on greater compaction levels, while rapid establishment of ground cover is needed to control erosion and sediment yields.

Establishment of native forest covers on reclaimed surfaces has recently become a priority and OSM directive focus of interest, which has led to advocating the use of loose-dumped spoils and low compaction grading to enhance reforestation success, in a process known as FRA (Angel et al., 2005; Sweigard et al., 2007). This new approach directs mine operators to employ lower levels of compaction to prepare a better medium for trees survival by increasing the chance of root penetration. Although this technique is advocated for all slopes including steep slopes, there is a critical need to understand the erosional geomorphology of steep sites.

Furthermore, pre-mining assessments termed probable hydrological consequences (PHC) in the Surface Mining Control and Reclamation Act (SMCRA) are conducted using the runoff CN method to generate runoff volume and hydrograph peaks for the study sites, and potential impacts are addressed through the design of on-site detention ponds. SMCRA requires post-mining runoff to match pre-mining runoff for a 10-year, 24-hour storm event. So estimating CN value for low-compacted steep-sloped reclaimed areas is key for investigating the hydrological properties of these reclaimed surfaces and it is vital for design of runoff and sediment control structures. This information provides regulators with the tools to assess probable future hydrologic/environmental consequences of these surface mining sites.

It is possible that climate change will affect soil erosion rates by changing future rainfall characteristics, but no study of the Appalachian coal region has been conducted to assess these potential effects. For all of North America except the south-western part of continent, future precipitation events are expected to be more extreme in terms of amount and frequency (IPCC, 2007). The increase in rainfall intensity will increase rainfall erosivity and as a result the erosion of and sediment delivery from disturbed areas. Estimating changes in rainfall erosivity is vital to assessing the future effectiveness of current best management practices (BMP) in reducing soil erosion and sediment delivery from coal mining sites.

1.3 Curve Number, CN

A common tool for investigating the hydrology of reclaimed areas has been the runoff-curve number (CN) method. The CN is an index used to indicate the runoff potential from a specific −generally ungagged− watershed. The runoff CN method developed by the US Department of Agriculture, Soil Conservation Service (now the Natural Resources Conservation Service, NRCS) is widely accepted for estimating runoff from rainfall on reclaimed mine lands due to ease of use and its general acceptance (Elhakeem et al. 2009). It was originally developed for agricultural lands (Barfield et al. 1981; Ritter et al. 1991; Schroeder 1994; Camorani et al. 2005; Taylor et al. 2008). The NRCS runoff method is fully described in the National Engineering Handbook (NEH), Section 4 on Hydrology, and updated in NEH Part 630 (SCS 1972; NRCS 2004). Design CNs can be determined from the tabulated values as a function of Hydrologic Soil Group (HSG), land use, and antecedent moisture condition (AMC).

CN selection for watersheds is typically based on: (1) curve number values using pre-mine soil classification and post mine land treatment and use; (2) calibrated curve number values based on rainfall-runoff data from watersheds disturbed by surface mining and reclamation; or (3)

simulated curve number values from rainfall infiltrometer tests on reclaimed-mine soils. A major problem associated with using the CN method for surface-mine permitting and reclamation design is the limited data available for adequate calibration of CNs from watersheds disturbed by surface mining, which is primarily due to inadequate record of data from disturbed mined watersheds and/or the lack of generally accepted procedure for CN value determination from mixed or limited land use data (Ritter et al. 1991).

To address the above issues, this study monitored a full calendar year of runoff events on three different active mine sites at East Tennessee reclaimed by the low-compaction FRA method. This research provided an opportunity to evaluate the potential impact of the FRA method on the hydrology of the study sites and to evaluate CN values for each site. A unique CN value for FRA-reclaimed sites was estimated, which can be used by mining engineer professionals for other FRA sites, if recommended standard procedures are followed. The results of this research can also help engineers in designing retention basins and BMPs for managing runoff and sediment leaving mine sites. It also aids regulators in predicting PHCs. Furthermore, SMCRA demands minimal variation from the pre-mining hydrological condition of area, which requires knowledge of the pre- and post-mining hydrologic conditions of these areas.

1.4 Erodibility, USLE K-factor

Soil erodibility reflects the susceptibility of a soil to erosion based on its physical and chemical properties. Soil erodibility depends on the organic matter and texture of the soil, its permeability, and profile structure (Wischmeier and Smith 1965; Renard et al. 2000).

Low compaction grading techniques in reclamation of disturbed areas are relatively well recognized, but the desire to maintain low levels of compaction is in direct conflict with traditional practice regarding the structural stability of slopes and their resistance to erosion. For

a given slope to be stable, soil must have sufficient strength to resist the gravitational and seepage forces acting on the soil mass. In general, soil strength will decrease as the density decreases. This is recognized in most discussions of low compaction grading techniques, as emphasized by Sweigard et al. (2007) in saying that if compaction is required for stability, the underlying compacted materials should be left in a rough configuration to assure a high strength interface with the weaker un-compacted material. At the same time, increasing the slope steepness increases the velocity of rill flow on the hillslope, resulting in an increase in the turbulent energy of eddies and the shear stress that develops between water and soil surface, in turn increasing the erosion rate. Steep slopes are defined in SMCRA refer as those that exceed 20 degrees, or 36%. The FRA reclamation technique tries to use both a steep slope gradient and a low level of compaction.

While FRA reclamation with low levels of compaction is reported to be effective in growing native forest species on reclaimed sites (Torbert and Burger 1994; Thomas et al. 1999; Angel et al. 2006), there is a lack of scientific information about its effect on erosion and sediment delivery in watersheds reclaimed by this method, especially on steep slopes. Steep-slope reclamation often causes reconstructed slopes to approach the angle of repose of the spoil material. Since establishment of protective vegetation or forest is a long-term process, the steep slope, back-to-contour surface mining is a long-term source of sediment (Dickens et al. 1985). Constructing slopes with low levels of compaction may increase erosion rate by increasing spoil erodibility, but it can also reduce sediment delivery by increasing infiltration rates and as a result reducing runoff volume. Decreasing the level of compaction may effect erosion on the slopes. Lower soil compaction may result in the creation of fewer and less stable soil aggregates. Soils with isles aggregation are more vulnerable to erosive forces. Although lower levels of

compaction increases infiltration and reduces the amount of runoff, it is possible that the reduction in soil aggregation may ultimately increase erosion and sediment delivery.

One of the main factors in estimating soil loss is the property of soil erodibility, known as the K factor in the Revised Universal Soil Loss Equation (RUSLE). RUSLE is a revised version of Universal Soil Loss Equation (USLE) (Wischmeier and Smith 1965; 1978), which served as the most commonly used soil loss estimation model worldwide for 30 years (Toy et al. 1999). Soil-erodibility factors are best obtained from direct measurements on natural runoff plots (22.13m length and 9% slope) (Renard et al. 2000). Rainfall simulation studies are less accurate, and predictive relationships are the least accurate means of obtaining K values (Romkens 1985).

To investigate the potential effects of lower compaction and increasing slope steepness on the erosion rate of hillslopes built by coal mining waste material, and to trace its change during different seasons, three active coal mining sites in East Tennessee reclaimed under FRA guidelines were monitored for a 14-month period. This research will provide a unique opportunity to estimate the erodibility (K) of low compacted waste material in coal mining sites for the worst case scenario (a bare material) as a key parameter for estimating erosion and sediment delivery from disturbed areas.

1.5 Evaluating Performance of SEDCAD Model

SEDCAD is a comprehensive hydrology, sediment, and erosion modeling package which has been widely used in designing runoff and sediment control structures, primarily in the surface mining industry. SEDCAD has been used primarily on low- to moderate-sloped surfaces, so there is no estimate on its performance for low-compacted FRA-reclaimed steep slopes. To address this issue, this study investigated the use of SEDCAD in estimating erosion and sediment delivery from low compacted steep sloped reclaimed areas, and evaluated the sensitivity of

SEDCAD outputs with respect to curve number values (CN) and erodibility factors of reclaimed material (K), using real data obtained from monitoring three different coal mining sites in the southern Appalachian region for more than a year period. The results of this study can give a better understanding in interpretation of SEDCAD outputs and will be highly useful in designing runoff and sediment control structures and selection of best management practices (BMPs) in the mining industry.

1.6 Climate Change and Watershed Hydrology

Climate change will affect soil erosion by changing the amount, pattern, and erosivity of future rainfall events. From a broader perspective, it will influence soil erosion by causing shifts in land use necessary to maintain productivity under a new climatic system, and by changing plant biomass production, residue decomposition rates, soil microbial activity, evapotranspiration rates, and soil surface sealing and crusting (Williams et al., 1996). Variations in rainfall erosivity can have more significant impact on ecosystems than the general global warming due to its wide domain of influence (Sauerborn et al., 1999; Allen and Ingram, 2002; Diodato et al. 2009). Based on the historical weather records, over the last century the number of rainfall events and intensities are both increasing across most of the U.S. (IPCC 2007; Nearing 2001). In a warmer climate, extreme precipitations and temperatures will increase more significantly than their related means (Hegerl et al. 2004). Studies using erosion models indicate that erosion response is much more sensitive to changes in the rainfall amount and intensity than to runoff (Nearing et al. 1990; Zhang et al. 2010). The global average soil erosion is projected to increase approximately 9% by 2090 due to climate changes (Yang et al. 2003).

While data from most Global Circulation Models (GCMs) can provide scenarios of monthly and annual changes in total precipitation around the world (Nearing et al. 1990), they do

not have enough precipitation detail at specific locations in order to directly enable computation of erosivities for physically based erosion models like RUSLE, which uses the R factor as a measure of erosivity (McFarlane et al. 1992; Johns et al.1997; Nearing M.A, 2001; Zhang et al. 2010). Even GCMs that provide daily values at their grid scales still require spatial downscaling to generate climate data for a specific location of interest. If monthly projections from GCMs are to be used in erosion modeling, which is the case in most erosion studies, then both spatial and temporal downscaling are required (Zhang 2007). Daily weather series generated by different downscaling methods usually are statistically different and result in different soil erosion and runoff predictions for a specific climate change scenario (Zhang 2007).

Statistical downscaling methods have been used as a tool to investigate the change in R factor caused by changes in monthly and annual precipitation amounts obtained from GCM outputs, and the resulting effect on soil erosion (Zhang et al. 2010; Nearing, 2001; Renard and Freidmund, 1994). However, these relationships have limitations, primarily with regard to snow dominated areas, and do not consider the impact of large changes in the storm intensity or duration on rainfall erosivity (Zhang et al. 2010). A new approach by Zhang et al. (2010) combines the earlier method developed by Zhang et al. (2005, 2007) for downscaling monthly precipitation products at time scale meaningful for modeling erosion processes, and the validated method developed by Yu (2002, 2003) for using a weather generator (CLIGEN) (Nicks and Gander, 1994) to generate accurate RUSLE erosivity factors (Zhang et al. 2010). This new approach was used in this study to estimate climate-change changes in R-factor values in the New River Basin at East Tennessee.

Stochastic weather generators are common tools in generating daily climate data from monthly data obtained from GCMs (Mearns et al. 1997; Wilks 1999; Pruski and Nearing 2002;

Zhang 2005, Zhang et al. 2010). Previous studies showed that R factors generated by CLIGEN are highly correlated with the measured R factors (Yu 2002, 2003; Zhang et al. 2010). Thus, a method using CLIGEN together with calibration formulas to adjust the generated R factor is able to adequately generate R-factor for RUSLE (Zhang et al. 2010).

1.7 Research Questions

1.7.1 Curve Number Hydrology for Low-Compacted Steep-Sloped Reclaimed Surface Mine Lands in the Southern Appalachian Region

The first part of this research focused on estimating a CN that can be used for runoff prediction from steep-sloped low-compaction spoil materials in the Appalachian coal-mining region. This information supports the regulatory agencies charged with the reclamation of natural hillslope topography and native forests under the FRA. The hydrological conditions immediately following hillslope construction must be understood in order to model and design adequate runoff retention and erosion control structures. In this study, runoff was measured using the flow divider buckets described by Pinson et al. (2003), and analyzed using the Asymptotic method as described by Hawkins (1993).

Question 1: What is the range of CN value for mine spoils on low-compacted steep-sloped reclaimed surfaces, and is it possible to estimate a unique CN value for those surfaces?

Task 1.1: Estimate a range for CN values for several coal mining sites which employed low level of compaction method for reclamation, using measured rainfall and runoff data.

Task 1.2: Investigate the relationship between the CN values, rainfall depth, and the 30-minute rainfall intensity.

Task 1.3: Estimate a unique CN value that will be useful for estimating the runoff leaving low compaction reclaimed sites, in order to help engineers in designing retention basins and BMPs for managing runoff and sediment leaving mine sites.

1.7.2 Evaluating the Erodibility of Low-Compacted Steep-Sloped Reclaimed Surface Mine Lands in the Southern Appalachian Region

The second part of this research focused on the erosional geomorphology of steep (>20%) reclaimed areas on which low levels of compaction method was employed during their construction, particularly in the Southern Appalachian Region of the USA. This includes estimation of erosion rate, calculation of the erodibility of the reclaimed material, and investigating the change in particle size distribution of eroded materials leaving study sites. The result of this study is significant as it provides valuable erosion data, for designing BMPs, and reclamation management input to the coal mining industry and regulatory agencies. This helps them to adequately design BMPs as required by the SMCRA.

Question 2: What is the erodibility for mine spoils on low-compacted steep slopes, and does it change with time?

Task 2.1: Estimate the range of erosion rates ($t \cdot ha^{-1}$) for low-compacted steep-sloped reclaimed mine lands during the total 14-month period of the study.

Task 2.2: Determine soil erodibility (the RUSLE K-factor) for low-compacted steep-sloped reclaimed surfaces, and investigate the potential influence of rill development on the RUSLE K factor over time.

Task 2.3: Investigate the change in particle size distribution of eroded material leaving low-compaction steep-sloped reclaimed surfaces during the 14-month monitoring period.

1.7.3 Evaluating the Performance of the SEDCAD Model

The third part of this research focused on evaluating the performance of SEDCAD model on reclaimed mining surfaces. This study investigated the performance of SEDCAD in estimating erosion and sediment delivery from low-compaction, steep-sloped mine lands reclaimed using the FRA. In addition, SEDCAD model input parameters were assessed with respect their sensitivity to SEDCAD outputs. The input parameters included CN value and erodibility (K) factor of reclaimed spoil material. Model outputs were compared to measured sediment yields from three mine study sites in East Tennessee. The results of this study can give a better understanding of the interpretation of SEDCAD outputs and will be useful in designing runoff and sediment control structures and selection of best management practices (BMPs) in the mining industry.

Question 3: How well does the SEDCAD model perform in predicting runoff and sediment delivery from reclaimed surfaces?

Task 3.1: Use estimated values of mine spoil erodibility (RUSLE K factor) and curve number (CN) obtained from previous parts of the study on reclaimed surfaces as input data for the SEDCAD model in order to estimate erosion and sediment yield from study plots and to compare results with measured data from the monitoring period.

1.7.4 Climate Change and Hydrology

The fourth and final part of this research focused on assessing potential changes in projected future rainfall erosivity due to climate change using as a case study the New River basin of East Tennessee, during the period 2010-2099 and for multiple greenhouse gas emission scenarios. To perform this assessment, a new approach was used which combines the methods

developed by Zhang (2005, 2007) for downscaling monthly precipitation products at time scales meaningful for modeling erosion processes, and the validated method developed by Yu (2002, 2003) for using a weather generator (CLIGEN) to generate accurate RUSLE erosivity factors. The results from this study can widely be used to assess potential future change in soil erosion in this area, and to evaluate the future effectiveness for current best management practices (BMP) in reducing soil erosion and sediment delivery from coal mining sites. The same method and technique is applicable for other regions of interest, in order to investigate the potential future change in rainfall erosivity.

Question 4: Will the future rainfall erosivity and its distribution throughout the year in the New River basin change due to climate change?

Task 4.1: Utilize a statistical downscaling method to produce enough precipitation details from a global circulation model to directly enable computation of R-factor values for the New River basin at East Tennessee.

Task 4.2: Assess potential changes in projected future rainfall erosivity due to climate change in New River basin in the Southern Appalachian region of East Tennessee.

1.8 Presentation of this Research

This dissertation is presented in seven chapters. Chapter 2 provides a literature review and background on erosion, erodibility, runoff generation, CN estimation, SEDCAD model usage, and climate change effect on erosion of reclaimed mine sites as they relate to the research completed within this dissertation. Chapter 3 describes the study area, site construction, monitoring equipment, and field data collection. Chapter 4 is devoted to runoff and CN estimation for low-compaction steep reclaimed slopes. Chapter 5 is devoted to erosion and

sediment delivery of low-compaction steep reclaimed slopes. Chapter 6 discusses performance of SEDACD model on reclaimed surfaces. Chapter 7 discusses climate change effect on future rainfall erosivity of study area. Conclusions and recommendations are included at the end of each chapter.

Chapter 2

Literature Review and Background

2.1 Runoff Generation & CN Estimation for Reclaimed Mine Surfaces

The runoff CN method developed by the US Department of Agriculture, Soil Conservation Service (now the Natural Resources Conservation Service, NRCS) is widely accepted for estimating runoff from rainfall on reclaimed mine lands, although its original development was for agricultural lands (Barfield et al. 1981; Ritter et al. 1991; Schroeder 1994; Camorani et al. 2005; Taylor et al. 2008). The NRCS runoff method is fully described in the National Engineering Handbook (NEH), Section 4 on Hydrology, and updated in NEH Part 630 (SCS 1972; NRCS 2004). In addition, Hawkins et al. (2009) recently completed a technical review on curve number hydrology.

Several studies have generated CN values for use on reclaimed surface coal mine lands, but none provide CN validated through field studies on steep-sloped reclaimed mine lands with loose spoils supporting the FRA. Also, estimated CN values from precipitation–runoff depth pairs obtained from the monitoring study sites are dependent on the precipitation depth, with CN value tending to decline as precipitation depth increases. Estimating a precipitation-independent CN value (P-independent CN) is important as it can be highly useful in practice to estimate runoff leaving low compacted reclaimed sites and also in designing retention basins and BMPs for managing runoff and sediment leaving mine sites. The widely recognized asymptotic method described by Hawkins (1993) was developed for estimating curve numbers from rainfall-runoff data sets and has the potential advantage of estimating unique CN value for watersheds. This method determines CN as an asymptotic limit to the CN values calculated from ranked data pairs as precipitation depth approaches infinity (Hawkins, 1993). The SCS (1985) National

Engineering Handbook, Section 4, suggests that soil-based tables be used as a guide to estimate CN, but if local rainfall-runoff values are available, they are to serve as the primary source of reference. For design flood estimation use of measured CN data is preferred, but the standard tabulated CN values are generally used when there are no or limited runoff measurement data. It would be expected that CN values for reclaimed mine lands with compacted soils are greater than values on loose spoils, inferring a greater initial abstraction with increased infiltration for the loose spoils. NEH Section 4 reports CN values for reclaimed mines lands in the range of 74 – 77. Ritter and Gardner (1991) found CN values to range from 83 to 88 for an initial abstraction of 0.2 for three watersheds in Central Pennsylvania. The three sites were 3.1 ha, 11.6 ha and 32.2 ha in area, but slope steepnesses were not provided. This study represented post-mined lands fully vegetated with trees and grasses, so these CN values do not represent estimates for recently disturbed mine lands. Barfield et al. (1984) also concluded that CN values reported by NEH Section 4 tables were too low for reclaimed mine lands with compacted spoils. They simulated rainfall on erosion plots in western Kentucky consisting of three treatments, including mine spoils, top soil, and subsoil. On compacted mine spoils Barfield et al. (1984) reported a CN of 91, a similar value for compacted gravel or dirt roads, and a Hydrologic Soil Group (HSG) classification of D representing a surface condition with little or no infiltration.

Bonta et al. (1997) investigated the effect of mining and reclamation on three small watersheds in East-Central Ohio by monitoring hydrological conditions for the pre-mining (Phase 1), mining and reclamation (Phase 2), and post-reclamation (Phase 3) periods. Reclamation construction used a high level of compaction on 9% slopes. By using rainfall simulation, they showed that CN values increased due to mining and reclamation activities (Phase 2) with the range 83 to 91, while during Phase 3, CN values remained approximately the

same as for Phase 2, within the range of 87 to 91. Interestingly, CN values were not significantly different between Phases 2 and 3, though land cover for Phase 3 post-mining period included grass and trees.

Other studies have reported CN values for compacted soils. Meadows and Blandford (1983) used rainfall simulators on un-mined and reclaimed coal mine sites in Wyoming. In this semi-arid region, average annual precipitation is approximately 38 cm, with high-intensity rainfall events from local thunderstorms. CN values ranged from 91.7 to 92.8 for un-mined sites and 88.4 to 97.5 for the reclaimed mine sites. In a similar study by Schroeder et al. (1987) in West-central North Dakota using simulated rainfall on 40 plots with fine-textured reclaimed mine spoils, CN values ranged from 88 to 97 for an initial abstraction of 0.20.

It is evident that compaction of spoil materials on reclaimed mine lands can increase CN values above 87 from pre-mining to post-mining surface conditions. Applying the FRA utilizing loose-dumped spoils in eastern Kentucky, Taylor et al. (2009) found CN values in the range of 60 to 92 for an initial abstraction of 0.2, and a range of 35 to 88 for an initial abstraction of 0.05. In this study, loose spoils were dumped on a longitudinal grade of 2% for drainage, with 3-10% lateral side-slopes, and an under-drain perforated PVC pipe was installed. Low slope steepness, very low level of compaction by single pass of a dozer, a very rough surface topography, the presence of large rocks which created big gaps for rapid infiltration, and occurrence of relatively moderate intensity rainfall events provided a situation for which surface runoff was not observed in the study, thus CN values represent interflow contributions only. No difference in CN values were found among the three spoil treatments, consisting of weathered brown sandstone, un-weathered grey sandstone, and a mixture. In addition, precipitation-independent CN values were not estimated from their dataset. Although their study duration was two years, their CN

investigation for loosed-dumped spoil material covered only one mine site and was limited to 12 data points. In the Appalachian Coal Belt (ACB) region, the pre-mining land use is predominantly steeply sloped, and since FRA requires that reclamation of mine sites follows the natural hillsope topography, study on reclaimed areas will better match reality for study sites constructed with steep slopes. Limitations in Taylor et al. (2009) make it difficult to extend their findings to steep-sloped mine sites.

2.2 Erosion, and Erodibility of Reclaimed Mine Surfaces

Steep slope generally have higher erosion rates. Zhang et al. (2009) showed that sediment transport capacity increases as a power function with slope gradient. Meyer and Harmon (1989) showed that slope steepness affects erosion for the more erodible soils, while rills are under formation. Rills are considered as the first signs of major soil erosion. Rills begin to form when the runoff shear stress−which is the ability of surface runoff to detach soil particles−overcomes the soil's shear strength, which is the ability of soil to resist forces working parallel to the soil's surface. This begins the erosion process, as water breaks the soil particles free and carries them downslope (Torri et al. 1987). The slope steepness controls the depth of the rills, while the length of slope controls their number. After rills begin forming, they are subjected to a variety of other erosional forces which may increase their size and output volume. Up to 37% of erosion in a rill-driven area may originate from mass movement, or collapse, of rill sidewalls. As water flows through a rill, it will undercut the channel walls, triggering collapse. Also, as water seeps into the soil of the walls they weaken, amplifying the chance of wall collapse. The erosion created by these forces increases the size of the rill while also swelling its output volume (Govers 1987).

A high level of compaction provides slope stability and reduces the amount of erosion and sediment delivery from disturbed surfaces. However, a lower level of compaction produces a

better medium for tree survival. The low compaction technique has been reported to be effective on low to moderate gradient slopes (Torbert and Burger 1994; Thomas et al. 1999; Angel et al. 2006). Torbert and Burger (1994) studied survival of different species of trees (white pine, Virginia pine, sugar maple, sycamore, red oak and black walnut) on compacted and un-compacted reclaimed sites. After 2 years, 42% survival of seedling plants on compacted sites was reported, while 70% of plants on un-compacted sites survived. Also, trees on un-compacted sites were taller. Thomas et al. (1999) performed a field study on surface mine lands in eastern Kentucky to investigate effects of two levels of compaction on white ash (Fraxinus americana), yellow poplar (Liriodendron tulipifera), and northern red oak (Quercus rubra) growth. They concluded that low compaction of spoils result in higher vigor and survival of plants. Angel et al. (2006) studied survival of white oak (Quercus alba), white ash, eastern white pine (Pinus strobus), northern red oak, black walnut (Juglans nigra), and yellow-poplar under compacted, lightly compacted, and uncompacted mine spoil. All species with the exception of white ash, showed increased survivability as compaction was decreased.

Sweigard et al. (2007) proposed techniques for constructing low-compaction spoils in order to maximize reforestation success on reclaimed coal mine surfaces. Their technique focused on leaving spoil loose, leveling with the lightest equipment available with the fewest passes possible during dry conditions, and permanently removing all equipment from the area after leveling. Fields-Johnson et al. (2009) assessed the effects of grading and groundcover treatments on reforestation and successful growth of mixed hardwoods and American chestnut trees in active coal-mining sites in Virginia. The result of their study showed that compaction had no significant impact on survival of mixed hardwood trees and Chestnuts growth, but loose grading reduced soil loss compared to smooth high compaction grading.

Erodibility of naturally formed agricultural soils has been studied extensively over the past years (Mcintosh et al. 1993), but there is limited information about the erodibility of both reclaimed and un-reclaimed surface mined lands, especially those constructed by low compaction techniques on steep slopes. Most research evaluates erodibility and/or soil loss from areas using rainfall simulation methods rather than in-situ field approaches. An erosion study under natural rainfall conditions is labor intensive, time consuming, and costly (Carroll et al. 2000). At the same time, researchers studying erosion of mine spoil have been more focused on low to moderate over-compacted reclaimed slopes.

Gilley et al. (1977) used rainfall simulations to compare runoff and sediment yield of native rangeland sites (sandy loam texture and 9.0 percent slope) with surface mined sites, representing pre-mined and mined conditions, respectively. Study plots were constructed in western North Dakota using bare spoil materials with slope gradients of 4.6 and 17.0 percent on a sandy clay loam material. Also, plots with 10.0 and 12.9 percent slope gradient were constructed on clay loam and silty clay loam spoils. Average sediment delivery of 74,000 $kg \cdot ha^{-1}$ for the bare topsoil, 18,000 $kg \cdot ha^{-1}$ for bare spoil, and 200 $kg \cdot ha^{-1}$ for rangeland were reported.

Hartley (1982) ran rainfall simulations on four loam-texture spoil study plots to investigate runoff and soil loss from different reclaimed treatments. Their study was conducted on plots with slopes ranging from 6% to 15%, which were located on a coal mine site in northwestern Colorado. The four plots included one straw mulch plot, one standing grain mulch plot, and a pair of rototilled fallow plots (bare and recently disturbed spoils). The test plots were reported to be hydrologically similar. The rototilled plots yielded four and ten times as much soil loss per unit of runoff as what the standing grain mulch and straw mulch plots showed, respectively. The standing grain mulch plot yielded about 2.5 times as much sediment per unit of

runoff as the straw mulch plot. A soil loss between 2.39 to 3.53 $t \cdot ha^{-1}$ was reported for the rototilled plots, 0.31 $t \cdot ha^{-1}$ was reported for the straw mulch, and 0.01 to 0.71 $t \cdot ha^{-1}$ was reported for standing grain mulch.

Mitchell et al. (1983) studied erodibility of un-mined soil (Clinton silt loam soil on 2 to 18% slope) and reclaimed material (mixture of Keomah silt loam, Hickory loam, and Clinton silt loam on 5% slope), for two sites in western Illinois and one in southern Indiana. For each condition at each mine, six plots were constructed with a high compaction level. Rainfall simulations with 64 $mm \cdot hr^{-1}$ intensity were performed. Their experimental procedure consisted of a 60-min dry run, and then within an hour, 30 min of wet run, followed by a 15- to 20-min pause before conducting 30 min of very wet run. Reclaimed soil plots were determined to have lower K factors than those for the corresponding un-mined soil for the same mine. The estimated K factor for the reclaimed sites was on the average 74% of what was estimated for corresponding un-mined sites. They reported K factor values in the range of 0.21 to 0.65 $t \cdot ha \cdot h \cdot ha^{-1} \cdot MJ^{-1} \cdot mm^{-1}$ for compacted reclaimed sites.

Barfield et al. (1983), investigated the effects of placement technique and density on erosion rate of mine spoil and reconstructed topsoil by using standard erosion plots (4.6 m by 22.1 m on 9 percent slope) in western Kentucky. Plots were constructed with shale spoil material, topsoil (A horizon) and subsoil (B and C horizon mixture) under two compaction conditions. Rainfall simulations with a rate of 63.5 $mm \cdot h^{-1}$ in dry, field capacity, and very wet conditions were used to study erosion on the plots. Average erosion rates of 0.35, 0.94, and 1.013 $t \cdot ha^{-1}$ were reported for the spoil, subsoil, and topsoil plots, respectively. They found lower erosion rates on slopes as the level of compaction decreased.

Researchers who used natural rainfall events have generally studied erosion on low slope gradients with a high level of compaction. McIntosh et al. (1993) studied erodibility and sediment yield of reconstructed compacted mine soils (topsoil, subsoil, and mine spoil) using natural rainfall events and low gradient (9%) standard study plots in Kentucky. The subsoil and topsoil were Sadler silt loam (Glossic Fragiudalf, fine-silty, mixed, mesic) and spoil was from overburden above the coal bed, consisted of a mixture of shale, siltstone, and sandstone. K factors of 0.046 for topsoil, 0.067 for subsoil, and 0.051 for mine spoil with units of $t \cdot ha \cdot h \cdot ha^{-1} \cdot MJ^{-1} \cdot mm^{-1}$ were reported. Significant rill development was observed. Rill formation followed by greater erosion rate due to change in the runoff patterns from sheet to that of more concentrated flow patterns, where erosive energy from overland flow is greater. Their study showed that the erodibility of a given material can be quite variable through the year (McIntosh et al. 1993). They concluded that K factors will increase slightly in the winter due to higher antecedent soil moisture levels and to temperature fluctuations that result in freeze-thaw cycles that cause further instability in spoil material. Equal erodibility of topsoil and spoil was observed and assumed to be associated with an armoring effect imposed by the coarse fragments of spoil. They found a good prediction for erodibility of each reconstructed material by using the Wischmeier et al. (1971) nomograph.

Bonta (2000) tried to quantify the effects of coal surface mining and reclamation on suspended sediment concentrations and yields leaving three small study watersheds in Ohio. The study watersheds were monitored during three different phases: 1) undisturbed natural condition, 2) under mining and/or reclamation activities, and 3) completely reclaimed condition. The predominant land use for the undisturbed natural condition (Phase 1) was pasture and forest. For Phase 3 (reclaimed condition), grasses and legumes were used as cover. Area-average USLE K-

factors of 0.33 and 0.43 t· ha· h· ha^{-1}· MJ^{-1}·mm^{-1} were used for Phase 1 and Phase 3, respectively. Also, CN values ranging from 71-81 for Phase 1 and 88-91 for Phase 3 were determined. Erodibility was not estimated during phase 2, but a linear regression model was built between suspended-sediment concentration and corresponding flow rates.

In southeastern Ohio, McKenzie and Studlick (1979) used natural rainfall events to find the erodibility of un-vegetated, un-reclaimed spoils, and didn't follow reclamation techniques as mentioned by SMCRA. The calculated K-factor value for the spoil material was found to differ from values obtained from soil-size texture analysis, "possibly due too gully erosion which is not predicted by Universal Soil Loss Equation" (Dickens et al. 1985).

Curtis and Superfesky (1977) investigated erosion and sediment delivery of steep-sloped surface mining spoil in Campbell County, Tennessee. Over 20 months, 33 mm (526,000 kg/ha) average total soil loss (including slope failure) from a 0.73 ha site was reported. Almost 90% of the reported erosion occurred during the first year after mining. Lots of rill and gully erosion, as well as slope failure were observed. Dickens et al. (1985) studied erosion and sediment yield from compacted steep-slope surface mine spoil in the New River Basin of Tennessee. Two study plots were constructed on a newly reclaimed surface mining spoil. Protective mulch and soil stabilizing material were used at reclamation. Average suspended sediment yields per storm were reported to be 0.06 kg·ha^{-1}. The major sources for sediment were reported to be sheet and rill erosion on the mining spoil. Between the deterioration of mulch and vegetation establishment, progressive armoring effect was observed on the spoil surface. About 81% of sediment was delivered during the first the 204 days of monitoring. It was concluded that "slope stability, in addition to erosion, must be considered in the approximate original contour reclamation of steep-

slope surface mines" (Dickens et al. 1985). Curtis (1971) also observed an armoring effect after strip mining in disturbed watersheds within Kentucky.

Carroll et al. (2000) investigated the effect of slope steepness on erosion, runoff, and sediment yield from three coal mine sites located in Queensland, Australia. Study plots with low (10%), moderate (20%) and steep (30%) slopes were constructed on soil and spoil material. Also, different treatments (pasture and tree) on slopes along with bare conditions were studied to understand the effect of vegetative cover on the erosion of mine spoils. Formation of rills (particularly on the steep slopes) was reported: "Once [rills] formed they persisted until a dense sward of grass colonized and stabilized rills" (Carroll et al. 2000). Little difference in soil erosion rates due to slope gradients were observed once dense vegetation was established on the plots. Runoff from the spoils was reported to be almost double that observed from the soil plots. Average annual sediment loss of 78 -280 $t \cdot ha^{-1}$ for bare mine spoil was reported.

Zhang et al. (2009) showed that sediment transport capacity increases as a power function with slope gradient in natural soils. Hahn et al. (1985) reported a strong positive linear relationship between soil loss and slope steepness for reclaimed spoil, but no significant correlation was seen between slope steepness and flow velocity for reclaimed material in their study. Increased rill frequency was observed for increased slope steepness, and a positive linear correlation was reported between length of rills and slope steepness. They concluded that since a positive linear relationship also exists between soil loss and slope steepness, soil loss and rill formations were strongly related and dependent on slope steepness. Meyer and Harmon (1989) showed that slope steepness affects erosion for erodible soils, at least while rills are under formation. Berger et al. (2010) used laboratory rainfall experiments to investigate initiation and evolution of rill networks under different rainfall intensity and slope (10, 20, and 30%)

treatments. An increase in either slope or rainfall intensity increased soil loss due to rill erosion, but the effect of rainfall intensity was larger. Increased rill formation was observed in the lower part of the slope. Rill density was similar for the different slope steepness treatments under constant rainfall intensity, but total sediment delivery increased considerably for higher slope steepness. "The developed rill systems were therefore comparable, but more soil was lost at steep slopes" (Berger et al. 2010). Rill depth increased for larger slopes, while the rill cross-section width got narrower. Rill stabilization was reported after almost an hour of rainfall simulation for all rainfall intensities and slopes.

Nicolau (2002) showed that grass cover and soil moisture are controlling factors for runoff generation, routing, and sediment delivery on topsoil slopes, while on compacted mine spoil slopes, rill network density is the dominant factor. Runoff connectivity (runoff rates recorded at the rill-network scale over runoff rates recorded at the interrill-area scale) of rilled spoil material was reported higher than on the corresponding topsoil slope. A higher rill density was observed on mine spoil than topsoil, and it was reported as related to low infiltration capacity in the compacted mine spoil. Hancock et al. (2002) studied rill development on a newly constructed homogeneous bare mine spoil, at a slope equal to the angle of repose. The observed rills initiated near the top of slope and ran linearly down the slope as regularly-spaced distinct drainage lines with triangular cross-section.

2.3 SEDCAD Usage for Reclaimed Mine Surfaces

Design of the sediment control basins and stormwater best management practices (BMPs) is sometimes performed with the support of computer software such as SEDCAD program. SEDCAD is a suite of curve number-based watershed rainfall-runoff models, RUSLE-based sediment yield analysis, and channel and hydraulic structure design utilities (Warner et al. 1998).

SEDCAD is primarily used by OSM, state mining programs, industry, and engineering consultant firms for hydrologic, erosion and sediment control designs (OSM, 2010). OSM provides SEDCAD to the 24 states with primacy under the SMCRA for use in permit review and in design of abandoned mine lands (AML) reclamation projects and remediation plans for bond forfeiture sites. OSM also uses SEDCAD to review permit applications from industry, and in preparation of Cumulative Hydrologic Impact Assessments (CHIA) to determine the cumulative hydrologic effects of multiple mining operations on adjacent lands and watersheds during and after mining (SEDCAD 2007). SEDCAD includes hydrology and hydraulics design and can be used to evaluate the effectiveness of both individual and integrated systems of surface water, erosion, and sediment control measures with respect to sediment trap efficiency and prediction of effluent sediment concentration (Warner et al. 1998).

Specifically, SEDCAD has been used by engineers, geologists, hydrologists, and soil scientists to: 1) model hydrologic mine systems including channels, ponds, and sediment control structures; 2) evaluate the effectiveness of sediment ponds and other sediment control structures such as check dams, grass filters, and silt fences for a mining reclamation plan; 3) evaluate diversion channel designs, including riprap, grass-lined, and bar soil conditions; 4) evaluate culvert and plunge pool designs, and recommend changes for permits under review; and 5) analyze the impact of the addition or removal of a hydrologic structure - sediment pond, permanent impoundment, plunge pool, etc. under permit review (US Dept. of Interior, 2008).

SEDCAD's input parameters are basin size, stream and land slope, time of concentration, curve number, soil erodibility (RUSLE K factor), hydrologic soil group, hydrograph response, storm frequency, and particle size distribution of eroded material. SEDCAD allows division of the watershed into relatively homogenous sub-basins with respect to expected hydrologic and

sediment erosion responses. Hydrologic and sediment data are tabulated at a model position that SEDCAD refers to as a "structure." A "structure" can be a physical or non-physical entity and is simply a position in the model where hydrographs and sediment-graphs are generated. While SEDCAD has been used extensively as a tool in hydrologic, erosion, and sediment control designs, there is limited information on its performance estimating erosion and sediment yield from disturbed mine lands. Also, sensitivity of the software's results to its hydrologic and sedimentologic input parameters has never been investigated.

The overall objective of this part of research is to evaluate performance of SEDCAD in predicting runoff, erosion, and sediment yield from three coal mining study sites in the southern Appalachian region for a 14-month period. In addition, the sensitivity of SEDCAD to the main hydrologic and sedimentologic input parameters–curve number value (CN) and erodibility of reclaimed material (K)–was investigated with respect to the model's output, and the outputs were compared with measured data. Results of this study allows for a better interpretation of SEDCAD output, which will be useful to practitioners in the mining industry designing runoff and sediment control structures and selecting stormwater BMPs.

2.4 Climate Change and Erosivity

The potential effects of climate change on erosion have been studied using different approaches. Favis-Mortlock and Boardman (1995) investigated changes in erosion rates due to the effect of climate change by using the Erosion Productivity Impact Calculator (EPIC) model at the South Downs, United Kingdom. Their model, EPIC, was limited in its ability to model the complicated interactions in the erosional system as the climate changes (Pruski et al. 2002). The Water Erosion Prediction Project (WEPP) model was used by Favis-Mortlock and Savabi (1996) to determine the effects of change in CO_2 concentrations on water balances and crop biomass

production rates. Sensitivity of erosion to changes in CO_2 concentration and temperature was investigated by Savabi et al. (2001), but no further evaluation was performed on potential impact of precipitation changes on erosion. Using three different GCMs, soil erosion changes due to climate change effect in Mato Grosso State of Brazil was investigated by using a CO_2-sensitive version of WEPP, which showed 27% to 55% increase in soil erosion (Savabi et al. 2001). Nearing (2001) used results of climate change scenarios from two GCMs to study potential changes in rainfall erosivity due to climate change across the United States for the 21st century. Study results showed a potential for erosivity change across much of the U.S. during the 21st century, from 16-58% change (positive or negative). Based on this study, using the U.K. Meteorological Office's Hadley Centre HadCM3 coupled GCM, a 25-50% average increase in rainfall erosivity was projected for East Tennessee over the 80 years from 2000-2019 to 2080-2099. Pruski and Nearing (2002) used simulated climate data from the HadCM3 GCM to study potential impacts of climate change on soil erosion by water. They modeled erosion at eight locations within the U.S. using a modified version of WEPP model to consider the effects of changes in CO_2 concentrations on plant growth. Their investigation showed an increase in erosion rate when there is a significant increase in precipitation amount/intensity, while for decreases in precipitation amount/intensity either increases or decreases in overall erosion can be expected, depending on the interactions between plant biomass, runoff, and erosion. Also, changes in rainfall intensity have a more significant impact on erosion rates than do changes in the number of rainy days, but the study found that erosional studies under climate change should incorporate both factors. Finally, the study revealed that each 1% change in precipitation would result in a 2% change in runoff and approximately 1.7% change in erosion, if other environmental factors (CO_2 concentration, temperature, etc.) remained constant.

Stochastic weather generators have been widely used to statistically downscale regional climate models, RCMs, or GCMs projections to the location of interest (Wilks 1992; Semenov and Barrow 1997; Katz 1996; Mearns et al. 1997; Mavromatis and Jones 1998; Hansen and Ines 2005; Tisseuil et al. 2010; Zhang et al. 2010). In this method present-date climate parameters are adjusted to GCM-projected relative climate changes, then future climate series are generated using perturbed parameter values (Zhang 2007). The CLIGEN model (Nicks and Gander 1994) is a stochastic daily weather generator that uses a first-order two-state Markov chain to produce daily precipitation occurrence. The Markov chain is constructed per transition probabilities of a wet day following a wet day ($P_{w/w}$) and a wet day following a dry day ($P_{w/d}$). The daily mean precipitation is generated using a transformed skewed normal distribution, while the daily maximum and minimum temperatures are generated using normal distributions (Zhang 2007). Zhang et al. (2010) investigated rainfall erosivity changes under climate change using six GCM models under three emissions scenarios (A2, A1B, and B1). They computed downscaled mean annual precipitation and USLE rainfall erosivity (R factor) for time periods 2030 through 2059 and 2070 through 2099 for northeast China. They established a new approach that combines the methods developed by Zhang (2005, 2007) to downscale monthly precipitation data from GCMs at time scales meaningful for modeling erosion processes, and the method developed by Yu (2002, 2003) that uses a weather generator (CLI GEN) to generate accurate RUSLE erosivity factors. Their study revealed that changes in rainfall erosivity under the higher greenhouse gas (GHG) emissions scenarios, A1B and A2, show the highest projected changes, and changes in erosivity do not uniformly correspond spatially to changes in total annual rainfall depths. The same approach by Zhang et al. (2010) is utilized in this study to estimate R factor trends caused by climate change for the New River Basin at East Tennessee.

Chapter 3

Low-Compaction Steep-Sloped Reclaimed Surface Mine Lands in the Southern Appalachian Region

3.1 Study Area

The three study sites were located in the Appalachian Plateau physiographic region, locally referred to as the Cumberland Plateau and extending in a north-south direction through Kentucky, Tennessee, and Alabama (USGS 2003). The Cumberland Plateau consists of Mississippian and Pennsylvanian geological formations holding coal, shale, sandstone, and limestone (NPS 2007). Soils in this mountainous region consist of moderately deep clay sub-soils and silty clay topsoils on ridge tops, and well-drained silty clay loam soils lower in the valley (Overton 1980). In undisturbed forested areas, the surface soil horizon is rich in organic matter. Native forest cover is classified as Appalachian Mixed Mesophytic Forest, dominated by oaks (*Quercus spp*), hickories (*Carya spp*), maples (*Acer spp*), ashes (*Fraxinus spp*), and elms (*Ulmus spp*). However, the study sites were devoid of trees and the spoils on the reclaimed slopes were predominately silty clay soils mixed with larger gray shale and brown sandstone rocks.

The three sites are in East Tennessee north of the city of Knoxville, and all sites were active with surface coal mining operations (Figure 1). Named in this report based on mine operator, the three sites were: 1) Premium, located in Anderson County at N 36^{o} 6’ 36”, W 84^{o} 19’ 30”; 2) National, located in Campbell County at N 36^{o} 30’ 30”, W 84^{o} 16’ 12”, and 3) Mountainside, located in Claiborne County at N 36^{o} 31’ 30”, W 83^{o} 57’ 23”. A humid subtropical climate prevails in this region, where July is the warmest month and January the coldest. Average annual precipitation at the Premium site is 129.2 cm, with typical temperature

ranges between -17 and 33^{o}C (NOAA webpage). The National site has an average annual precipitation of 136.9 cm, and the temperature ranges between -15 and 33^{o}C, whereas the Mountainside site has an average annual precipitation of 129.5 cm and a temperature range between -14.5 and 33.2^{o}C. During the study period the annual precipitation, averaged among all three sites, was 136.5 cm. In East Tennessee, long-term average precipitation for the months of May, June, July and August are 12.8 cm, 12.3 cm, 13.7 cm, and 10.7 cm, respectively (NOAA webpage). During the initial four months of the monitoring period for this study (May through August 2009), the monthly precipitation measurements averaged across study sites were 14.6 cm, 13.4 cm, 28.6 cm, and 19.3 cm, respectively, or a total of about 53% over the normal. As will be seen later, this was also the period of most active rill formation.

3.2 Site Construction and Monitoring Equipment

The study sites were constructed in late 2008 and early 2009 based on FRA techniques, employing low-compaction grading practices. Various reclamation methods to restore hillslopes to their original topography are used by coal mining operators, but the "contour haul back" is the most widely used method in the Appalachian region (Burger et al., 2005; Sweigard and Kumar, 2010). In this method a ramp is constructed on the contour bench, where soil is hauled and dumped over the ramp edge. Compaction levels are achieved by the number of grading equipment passes during construction, creating dense spoils at the slope core. In the upper 1 to 2 meters, loose spoils and stock-piled topsoils and subsoils are deposited as the final surface with no or limited grading passes.

Premium, National, and Mountainside study sites were designed and constructed in March 2009 with four plots separated by earthen berms approximately 0.5 m in height serving as physical barriers to isolate runoff and sediment (Figure 2). Cover crops were not established

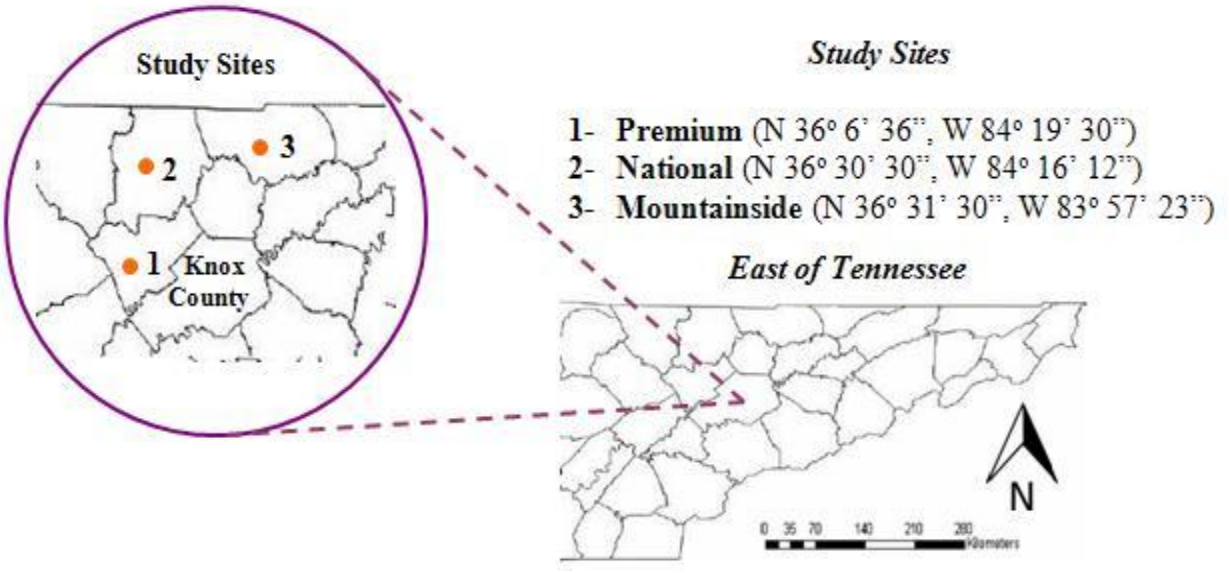

Figure 1. Location of study sites at Premium, National, and Mountainside surface coal mining sites in East Tennessee, USA.

during the first year after construction, so this research represents the worst-case scenario for runoff and sediment yield from these reclaimed mine sites. Plot sizes were approximately 45 m long by 25 m wide, with slopes ranging from 19^{o} to 3^{o} (Table 1). Unit weights were measured by a Nuclear Density Gauge (NDG) device (Troxler 3411 B) between June and August 2009, and ranged from 16.2 to 20.4 KN$\cdot$m^{-3} (Jeldes et al., 2010).

At the bottom of each plot, earthen berms and paved chevrons with a rubber mat liner directed runoff and sediment to a ¾ -ft (0.23 m) standard USDA H-type flume (Figure 3). Each H flume was equipped to measure flow depth utilizing the Tennessee fluid level indicator (TFLI) as developed by Yoder et al. (1999). Downstream of each H-flume, runoff and sediment were directed into a 0.378 m^{3} (100-gal) pre-sedimentation tank, and then into a collection system of three flow divider buckets and a terminal collection bucket, all of which were 5-gal (18.9 L) in size (Hoomehr et al., 2010).

Figure 2. Photo of the study site construction on the National Coal Company property.

Table 1. Study site and field plot constructed characteristics.

Site	Plot	Angle of Slope, Degrees	Length (m)	Width (m)		Unit Weight (KN/m^3)		
				Top	Bottom	Type	Mean	SD
Mountainside	1	27	48.8	21.5	21.5	*Dry*	18.9	2.2
	2	29	46.0	21.5	25.0			
	3	28	44.6	25.1	22.4	*Wet*	20.4	2.2
	4	27	42.3	25.7	23.3			
National	1	21	47.6	23.1	19.7	*Dry*	18.5	1.0
	2	20	48.4	22.1	25.3			
	3	19	49.2	23.5	28.4	*Wet*	20.3	1.0
	4	21	48.2	20.8	28.2			
Premium	1	28	33.5	24.8	21.7	*Dry*	16.2	1.3
	2	28	33.3	28.8	27.2			
	3	28	33.3	27.7	25.3	*Wet*	18.5	1.3
	4	30	28.5	31.0	25.7			

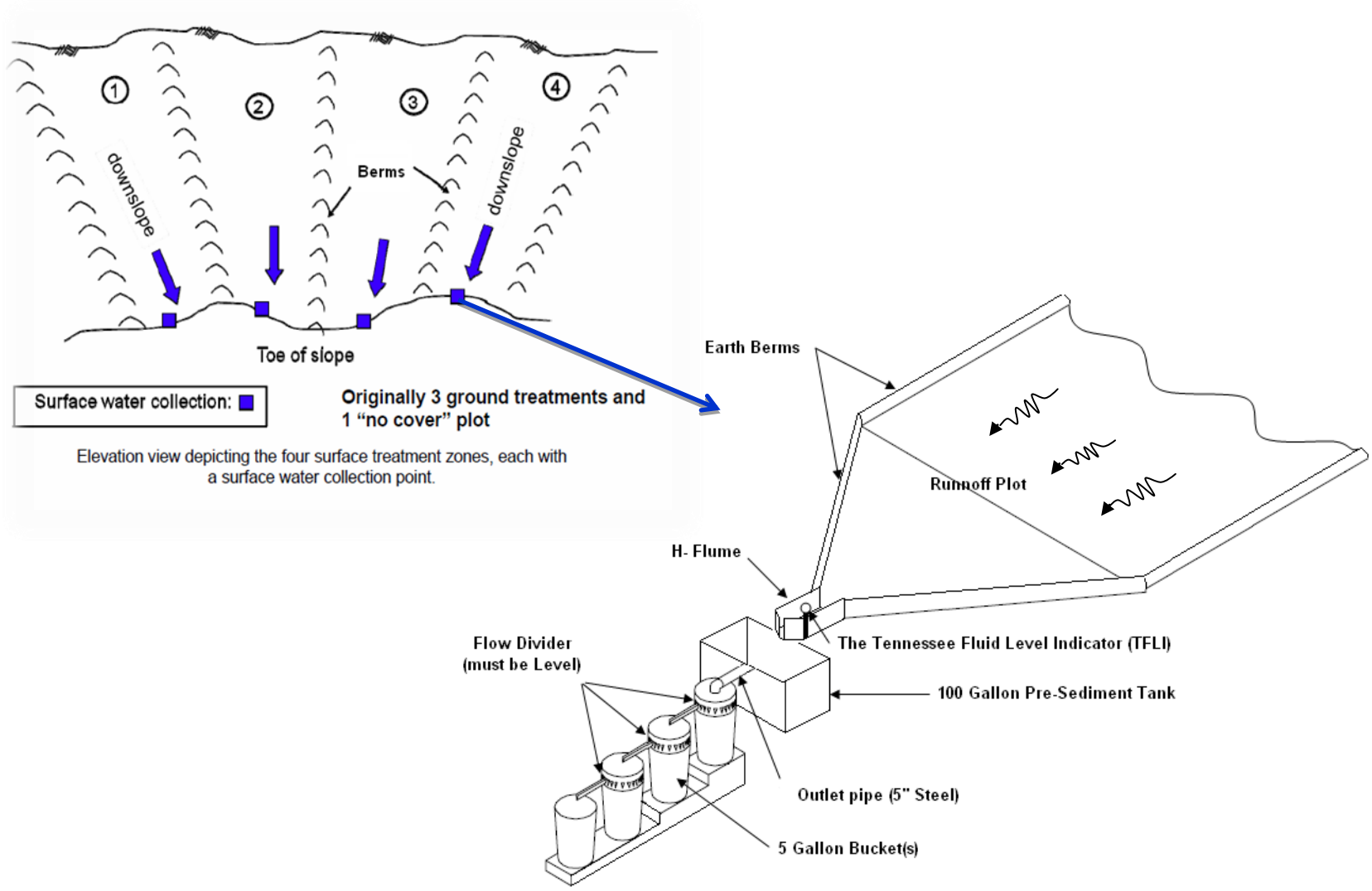

Figure 3. Field plot set up and instrumentation for measurement of water runoff and sediment erosion.

Based on Pinson et al. (2003), the flow dividers consisted of a stainless-steel circular crown containing 22.5^{o} V-notch weirs, with the crown screwed onto the bucket (Figure 3). The first divider consisted of 12 V-notches in order to handle the high initial flow rate, whereas the 2nd and 3rd dividers had 24 notches. Once the bucket completely filled, water and sediment overflow was evenly divided among the V-notches, and flow from a single notch was directed to the next bucket. A triangular leveling device constructed of angle iron and stainless steel adjustment bolts at each corner was used to ensure that the flow divider was level so outlet flow from the buckets was evenly divided. The first flow divider limits the maximum peak runoff rate that can be handled with this arrangement, which for a 12-weir divider is about 30 L·s^{-1}. The corresponding peak runoff rate for this size of plot is 27.5 L·s^{-1}, corresponding to a 76 mm·h^{-1} runoff intensity. The maximum measurable runoff volume for this system was 136.52 m^{3} (36,065 gal) corresponding to a 10.5 cm runoff depth over a study plot (Hoomehr et al., 2010). Estimates of measured runoff and sediment yield from these devices are explained in the next section.

Each study site was equipped with a Campbell Scientific Inc. (CSI) CM10 full weather station consisting of: 1) CSI 21X data logger; 2) Vaisala HMP-45C temperature/relative humidity sensor in a UT12VA gill radiation shield; 3) Texas Electronics TE525 tipping bucket rain gauge; 4) Li-Cor model LI-200sz solar radiation pyranometer, 5) RM Young 03001 wind sentry for wind speed and direction, 6) CSI MSX20R solar panel; and 7) 115 amp-hour deep cycle marine battery. The devices were tested and calibrated before use. Measurement accuracy for rainfall rates less than 25.4 mm·h^{-1} (1 in·h^{-1}) was ± 1%, and for rates greater than 25.4 mm·h^{-1} was not greater than 3%. Weather sensor data was measured every minute, including air temperature, relative humidity, wind speed and direction, and solar radiation. Each hour, the CSI data logger computed and recorded averages for air temperature, relative humidity, wind speed

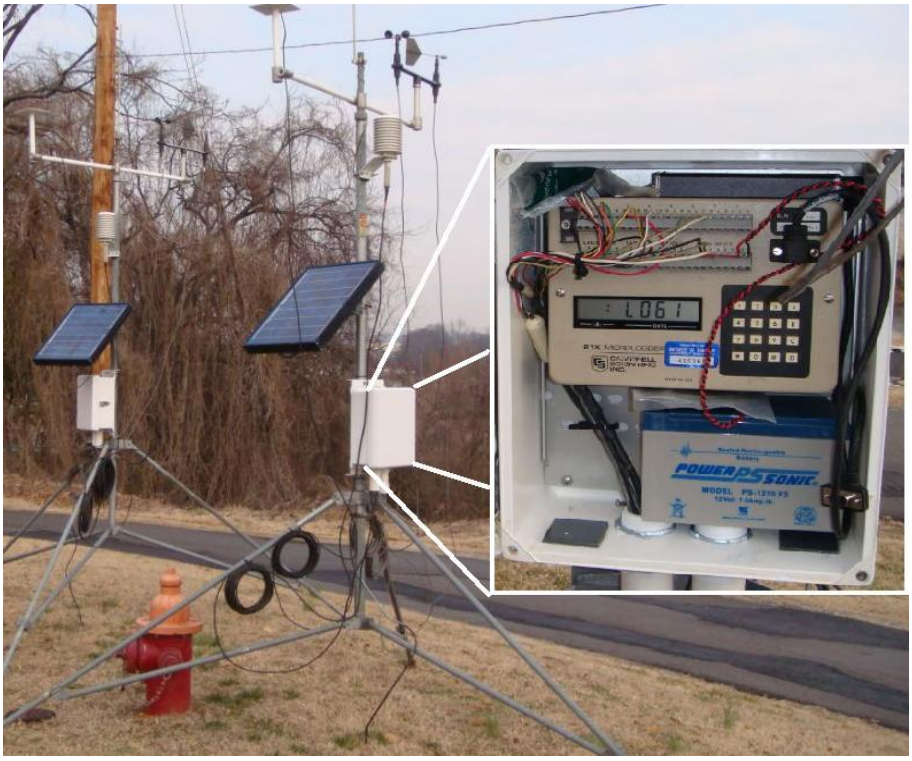

Figure 4. Typical weather stations and data logger used at study sites.

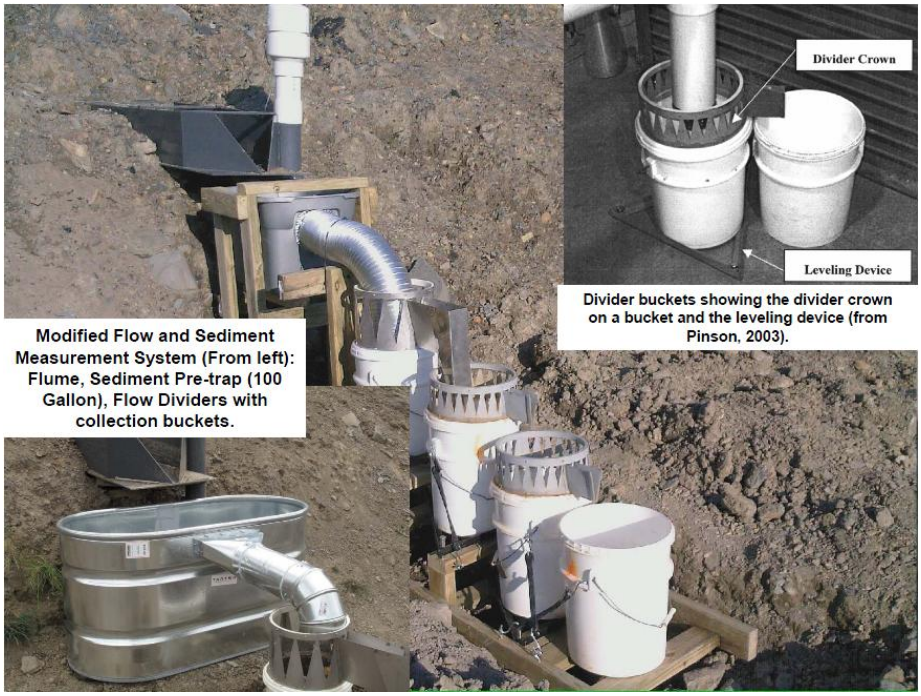

Figure 5. Typical sediment and runoff collection systems at study sites.

and direction, and a total for solar radiation. A total for precipitation and an average flume stage was recoded every five minutes. Daily values of maximum and minimum air temperature, totals of precipitation and solar radiation, and averages of air temperature, relative humidity, and wind speed and direction were also recorded.

Chapter 4

Curve Numbers for Hydrology on Reclaimed Mine Lands

Hoomehr S., J.S. Schwartz, S.C. Yoder, W.C. Wright, and E.C. Drumm. "Curve numbers for hydrology on low-compaction, steep-sloped reclaimed mine lands in southern Appalachian region." *ASCE Journal of Hydrologic Engineering*. Under Review

4.1 Introduction

Under the Surface Mining Control and Reclamation Act of 1977 (SMCRA), hydrologic impacts of coal surface mining operations must be assessed and mitigated (Tolbert et al. 1994; Graves et al. 2000). Pre-mining assessments − termed probable hydrological consequences (PHC) in SMCRA − are conducted using the runoff CN method to generate estimates of runoff volume and hydrograph peaks for the mine sites, and potential offsite runoff impacts are addressed with on-site detention ponds. SMCRA requires post-mining runoff to not exceed pre-mining runoff for a 10-year 24 hour storm event. Recent advancements in surface mining reclamation advocates the use of loose spoils and low compaction grading to enhance reforestation success, in a process known as the Forest Reclamation Approach (FRA). Swiegard et al. (2007) describes grading practices under the FRA on steep slopes where spoils are compacted for slope stability in terraced layers following the natural topography, and surface finished with 1 to 2 meters of a loose spoils and top soil with minimal grading. Currently, CN values for conducting PHCs in the Appalachian region are limited to highly-compacted non-FRA mine lands and mild-sloped FRA sites with a 2% grade (Taylor et al. 2009). Better CN values are needed in order to adequately design detention ponds and other runoff controls for slopes in the 25% to 35% range on loose spoils constructed in the Appalachian region for FRA.

The runoff CN method developed by the US Department of Agriculture, Soil Conservation Service (now the Natural Resources Conservation Service [NRCS]) is widely

accepted for estimating runoff from rainfall on reclaimed mine lands, although its original development was for agricultural lands (Barfield et al. 1981; Ritter et al. 1991; Schroeder 1994; Camorani et al. 2005; Taylor et al. 2008). The NRCS runoff method is fully described in the National Engineering Handbook (NEH) Section 4 on Hydrology, and updated in NEH Part 630 (SCS 1972; NRCS 2004). In addition, Hawkins et al. (2009) recently completed a technical review on curve number hydrology. In the Appalachian coal mining region, design professionals commonly use the SEDCAD model to estimate runoff volumes and peaks and soil erosion for detention pond design in order to meet SMCRA requirements (Taylor 1995). SEDCAD also needs CN inputs as it employs the curve number method for runoff volume prediction, although other rainfall-runoff models could be effectively utilized as well.

Several studies have generated CN values for use on reclaimed surface coal mine lands, but none provide CN values validated through field studies on steep-sloped reclaimed mine lands with loose spoils supporting the FRA. It would be expected that CN values for reclaimed mine lands with compacted soils are greater than values on loose spoils, inferring greater initial abstraction with increased infiltration for the loose spoils. NEH Section 4 reports CN values for reclaimed mines lands in the range of 74 – 77. Ritter and Gardner (1991) found CN values to range from 83 to 88 using an initial abstraction coefficient $\lambda = 0.2$ for three watersheds in Central Pennsylvania. The three watersheds were 3.1 ha, 11.6 ha and 32.2 ha in area, but average slope values were not provided. This study represented post-mined lands fully vegetated with trees and grasses, so these CN values do not represent estimates for recently disturbed mine lands. Barfield et al. (1984) also concluded that CN values reported by NEH Section 4 tables were too low for reclaimed mine lands with compacted spoils. They simulated rainfall on erosion plots in western Kentucky consisting of three treatments including mine spoils, top-soil, and subsoil. On

compacted mine spoils Barfield et al. (1984) reported a CN of 91, a similar value for compacted gravel or dirt roads, and a hydrological soil group (HSG) classification of D representing a surface condition with little or no infiltration.

Bonta et al. (1997) investigated the effect of mining and reclamation on three small watersheds in East-central Ohio, monitoring hydrological conditions for pre-mining (Phase 1), mining and reclamation (Phase 2), and post-reclamation (Phase 3) periods. Reclamation construction used a high level of compaction on 9% slopes. By using rainfall simulation, they showed that CN values increased due to mining and reclamation activities, resulting in a CN grange of from 83 to 91. During Phase 3, curve numbers remained approximately unchanged from the values for Phase 2, with a range of 87 to 91. Interestingly, CN values were not significantly different from this for Phase 3, though land cover for the Phase 3 post-mining period included grass and trees.

Other studies have reported CN values for compacted soils. Meadows and Blandford (1983) used rainfall simulators on un-mined and reclaimed coal mine sites in Wyoming. In this semi-arid region, average annual precipitation is approximately 380 mm, with high intensity rainfall events from local thunderstorms. CN values ranged from 91.7 to 92.8 for un-mined sites and from 88.4 to 97.5 for the reclaimed mine sites. In a similar study by Schroeder et al. (1987) in West-central North Dakota using simulated rainfall on 40 plots with fine-textured reclaimed mine spoils, CN values ranged from 88 to 97 for an initial abstraction of 0.20.

It is evident from these studies that compaction of spoil materials on reclaimed mine lands can increase CN values above 87 from pre-mining to post-mining surface conditions. Applying the FRA utilizing loose-dumped spoils in eastern Kentucky, Taylor et al. (2009) found CN values ranged from 60 to 90 ($\lambda = 0.2$), with a mean CN of 82 based on 11 storms and 64

sampled events. For $\lambda = 0.05$, CN values ranged from 32 to 87 with a mean of 67. In the Taylor et al. (2009) study, loose spoils were dumped on a 2% profile grade with 3-10% lateral side-slopes, and a perforated PVC pipe was installed as an under drain. Three spoil treatments were used in the study, consisting of weathered brown sandstone, unweathered grey sandstone, and a mixture. They found no statistical differences in CN values among the treatments. Surface runoff was not observed in this study, so CN values represent interflow contributions only. The lack of surface runoff was attributed to the low steepness and low compaction, the rough surface comprised of large rocks and crevices, and occurrences of relatively moderate intensity rainfall events during the two-year study period. In addition, precipitation-independent CN values (as described below) were not estimated for their dataset.

Hawkins et al. (2009) recommends computing a precipitation-independent CN by the asymptotic method. In contrast to a range of CN values or a mean based on skewed measured rainfall-runoff data, Hawkins (1993) developed the asymptotic method, which can estimate a unique CN value for a land condition. It also reduces variation in calculated CN values. CN values are determined by taking the asymptotic limit of calculated CN values from ranked data pairs as precipitation depth approaches infinity. Use of a precipitation-independent CN provides a better solution for estimating runoff, especially when runoff estimates are used in detention/retention basin design for stormwater management.

The objective of this study was to estimate CN values for use in runoff prediction from steep-sloped, loose spoil materials in the Appalachian coal mining region. This information will support the regulatory agencies charged with the reclamation of natural hillslope topography and native forests under the FRA, as understanding the hydrological conditions immediately following hillslope construction is necessary in order to engineer adequate runoff retention and

erosion control structures. In addition, this new information supports reforestation research efforts to improve native tree regeneration using the FRA. In this study, runoff was measured by the method described by Pinson et al. (2003) using flow divider buckets, and the hydrological analysis was completed using the Asymptotic method as described by Hawkins (1993). It should also be noted that during the monitoring period rill development occurred on the study sites, as commonly occurs on steeply-sloped reclaimed mine lands without adequate surface cover.

4.2 Materials and Methods

4.2.1 Rainfall and runoff measurement

Rainfall and runoff measurements began in June 2009 and continued through July 2010 for the Premium, National, and Mountainside sites. Site monitoring was temporally halted in January and February 2010 because during these winter months the locations remained below freezing temperatures with no runoff. In addition, access to the monitoring sites was impossible due to poor road conditions. Downloads for CSI data loggers occurred on approximately a weekly basis, which was necessary with a 5-min (on rainfall − but hourly on weather data) recording interval from the weather stations and 5-min interval from the TFLIs. In addition, site equipment was inspected on these routine visits, and maintenance performed as required.

Although the sites were equipped with H-flumes, runoff volume was measured using the Pinson et al. (2003) flow dividers. Data from the H-flume was not usable due to sediment deposition in the flume channel. Also, the 5-minute recording interval for flow stage was not adequate to accurately estimate runoff volumes. In addition, this interval was inadequate to estimate time of concentration. Limitations on memory storage capacity prevented reducing the recording interval from the TFLIs.

4.2.2 CN Computations

The Curve Number method developed by the USDA Soil Conservation Service (SCS), presently the National Resource Conservation Service (NRCS) provides a means to estimate runoff volumes from rainfall event depths. This method is defined in Section 4 of the National Engineering Handbook, NEH-4 (SCS 1985). Briefly, the fundamental rainfall-runoff relationships are as follows:

$$Q = \frac{(P - I_a)^2}{(P - I_a) + S} \quad \text{for} \quad P \geq I_a \quad \text{..... (1)}$$

$$Q = 0 \quad \text{for} \quad P \leq I_a \quad \text{..... (2)}$$

$$S = I_a / \lambda \quad \text{..... (3)}$$

where Q is direct storm runoff, P is rainfall event depth, I_a is the initial abstraction, S is the maximum retention or storage, and λ is the initial abstraction coefficient. The values of Q, P, I_a, and S are in units of mm, and λ is dimensionless. Estimation of CN for a particular area depends on the maximum storage, S, which is in turn the function of initial abstraction, I_a, (Eq. 3). Initial abstraction is the amount of rainfall that falls before runoff begins, so it includes interception, filling of surface storage elements, and initial infiltration. This means that estimation of the maximum storage, S, requires an assumption for the initial abstraction coefficient, λ, if P and Q already exist. Although λ can take any value between 0.01 and 0.2 (Schneider and McCuen 2005), the 0.2 value is commonly used for CN calculations, while a λ of 0.05 was recommended by Hawkins (1993) and Hawkins et al. (2002) for general application. In this study values for λ of both 0.05 and 0.2 were used in CN computations to investigate the effect of this assumption on computed runoff values.

CN estimation for a specific area can be done either by using tabulated values as shown in NEH-4 Part 630, or by direct investigation using measured rainfall-runoff data from that area. NEH classifies soils into one of four Hydrologic Soil Groups (HSG) −A, B, C, or D, in order of increasing runoff − according to expected infiltration rates. Based on the cover type, hydrologic condition, % impervious area, and soil HSG, CN values are suggested by NEH. Because low-compaction mine spoils cannot be classified by one of the HSGs, direct estimation for CN was performed in this study by two methods. The first approach utilized the raw rainfall-runoff data following the method of Hawkins (1973), and the second performed a CN computation utilizing the asymptotic method, proposed by Hawkins (1993). The asymptotic method recombines rainfall and runoff data based on frequency matching to back-calculate CN values. Fitting of data was based on the least squares method, performed using SAS 9.3 and JMP 9.0 statistical software packages.

By having measured data for P and Q, the variable S can be determined by (Hawkins 1973). Equation (4) was used to calculate storage (S) values from different P- Q data pairs obtained by monitoring study plots. Using Eq. (5), the storage (S) values were converted to CN values for each study plot. The CN values can vary from 0 to 100, while S varies from 0 to ∞. A CN value of 100 shows maximum possible runoff potential.

$$S = [P + 2Q - (4Q^2 + 5PQ)^{0.5}] \quad \text{..... (4)}$$

$$S = \frac{25400}{CN} - 254 \quad \text{..... (5)}$$

The asymptotic method (Hawkins et al. 1993), a frequency matching method, is based on equating the return periods of rainfall and runoff events. It assumes that the data do not show a constant CN −which is true in most cases − but that a trend toward steady-state is recognizable, in which case using asymptotic least squares fitting can extend that trend to a constant value. As

the first step in this process, all precipitation events and runoff amounts are sorted separately in descending order. Each rainfall depth is then paired with its corresponding runoff amount in ranked position, a process called frequency matching, which does not necessarily associate the rainfall amount with its produced runoff (Hawkins 1993). This method causes a secondary relationship between CN and rainfall depth to emerge. Watersheds can be categorized into three groups based on these secondary relationships. These categories are (i) watersheds with Complacent Behavior, (ii) watersheds with Standard Response and (iii) watersheds with violent responses. Detailed description for each category can be found in Hawkins et al, 1993.

Watersheds with standard response behavior are those whose CN values tend to decline and then approach a constant value with increasing P; that constant value defines the P-independent CN. Equation (6) has been found to fit P-CN data sets, where CN_∞= constant value approached as P $\rightarrow \infty$, and K = fitting constant. This approach has been found to work well for a variety of watershed data sets (Hawkins et al, 1993).

$$CN(P) = CN_\infty + (100 - CN_\infty) \cdot \exp(-K_1 P) \quad \text{(6)}$$

The asymptotic method may be enhanced by incorporating the effect of rainfall distribution on the CN value, or in other words by using a measure of rainfall intensity instead of precipitation depth. The traditional asymptotic method assumes that rainfall amount is evenly distributed over the event duration and uses P to match frequencies. Rainfall intensity simultaneously represents both rainfall depth and its time variation, so can provide a more meaningful relationship.

Because CN method runoff estimations are usually for the purpose of sediment transport modeling or design of detention basins, the 30-minute rainfall intensity (I_{30}) as defined by the Universal Soil Loss Equation (USLE) (Wischmeier and Smith 1965; 1978) or its more modern

offspring the Revised Universal Soil Loss Equation (RUSLE) (Renard et al., 1997), may be a good candidate for an intensity value to replace the rainfall depth in an enhanced asymptotic method. For each rainfall event, using the 5-min rainfall depths that were recorded by the tipping bucket raingages and an energy-intensity relationship from Renard et al. (1997), the storm erosivity (I_{30}) can be computed. To incorporate the effect of rainfall distribution over time in estimating an independent CN, the same asymptotic frequency match method can be used, but with storm erosivity (I_{30}) instead of storm rainfall depth. This method was conducted in two ways: 1) replacing sorted P measurements as used in the original method with their corresponding I_{30}; and 2) sorting rainfall I_{30} and runoff depths separately and then realigning the pairs on a ranked-order basis to form I_{30}-Q pairs of equal return periods. The individual runoffs were not necessarily associated with the original causative rainfall I_{30}.

The Antecedent Moisture Condition (AMC) is defined as the soil moisture prior to a precipitation event, and affects runoff generation and as a result the estimated CN for that event. Typically, there are three defined AMC conditions: dry (AMC I), average (AMC II), and wet (AMC III). Based on NEH-4 (1964), the median CN that divides the rainfall-runoff plot into two roughly equal portions is associated with AMC II, while AMC I and AMC III are defined based on the lower enveloping CN and upper enveloping CN, respectively. Plotting AMC curves on a rainfall-runoff graph is a trial and error process. An initial value for CN is assumed and that value is used with Equations (1), (2), and (5) to construct a CN curve on a rainfall-runoff plot for different initial P values. This process continues until a desirable curve is achieved (Figure 6). Based on the location of data points in relation to AMC curves, the related AMC for each of the computed CNs can be determined. Points are then given the AMC label of the nearest AMC curve. The AMCs provide an insight about average moisture condition of loose-dumped spoil

before rainfall events occur. CN values in this study were not adjusted based on the AMC condition, but the AMC conditions were reported for reference (Table 3).

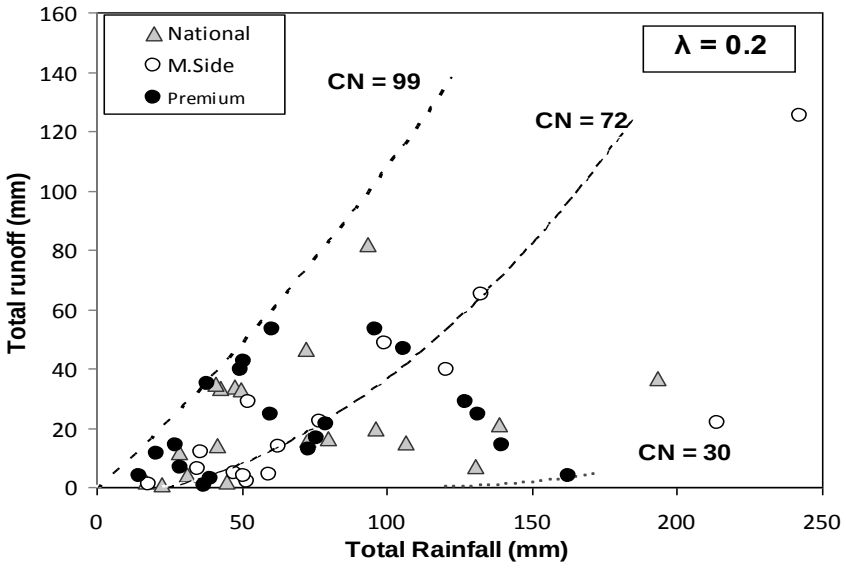

Figure 6. Observed rainfall – runoff data points in relation to median AMC II CN (CN=70) and enveloping CN curves (AMC I and III).

4.3 Results and Discussion

4.3.1 Hydrologic Data

A total of 60 sampling measurements were obtained from June 2009 through July 2010, in which six measurements were deemed to be outliers, falling three standard deviations [σ] or more from the mean. Table 2 summarizes the remaining 54 rainfall-runoff events from the three study sites that were used to estimate a CN. The cumulative rainfall duration for a sampling event varied from 3.6 to 104.4 hr, the cumulative rainfall depth varied from 14.6 mm to 242.6 mm with an average of 75.34 mm, and the 5-minute rainfall intensity varied from 7.5 mm/hr to 133.1 mm/hr, with an average of 54.0 mm/hr. Because high intensity and short duration storms were typical during the summer months at the study sites, rainfall intensities during a 5-min

window were calculated to better illustrate event intensity. As shown in Table 2, study sites experienced storm events with a variety of rainfall depths, durations, and intensities during the one-year monitoring period, providing sufficient data for estimating a representative CN for steep-sloped, low compaction reclaimed surfaces for which ground cover was not yet been established.

4.3.2 CN and Initial Abstraction coefficient

Using $\lambda = 0.2$, single-storm CN values for the Premium site ranged from 30.7 to 98.8 with a mean of 76.3 and σ of 19.5 (Table 3). CN values for the National site ranged from 40.5 to 97.8 with a mean of 76.0 and σ of 19.0; and for the Mountainside site they ranged from 34.0 to 89.5 with a mean of 70.6 and σ of 13.5. CN values using a $\lambda = 0.05$, also presented in Table 3, were generally observed to be lower and more variable than those based on $\lambda = 0.2$. Hawkins et al. (2002) also note that CN estimates based on $\lambda = 0.05$ will be lower than for $\lambda = 0.2$. Results from this study indicate a $\lambda = 0.2$ provides a better fit to the data and appears to be more appropriate for use in hydrology computations for steep, low-compaction reclaimed mine lands.

The resulting CN values in Table 3 can be compared to CN values listed in NEH Part 630, for different Hydrologic soil groups. For fallow bare soil and $\lambda = 0.2$, NEH CN values are 77, 86, 91, and 94 for soils with respective HSG A, B, C, and D. The mean CN values calculated based on Equations (4) and (5) for different sites suggest that the loose-dumped waste material from steep-sloped reclaimed mine sites has hydrologic properties most similar to HSG A. Comparison with HSG D that Meadows and Blandford (1983) reported for low-gradient highly-compacted reclaimed sites, shows a 19% reduction in CN value for low compaction slopes due to a decrease in compaction level and the resulting increase in infiltration rate. While previous studies reported

Table 2. Rainfall event data summarized for the Premium, National, and Mountainside study sites by collection date, and cumulative depth in mm, cumulative duration in hr, and maximum 5-min intensity (mm/hr).

No.	Site	Sampling Date	Cum. Rainfall Depth, (mm)	Cum. Rainfall Duration,(hr)	Max 5 min. Intensity, (mm/hr)
1	Premium	June 24, 2009	38.1	17.5	31.5
2		July 17, 2009	127.3	44.9	75.0
3		August 3, 2009	106.1	48.0	39.0
4		August 13, 2009	20.8	5.6	37.5
5		August 24, 2009	75.9	28.0	82.5
6		September 22, 2009	162.9	99.0	67.5
7		October 1, 2009	96.0	25.0	79.5
8		October 13, 2009	60.3	51.8	40.5
9		October 20, 2009	73.4	48.2	19.5
10		October 27, 2009	37.3	21.5	18.0
11		November 3, 2009	14.6	17.8	9.0
12		November 24, 2009	49.8	43.8	10.5
13		December 3, 2009	39.3	30.8	27.0
14		December 17, 2009	139.8	31.3	42.0
15		March 24, 2010	50.625	32.3	22.5
16		May 7, 2010	131.5	64.4	105.0
17		May 18, 2010	27.375	4.4	43.5
18		June 8, 2010	60.625	14.2	54.0
19		June 25, 2010	29.125	5.4	31.5
20		July 20, 2010	79.125	17.8	52.5
21	National	June 25, 2009	96.1	12.8	114.0
22		July 15, 2009	72.6	11.0	100.4
23		August 14, 2009	47.6	11.0	111.0
24		September 25, 2009	138.8	104.4	43.5
25		September 29, 2009	49.5	14.9	36.0
26		October 8, 2009	41.3	33.5	45.0
27		October 22, 2009	106.3	94.6	81.0
28		October 29, 2009	22.1	15.3	9.0
29		November 5, 22009	31.3	16.8	21.0
30		November 12, 2009	16.9	13.6	7.5
31		December 1, 2009	44.9	35.6	16.5
32		December 14, 2009	130.6	52.7	33.0
33		March 19, 2010	42.75	21.1	19.5
34		April 13, 2010	72.25	26.1	52.5
35		May 7, 2010	193	59.7	49.5
36		May 19, 2010	41	5.8	111.0
37		June 23, 2010	79.5	14.5	87.0
38		June 29, 2010	28.5	4.3	72.0
39		July 16, 2010	93.245	10.4	109.4
40	Mountain Side	July 2, 2009	132.8	3.6	54.4
41		July 14, 2009	62.6	21.9	75.6
42		July 27, 2009	214.0	28.8	101.3
43		September 22, 2009	120.7	75.8	86.2
44		October 13, 2009	59.6	33.8	65.0
45		October 20, 2009	51.7	70.6	33.3
46		November 3, 2009	36.0	21.3	13.6
47		December 1, 2009	18.1	14.6	10.6
48		December 10, 2009	99.3	35.3	24.2
49		December 14, 2009	35.0	8.8	10.6
50		March 26, 2010	77.1	37.1	54.4
51		May 13, 2010	242.6	57.3	66.5
52		May 18, 2010	47.5	7.3	98.3
53		June 8, 2010	52.7	7.8	83.2
54		June 25, 2010	50.5	6.8	133.1

Table 3. Curve number computations summarized for the Premium, National, and Mountainside study sites by collection date, AMC, and λ. Per collection date, measured rainfall and runoff depths (mm) and maximum I_{30} (mm/hr) are also reported for reference.

Site	Date	D (mm)	$I_{30,\ max}$ (mm/hr)	Q (mm)	AMC	CN λ = 0.2	CN λ = 0.05
Premium	June 24, 2009	38.1	13.5	34.8	III	98.8	98.6
	July 17, 2009	127.3	51.5	28.8	II	57.4	44.3
	August 3, 2009	106.1	21.5	46.7	II	75.5	68.8
	August 13, 2009	20.8	10.0	11.1	III	95.5	94.1
	August 24, 2009	75.9	34.2	16.5	II	68.7	56.2
	September 22, 2009	162.9	31.0	3.8	I	30.7	13.4
	October 1, 2009	96.0	44.5	53.3	II	83.0	78.8
	October 13, 2009	60.3	23.2	24.6	II	83.1	77.5
	October 20, 2009	73.4	11.2	12.9	I	66.4	52.0
	October 27, 2009	37.3	8.7	0.6	II	64.9	38.1
	November 3, 2009	14.6	5.7	3.6	III	92.6	88.4
	November 24, 2009	49.8	5.5	1.8	III	96.3	37.6
	December 3, 2009	39.3	8.2	2.7	II	70.7	50.9
	December 17, 2009	139.8	19.7	14.1	I	44.0	27.1
	March 24, 2010	50.625	16.0	42.5	III	97.1	96.5
	May 7, 2010	131.5	22.7	24.6	I	53.4	39.1
	May 18, 2010	27.375	20.0	14.0	III	93.7	91.8
	June 8, 2010	60.625	32.5	53.4	III	97.5	97.0
	June 25, 2010	29.125	13.2	6.6	II	85.5	77.7
	July 20, 2010	79.125	23.0	21.0	II	71.0	60.3
National	June 25, 2009	96.1	40.5	19.7	II	62.5	48.9
	July 15, 2009	72.6	51.5	16.0	II	69.8	57.6
	August 14, 2009	47.6	37.0	34.0	III	94.7	93.5
	September 25, 2009	138.8	30.2	21.0	I	48.9	33.6
	September 29, 2009	49.5	17.5	32.7	III	93.3	91.7
	October 8, 2009	41.3	20.2	14.3	II	85.7	80.1
	October 22, 2009	106.3	37.5	15.1	II	54.8	38.6
	October 29, 2009	22.1	4.2	1.2	II	79.8	61.6
	November 5, 2009	31.3	10.5	4.2	II	80.1	67.3
	November 12, 2009	16.9	6.5	1.84	II	87.0	76.4
	December 1, 2009	44.9	11.7	1.81	II	64.4	41.0
	December 14, 2009	130.6	12.0	7.3	I	40.5	21.8
	March 19, 2010	42.75	12.2	33.5	III	96.5	95.8
	April 13, 2010	72.25	21.7	46.4	III	89.8	87.4
	May 7, 2010	193	24.0	36.9	I	44.2	30.9
	May 19, 2010	41	41.2	34.8	III	97.8	97.4
	June 23, 2010	79.5	20.2	16.7	II	67.1	54.2
	June 29, 2010	28.5	17.2	11.8	III	91.4	88.2
	July 16, 2010	93.245	33.5	82.0	III	96.1	95.5
Mountain Side	July 2, 2009	132.8	16.4	64.8	II	74.0	67.7
	July 14, 2009	62.6	48.1	13.5	II	72.5	60.7
	July 27, 2009	214.0	62.0	21.8	I	34.0	19.6
	September 22, 2009	120.7	35.3	39.3	II	65.8	55.8
	October 13, 2009	59.6	33.0	4.3	II	61.8	41.3
	October 20, 2009	51.7	13.4	1.9	II	60.7	36.8
	November 3, 2009	36.0	9.3	11.8	III	86.6	81.0
	December 1, 2009	18.1	7.3	0.8	II	82.3	64.8
	December 10, 2009	99.3	11.6	48.5	II	79.2	73.7
	December 14, 2009	35.0	9.3	6.2	II	80.7	69.8
	March 26, 2010	77.1	15.9	22.3	II	72.9	63.1
	May 13, 2010	242.6	36.8	125.3	II	63.1	56.0
	May 18, 2010	47.5	40.6	4.6	II	69.5	51.7
	June 8, 2010	52.7	39.3	28.5	III	89.5	86.6
	June 25, 2010	50.5	40.8	3.7	II	65.7	69.8

CN ranging from 83 to 97.5 for highly-compacted low-gradient reclaimed sites (Meadows and Blandford 1983; Schroeder et al. 1987; Ritter and Gardner 1991; Bonta et al. 1997), this study found the average CN to be in the range of 70.6 -76.3, with at least a 15% reduction in CN values, perhaps due to the lower level of compaction in this study. This study reflects runoff estimates from high-gradient slopes with intense rainfalls events, where a wide range of runoff events were generated (0.6 -125.3 mm). In contrast to the study of Taylor et al. (2008), it appears that in this study the steep-sloped reclaimed sites with loose spoils considerably increased infiltration rates, causing less runoff.

4.3.3 CN and Precipitation Depth

The CN distribution in relation to precipitation depth for each study site was investigated, with results shown in Figures 7 and 8. All three sites had similar runoff responses to rainfall events. The Mountainside site reported a lower R squared due to one extreme data point (P = 242.6 mm and CN = 63.1) related to the 09/13/2010 sampling event. Although this data point was not an outlier (2.37 σ from the mean), its high rainfall depth increased variation in the regression model. So, if two σ from mean are considered as the lower bound for outliers, then this point would be excluded and the R^2 for Mountainside site would be 49% ($\lambda = 0.2$), close to what was computed for the other two study sites. Four out of the six total outliers were measured at the Mountainside site, and they were related to the early monitoring period in June 2009 during high-intensity storm events (P= 150-200 mm). During that period, the sediment and runoff collection system at Mountainside site failed to capture the generated runoff from one of the events, but the monitoring system was reconstructed for that site, explaining the gap in Mountainside's data in Figures 7 and 8.

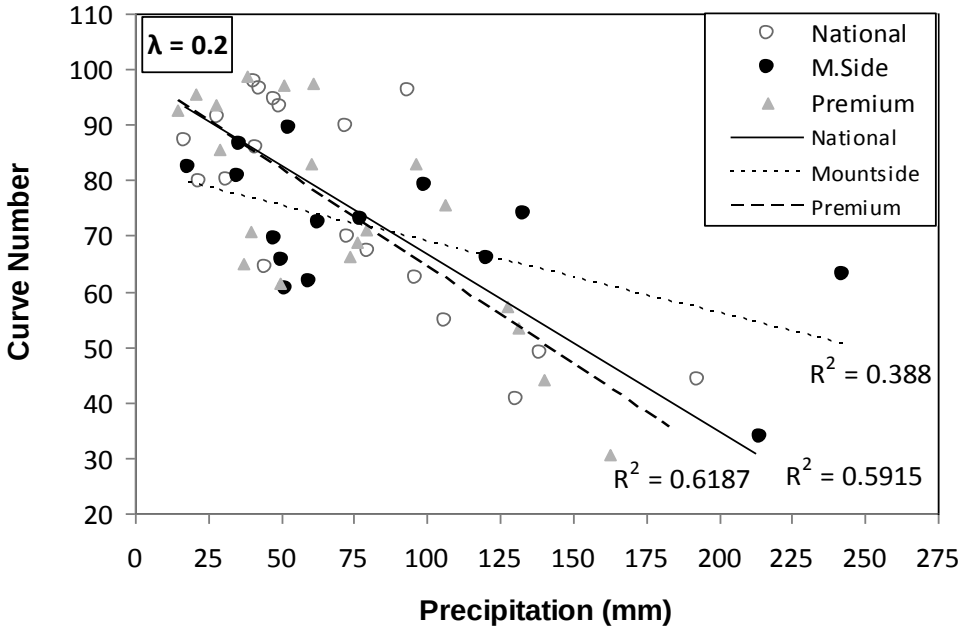

Figure 7. Curve numbers for each of the three sites in relation to precipitation amounts for λ = 0.2.

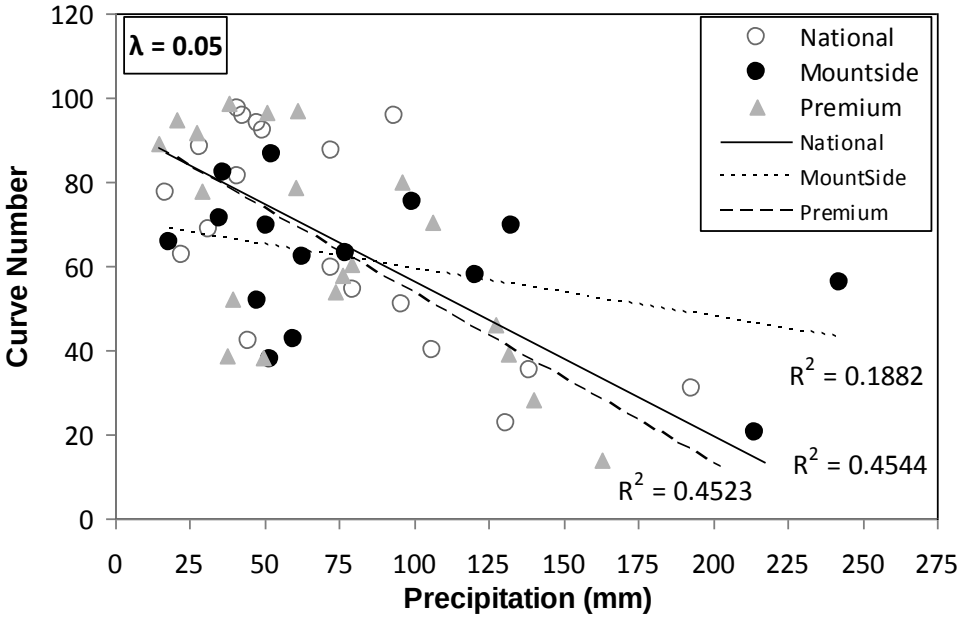

Figure 8. Curve numbers for each three sites in relation to precipitation amounts for λ = 0.05.

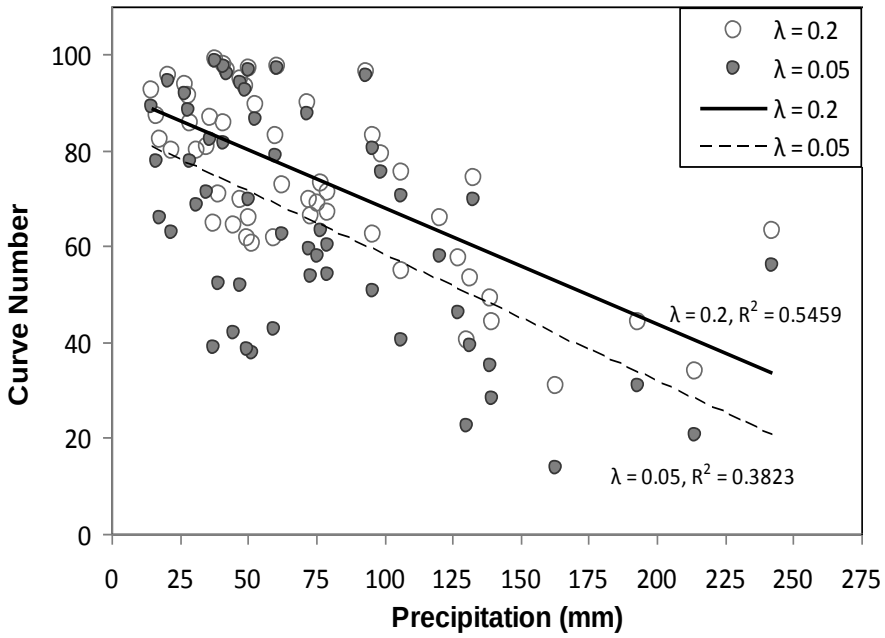

Figure 9. Curve numbers for the combined three sites in relation to precipitation amounts for λ = 0.2 and 0.05.

Using a t-test, the hypothesis that the CN means for the three study sites are statistically different was rejected at the 5% significance level, so the CN values from the three sites were combined and compared against their corresponding precipitation depths (Figure 9). Using λ = 0.2, CN calculation result in less variation than did λ = 0.05, which suggests that using 0.2 for initial abstraction may give a better estimates for low compaction spoils on steep slopes.

CN and precipitation depth were inversely correlated, with higher CN estimates for smaller precipitation depths ($r = 0.77$, $p = 0.05$), as shown in Figures 7 and 8. This phenomenon was first observed by Sneller (1985) and then noted by Hawkins (1993) and Hjelmfelt (1996). They attribute this phenomenon to several factors, including data censoring, hydrologic partial area effects, and basic error in the model or data. Data censoring results from excluding all rainfall events without direct runoff from the data sets to assure $P \geq 0.2S$, and to meet the

requirements that100 / (1+P/2) < CN < 100. On the other hand, Hawkins (1993) states "to the extent that any CN is manifested at low rainfalls, for which there are many storms, they would by definition predict high CNs".

Frequency distributions of CN estimates were compared for λ values of 0.2 and 0.05, utilizing data summarized from all three sites and categorized within 14 sub-groups (Figure 10). The CN frequency distribution for λ = 0.2 showed a near uniform distribution except for lower CN values below 40, while the distribution for λ of 0.05 showed a higher tendency toward mid and high CN values. To note, 78% of the CN values were higher than 51 for λ = 0.2, while 81% of CN values were higher than 61 for λ = 0.05, with the maximum occurrence between 61 and 65. Based on Hawkins' (1993) contention that a λ = 0.05 produces greater consistency for practical runoff estimation applications, a CN value for the low-compaction steep-sloped reclaimed spoils should be approximately 61-65 (Figure 10).

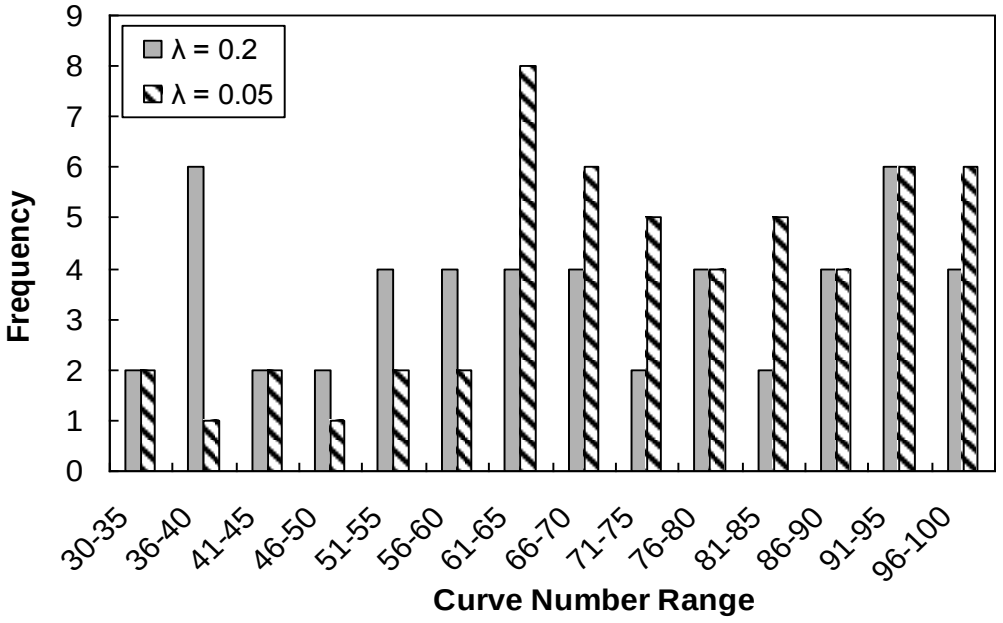

Figure 10. Frequency distribution of curve numbers for combined data from all study sites, comparing CNs for λ = 0.2 and 0.05.

4.3.4 CN Asymptotic Method

In Figure 11, CN estimates obtained from original rainfall-runoff data were compared with CN estimates calculated using frequency matched rainfall-runoff data. The size of each data point's bubble was scaled based on its corresponding rainfall intensity, where a larger bubble size represents higher storm rainfall intensity. The plot displays a standard asymptotic response using frequency matched rainfall-runoff data. CN estimates calculated using frequency matched data were more strongly correlated to precipitation depth ($R^2 = 0.88$), than were CN values obtained from the original data ($R^2 = 0.52$). The frequency match method considerably reduces CN estimate variation.

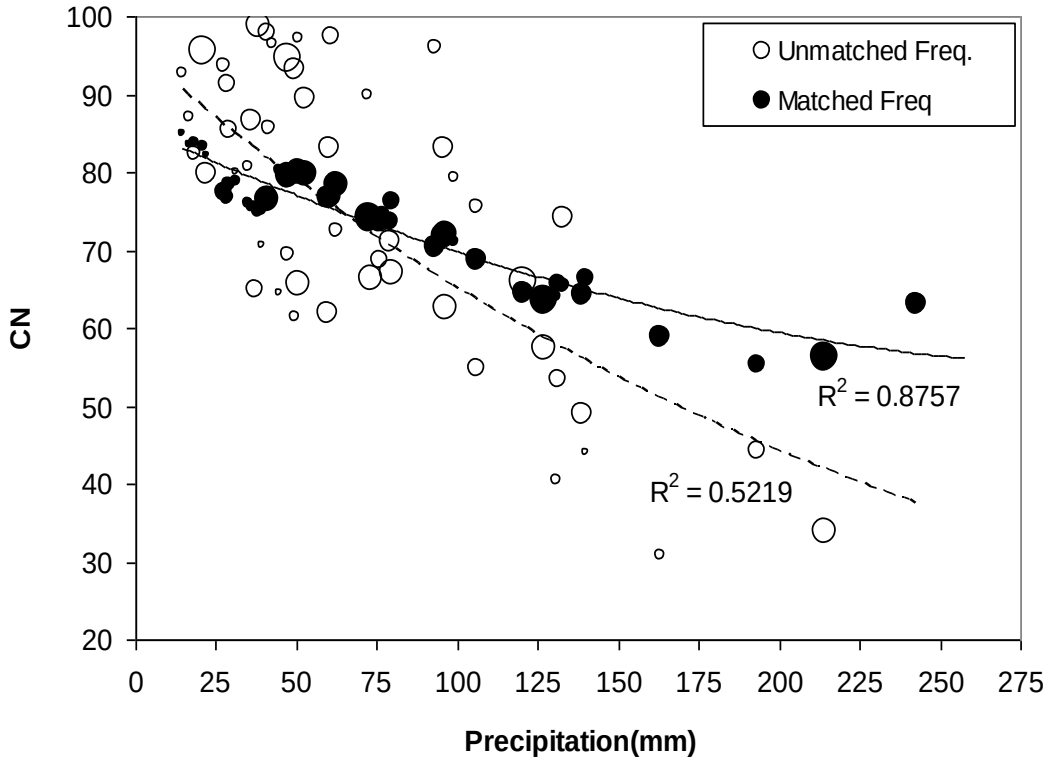

Figure 11. Original CN compared with ones obtained from matched frequency methods.

4.3.4.1 CN and P-Q Freq. Match

The best-fit exponential curve to the CN estimates for $\lambda = 0.2$ obtained from frequency matched rainfall-runoff data is shown in Figure 12 ($R^2 = 0.80$). The equation for the fitted curve follows:

$$CN(P) = 58.5 + (100 - 58.5)\exp(-0.02253\ P) \quad \text{..... (7)}$$

The CN_∞ was equal to 58.5, which is thus the P-independent CN value for steep-sloped low compaction reclaimed mine lands. This result was consistent with CN frequency distributions as shown in Figure 10, which suggests that CN estimates should be above 50 with an expected value of about 60.

For steep-sloped low-compaction reclaimed mine lands, the P-independent CN value was compared to CN values listed in NEH Part 630 for different HSGs. This comparison suggests that low-compaction spoils have hydrologic properties better than a soil of HSG A with the bare conditions (CN = 77).

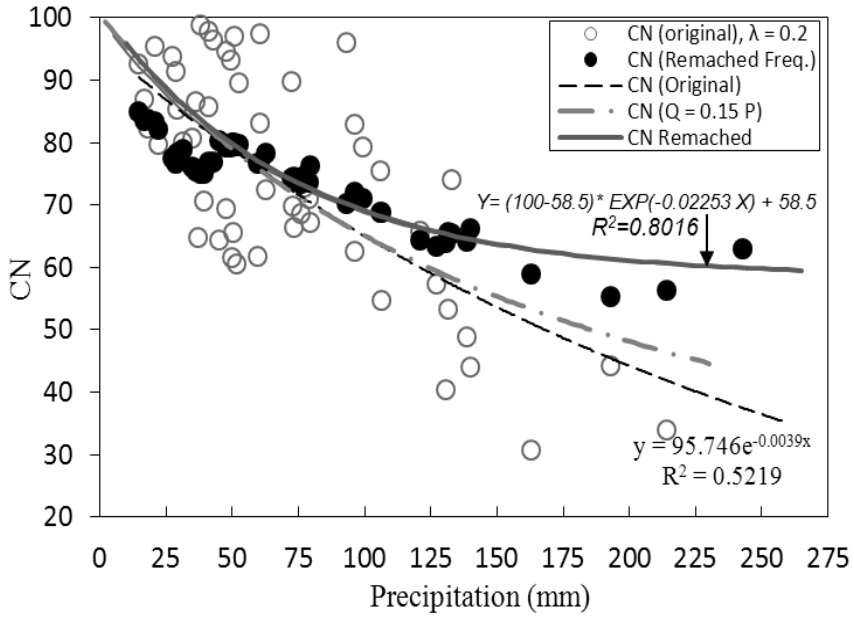

Figure 12. Best fit exponential curve for P-Q matched frequency pairs and $\lambda = 0.2$.

Previous studies on highly-compacted, low-gradient reclaimed sites reported CN values ranging from 83 to 97.5 (Meadows and Blandford 1983; Schroeder et al. 1987; Ritter and Gardner 1991; Bonta et al. 1997), so the simultaneous effect of increased slope gradient and reduced compaction appears to have resulted in at least a 29.5% reduction in CN value. The asymptotic method using the P-Q Frequency Match appears to provide a reasonable estimate for a CN value on low-compaction steep-sloped material (CN_∞ = 58.5).

4.3.4.2 CN and I_{30} -Q Freq. Match

Estimating CN values based on the I_{30} frequency match was done in two ways, 1) replacing the sorted rainfall depths (P) used in the original method with their corresponding I_{30} values, and 2) the rainfall I_{30} values and the runoff depths are sorted separately and then realigned on a ranked-order basis to form I_{30}-Q pairs of equal return periods. The individual runoffs are not necessarily associated with the original causative rainfall I_{30} values. Results of these new approaches and also the fitted curve to the CNs obtained from rainfall and the runoff depths sorted separately and then realigned on a ranked-order basis to form I_{30}-Q pairs of equal return periods are shown in Figure 13. Of the two methods, Method 2 resulted in less variation in calculated CN values than method 1, so the curve fitting was completed for CNs plotted from Method 2 (Figure 13). The curve fitting was accomplished with the same mathematical format as that of Eq. 6. The equation for the fitted curve is as follows:

$$CN(P) = 60 + (100 - 60)\exp(-0.05\,P) \quad \text{..... (8)}$$

The CN_∞ was equal to 60 (R^2 = 0.79). This CN value was 1.025 times that obtained from curve fitting the CNs calculated based on the P-Q frequency match data. Both frequency match methods cause reduction in CN variation. The asymptotic method that used rainfall I_{30} described the variation within observed data as well as the traditional asymptotic method described earlier.

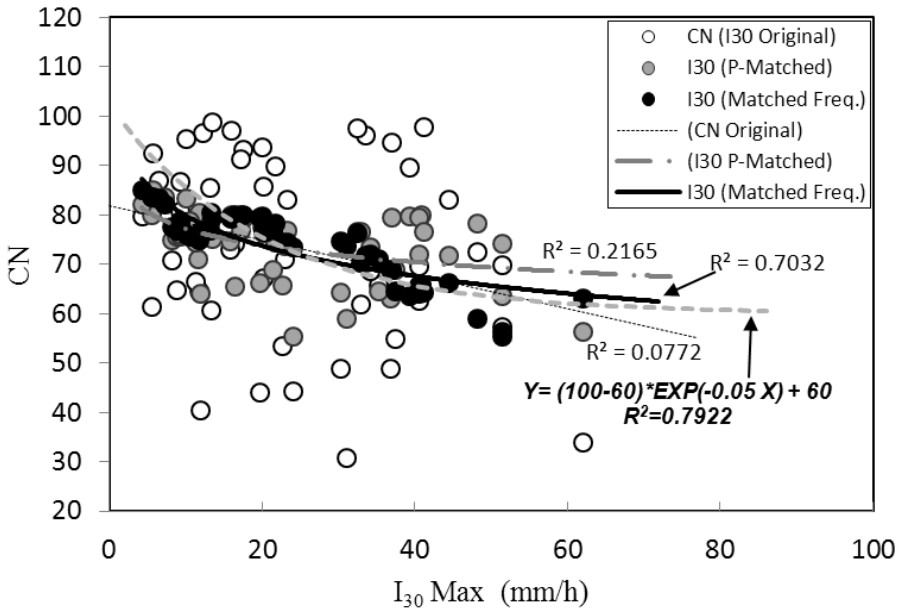

Figure 13. Best fit exponential curve for I_{30}–Q matched frequency pairs and $\lambda = 0.2$.

In this study, incorporating rainfall distribution in the asymptotic method didn't affect estimation of the P-independent CN value. This result was not conclusive and further investigations on watersheds with different rainfall distribution, land use, and level of compaction may lead to a better understanding of this new approach. Both frequency match methods suggest a CN value of around 58.5 ~ 60 for low-compaction reclaimed mine spoils on steep slopes.

The question then arises as to how the CN values found for this study should be adjusted to fit other locations of interest also using the FRA approach, but perhaps with greatly different soils. It is suggested that a correction factor be calculated using a standard infiltration test (e.g., ASTM D3385) on a series of oven-dried undisturbed samples to estimate surface water storage (S) for the waste material on reclaimed surface of interest. Using the following formula, a correction factor (α) can be calculated for a CN in the suggested range of 58.5 ~ 60:

$$\alpha = \frac{Storage\ calculated\ for\ a\ specific\ CN\ in\ range\ of\ 58.5{\sim}60\ using\ Eqn.\ (5)}{Average\ of\ estimated\ surface\ storage\ values\ for\ undisturbed\ samples}$$

If the estimated storage for location of interest is lower than what is estimated from this study, then $\alpha < 1$ and a lower CN value should be used; $\alpha > 1$ indicates that a higher CN value is required for the location of interest; and $\alpha = 1$ indicates that the suggested range of CN value is valid for the location of interest.

4.4 Conclusions

While the CN method is traditionally used to predict runoff from ungaged watersheds, the lack of CN values for low-compaction steep-sloped reclaimed mine surfaces has been an issue for mine operators and regulatory agencies. This study estimated CN values for low-compaction steep-sloped reclaimed surfaces in the Appalachian coal mining region by using natural precipitation-runoff data and utilizing both standard techniques and the asymptotic method as described by Hawkins (1993). Results showed that the differences due to spatial variation in rainfall and use of different reclaimed material between the original CN means estimated for three different study sites were not statistically significant. Both asymptotic methods – that based on Hawkins (1993) and its modified version which uses I_{30} instead of P − suggest a standard asymptotic behavior for the study sites, with P-independent CN values around 58.5~60. Determining a CN value for low compaction reclaimed surfaces is important, as it can be used to estimate runoff for adequate design of on-site retention basins and other BMPs for sediment erosion control. The US department of interior, Office of Surface Mining, OSM, and mining consultants use CN value for their SEDCAD designs of detention ponds and other practices, so the results from this study provide SEDCAD users better model input data. Furthermore, this new information supports re-vegetation efforts of the surface mined lands. Growth of vegetation on reclaimed slopes reduces runoff speed and increases chance of infiltration, which in turn reduces the runoff production on slopes and may decrease the estimated CN values.

Chapter 5

Erosion and Sediment Delivery of Low-Compacted Reclaimed Slopes

Hoomehr S., J.S. Schwartz, S.C. Yoder, E.C. Drumm, W.C. Wright. "Erodibility of low-compaction steep-sloped reclaimed surface mine lands in southern Appalachian region, USA." *Journal of Hydrological Processes.* Under Review.

5.1 Introduction

Improving reclamation approaches on surface coal mining sites is essential in order to reduce environmental impacts from excessive erosion in mountainous regions (Carroll et al., 2000; Harms and Chanasyk, 2000; Nicolau, 2002; Espigares et al., 2011; Fox, 2009). Improvements have occurred over time through an integration of science and policy, utilizing valuable information from studies relating spoil erodibility with physical site conditions. In the US, surface mining reclamation is mandated by the Surface Mining Control and Reclamation Act of 1977 (SMCRA), and regulated by the US Department of Interior, Office of Surface Mining (OSM). From the 1980s through 1990s, reclamation on coal mining sites in the Appalachian region consisted of back-to-contour compacted spoil placement to create stable steep slopes, which were then vegetated with moisture competitive grasses and tolerant black locus (*Robinia pseudoacacia*) trees (Dickens et al., 1985). Studies showed it was difficult to regenerate forests with a diversity of native species when spoils and top soil placement on reclaimed mine sites were compacted (Torbert and Burger, 1994; Thomas et al., 1999; Angel et al., 2006). In order to mitigate these impacts, more recently OSM has promoted the Forest Reclamation Approach (FRA) for constructing back-to-contour placement, utilizing minimally-compacted spoils in order to enhance reforestation success and improve long-term forest ecosystem health (Angel et al., 2005; Sweigard et al., 2007). This technique focuses on leaving a surface layer of about 1.5 m thick of loose spoil, leveling with the lightest equipment available with as few passes as

possible under dry conditions. SMCRA also mandates back-to-contour spoil placement to approximate natural slopes, which in the Appalachian region exceed 20% in many locations, and typically are on the order of 30 to 35%. Without achieving vegetative cover immediately following loose spoil placement on steep slopes, there is great potential for excessive erosion and reduced slope stability (Jeldes et al., 2010). Assessing whether FRA can be successfully applied on steep slopes is a critical research need, as is quantifying sediment yields from FRA sites. Such information on sediment yields will support improved designs of best management practices (BMPs) for mining site erosion control.

The susceptibility of surface mining reclamation sites to soil erosion has often been quantified in terms of erodibility, defined by the K factor in the Revised Universal Soil Loss Equation (RUSLE) (Mitchell et al., 1983; Barfield et al., 1983; McIntosh et al., 1993; Bonta, 2000). Developed originally from agricultural plots, RUSLE is the revised version of Universal Soil Loss Equation (Wischmeier and Smith, 1965, 1978) and has widespread use in predicting long-term average annual soil loss per unit area (Renard et al., 1997). RUSLE has the utility to estimate soil loss for varying soil properties, land condition, and management practices. Toy et al. (1999) indicated that RUSLE is applicable for surface mining reclamation sites, although K factor estimates deviate from the original studies and equation development due to the presence of large rock fragments and dynamic consolidation. Nonetheless, the K factor has been commonly used to characterize erodibility of reclamation site spoils, and the SEDCAD™ model which incorporates RUSLE is commonly used to predict sediment yields from proposed surface mining sites (Warner et al., 1998).

Previous studies estimating K factors for reclamation site soils have included both small-scale rainfall simulation plots and large-scale field sites under natural rainfall conditions.

Mitchell et al. (1983) studied erodibility on reclaimed material consisting of compacted loam and silt loam for two field plots in western Illinois and one in southern Indiana with 5% slopes. Rainfall simulations used an intensity of 64 $mm \cdot h^{-1}$, and resulting K factors were reported in the range of 0.21 to 0.65 $t \cdot ha \cdot h \cdot ha^{-1} \cdot MJ^{-1} \cdot mm^{-1}$. Under natural rainfall, McIntosh and Barnhisel (1993) estimated erodibility of reclaimed mine soils on 9% slopes in eastern Kentucky. Consisting of silt loam topsoil and subsoil, and overburden spoils of a mixture of shale, siltstone, and sandstone, K factors for these mine soils were estimated as 0.046, 0.067, and 0.051 $t \cdot ha \cdot h \cdot ha^{-1} \cdot MJ^{-1} \cdot mm^{-1}$, respectively. Hartley (1982) found reclaimed compacted soils under natural rainfall condition to have a K factor of 0.43 $t \cdot ha \cdot h \cdot ha^{-1} \cdot MJ^{-1} \cdot mm^{-1}$. In general, soil erosion as a function of erodibility appears to be highly variable depending on particle size composition, organic matter, and clay content (Wischmeier and Mannering, 1969; Torri et al., 1997; West and Wali, 1999). Also, soil erodibility varies with antecedent moisture and with freezing and thawing cycle (Mutchler and Carter, 1983). Previous studies have not investigated erodibility on steep-sloped, loose spoil conditions, but they do provide useful information in order to generally compare with results from this study.

Although a focus of this research was on determining erodibility, a general understanding of erosion behavior and sediment yields from low-compaction steep-sloped reclaimed sites was needed. Several studies reported erosion rates on surface mining reclamation sites, providing a means to compare differences in soil and land conditions per site. In contrast to erosion rates, which often cannot be compared across sites because of variable rainfall applications, erodibilities of different sites can be compared as they contain both soil medium and experienced rainfall erosivity effects (Gilley et al., 1977; Hartley, 1982; Barfield et al., 1983; Carroll et al., 2000). Two studies found that bare mine spoils eroded less than bare topsoil and subsoil. Gilley

et al. (1977) used rainfall simulators on varying slopes from 4.6% to 17.0% in western North Dakota, in which mine spoils yielded 18 $t \cdot ha^{-1}$ and loam topsoil yielded 74 $t \cdot ha^{-1}$. In eastern Kentucky, Barfield et al. (1983) investigated sediment yields on field plots with rainfall simulators for topsoil, subsoil, and shale mine spoils, and the effects of compaction on erosion rates. They found average erosion rates of 0.92, 0.85, and 0.32 $t \cdot ha^{-1}$ for topsoil, subsoil, and shale mine spoils, respectively. In addition, they found higher erosion rates for compacted topsoils and spoils compared with tilled surfaces, although rate differences were small for shale spoils in contrast to topsoil (Barfield et al., 1988). Expressed as soil loss per unit of erosivity (which is the definition of K), erosion rates for compacted spoils were 1.28 times larger than those for tilled soils, whereas for compacted topsoil the erosion rate was found to be 2.5 times greater than tilled. Relevant to this study, Curtis and Superfesky (1977) estimated an erosion rate on compacted spoils from a steep-sloped coal surface mine site in East Tennessee as 526 $t \cdot ha^{-1}$ over a 20 month period, with 90% of the soil loss occurring in the first year. They observed that rill development was a major source of soil loss from the mine site.

Others have also reported that rill development greatly influences soil loss from reclaimed surface mining sites, and as a result possibly the erodibility of material under the same erosivity, and they report that several factors control rill development, including: slope steepness, spoil size characteristics and bulk density, soil moisture, infiltration and runoff, surface hydraulic roughness, and vegetative cover (McKenzie and Studlick, 1979; Dickens et al., 1985; Hahn et al., 1985; Nearing et al., 1997; Carroll et al., 2000; Sheridan et al., 2000; Hancock et al., 2008; Smets et al., 2008; Taylor et al., 2009; Zhang et al., 2009; Espigares et al., 2011). Increases in rill erosion appear to be greatly influenced by increases in slope and rainfall intensity (Yao et al., 2008), although Berger et al. (2010) suggests that rainfall intensity has a greater influence than

does slope steepness. Precipitation volume and overland flow depth have also been suggested as key factors in rill development, exerting more influence than precipitation intensity (Nearing et al., 1997; Foltz et al., 2008). Spoil size characteristics indirectly influence overland flow depth by influencing infiltration, while percent of rock fragments also becomes a factor controlling rill development. Jean et al. (2000) found that surface runoff decreases with increased % rock fragments on slopes less than 9%, whereas runoff increased with increased % rock fragments on slopes of about 20%. Sediment yields from sites with large rock fragments appear to be greatly increased by steeper slopes, concentrating flow and forming rills (Hancock and Willgoose, 2004; Hancock et al., 2008). In general, rill control measures are more difficult to apply on steep slopes, where mulches and grass seed may be transported offsite prior to seed germination and root establishment (Dickens et al., 1985; Smets et al., 2008).

Objectives of this chapter were to estimate the soil erodibility K factor, and to estimate sediment yields and characterize erosion behavior for steep-sloped, low-compaction reclaimed surface mine lands. With the FRA emphasis promoted by OSM, understanding how to manage these mine lands immediately following reclamation construction is critical because bare soils represent the most vulnerable period prior to establishment of grass cover. In this part of study, erodibility was measured for bare soil conditions, and particle size distributions of transported sediment were characterized. K factors were determined over time as rills developed, and rill development was qualitatively noted during the study. Results from this study provide necessary input data for erosion and sediment delivery models, and generally support reclamation practices on surface coal mines.

5.2 Methods

5.2.1 Measurements for Runoff, Sediment Yield, and Rill Morphology

Runoff and sediment in each collection system were measured regularly based on rainfall event frequency and magnitude and system capacity. Measurements were taken on approximately every 10 days for each site from May 2009 through July 2010. Site monitoring was not possible during the winter months (mid-December to mid-March), when continuous temperatures below freezing caused ice formation in the sampling buckets. In addition, mountain road closures are common during winter conditions in the high-altitude areas of the Appalachian region.

Runoff volumes in each plot were estimated by measuring total depth of water and sediment in each bucket (Pinson et al., 2003). If the bucket was full, the total depth was considered as runoff depth for runoff volume calculation, while if the bucket was partially full, the depth of sediment was deducted from the total depth. For the partially-full bucket, the depth of rainfall that occurred since the previous sampling was deducted from the depth of water, because the buckets were not covered so part of water in the bucket was from direct precipitation. Evaporation from buckets was assumed negligible, as the samples were generally measured and collected soon after each event.

Sediment yield was measured by collecting coarse and fine sediment from the chevrons, 100-gal pre-sedimentation tank, and flow divider buckets. While most of the coarse sediment deposition occurred in the pre-sedimentation tank, there was also some deposition within the chevrons and flume. Sediment collected within the chevrons and flume was added to the amount from the pre-sedimentation tank. The coarse materials deposited within the tank, flume, and chevrons were completely mixed by shovel and a 5-gallon bucket of mixed material was taken as

a representative sample. The total amount of material was estimated by counting the number of 5-gallon buckets required to remove all the material. For the flow divider buckets, if coarse sediment was found within the bucket, the whole material was brought back to laboratory, dried using industrial ovens and then weighed. If the captured material within the bucket was fine sediment (clay or silt), each bucket was agitated for 45 sec. and immediate sub-sampling performed with 500 ml bottles moved from bottom to top of the bucket. The 500 ml bottles were also dried and then weighed to determine the amount of sediment in each bottle, and based on that the total weight of sediment in the bucket was estimated.

In order to document rill development that occurred on each of the study sites, six lateral cross-sections were surveyed across the four plots per study site. Rills were surveyed once with a GTS 800A robotic total station during September 2009, after the initial development period occurring through July 2009.

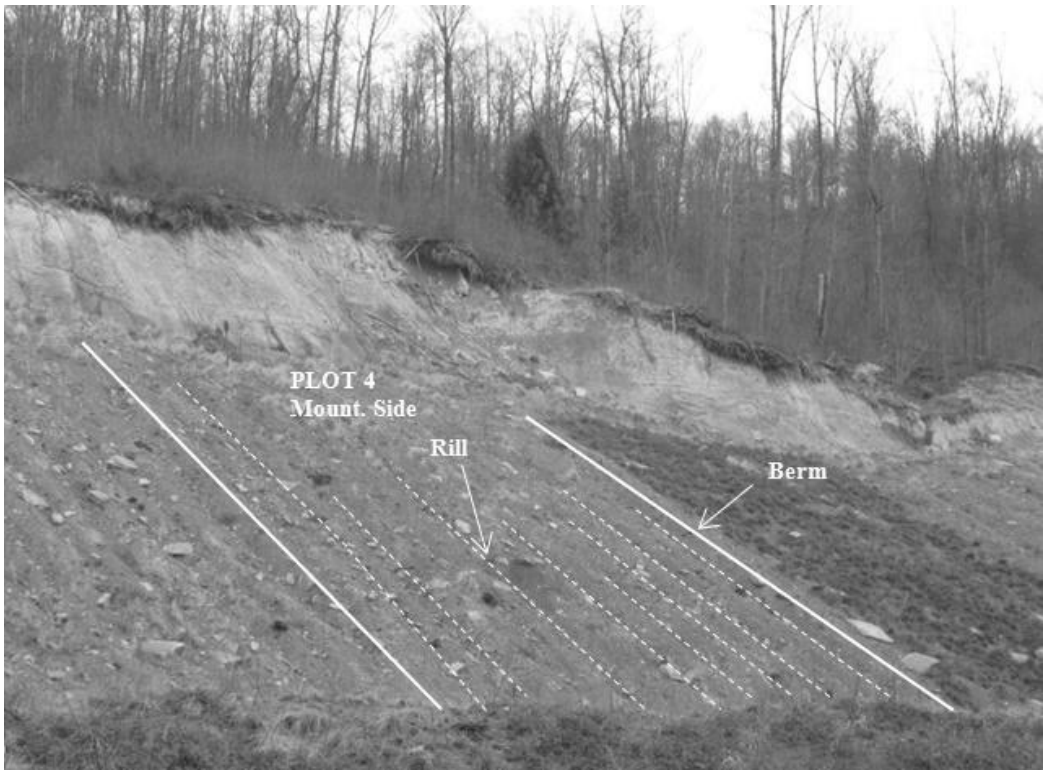

Figure 14. Rill development in Plot 4 at Mountainside study site, September 2009.

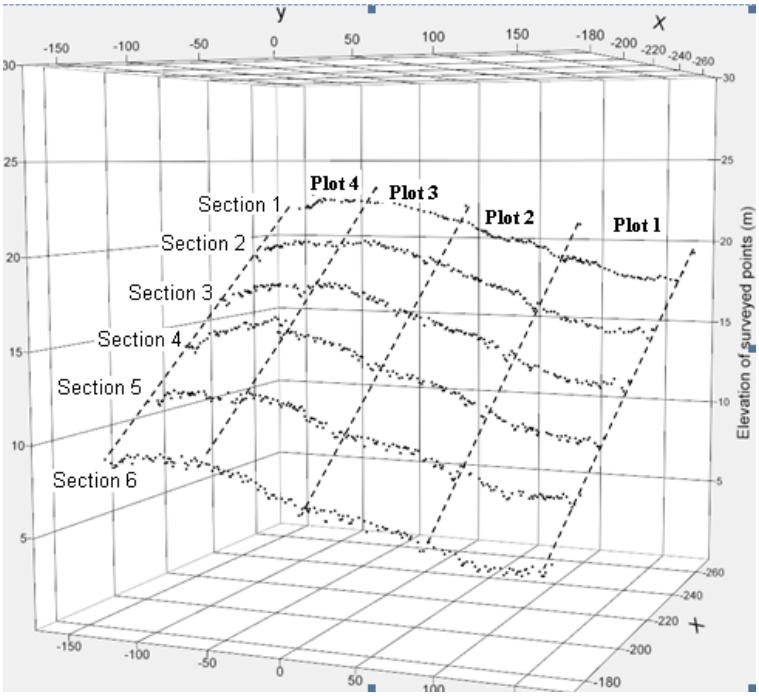

Figure 15. Illustration of rill morphology from survey of field plots at Mountainside study site, September 2009.

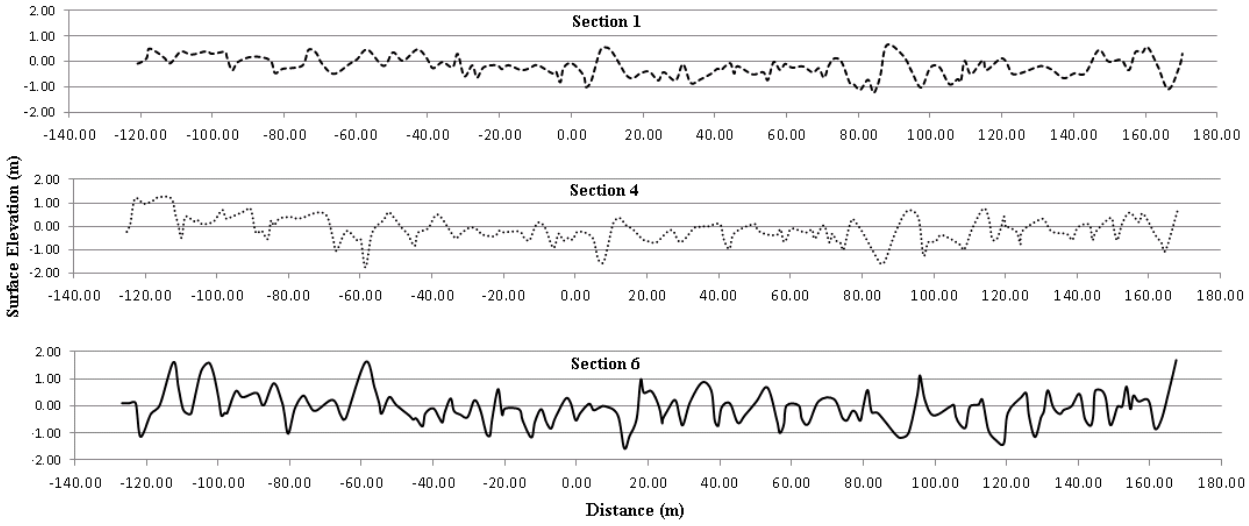

Figure 16. Surface elevations for three cross-sections illustrating rill morphology at Mountainside study site. Cross-section positions shown in Figure 15.

This study only presents results from the Mountainside study site because this effort was only to characterize the rills and document their presence (Figures 14, 15, and 16); no analysis was conducted with this data because the hypothesis regarding rill development was not part of the original study design.

5.2.2 Soil Loss Equation

RUSLE was used to estimate erodibility of reclaimed spoils without cover for each plot and averaged per study site (Wischmeier and Smith, 1978; SWCS, 1993, Renard et al., 1997). RUSLE estimates average annual erosion by the following equation:

$$A = R \cdot K \cdot LS \cdot C \cdot P \quad \ldots\ldots (1)$$

where,

A = amount of soil loss occurred (kg/m^2); R = rainfall and runoff erosivity factor; K = soil erodibility factor, soil loss rate per erosion index unit for a specified soil as measured on a standard plot (22.13 m length and 9% slope) under Unit Plot management conditions; LS = combined length-slope factor; C= cover management factor; and P = erosion control practice factor.

5.2.2.1 R Factor

Soil loss (A) is directly proportional to rainfall erosivity factor (R), based on the total storm energy (E) and the maximum 30-min intensity (I_{30}). The relationship between soil loss and EI_{30} is assumed to be linear, and individual storm parameter values are directly additive. Summation of EI_{30} values for a period shows the rainfall erosive potential during that period. Brown and Foster (1987) equations were used to compute rainfall energy (e_m) in this study as follows:

$$R = \frac{\sum_{i=1}^{n} EI_{30}}{N} \quad \text{..... (2)}$$

$$E = \sum e_m \times d_j \quad \text{..... (3)}$$

$$e_m = 0.29[1 - 0.72\exp(-0.05 i_m)] \quad \text{..... (4)}$$

where,

e_m has units of MJ·ha^{-1}·mm^{-1}of rain; i_m is rainfall intensity with units of mm· h^{-1}; d_j is rainfall depth in millimeters; and N is number of storms.

Rainfall amount and intensity data from each event were used to calculate R factors, as outlined in USDA Agricultural Handbook Number 703 (Renard et al., 1997). Storms with less than 13 mm (0.5 in.) of rainfall were ignored during analysis, with the exception of rainfall depths greater than 6 mm in any15–minute period (Wischmeier and Smith, 1978). Individual rainfall events were distinguished by a 6-hour dry period.

For each rainfall event, the five-minute rainfall depths that were recorded by the tipping buckets were used to compute 30-minute rainfall intensities (I_{30}). The maximum 30-minute rainfall intensity (I_{30}, Max) was used with total storm energy (E) to estimate erosivity of each rainfall event (Equations 2, 3, and 4). Summing all erosivities of rainfall events that occurred between two sampling events yielded total erosivity for that period.

5.2.2.2 K Factor

Per Equation 1, estimates for the soil erodibility K factor were based on measured soil loss (A) and computed R factors from measured precipitation data. The soil loss was averaged between four plots for each site at each sampling event. LS factors were computed based on the tabulated values in the USDA Agricultural Handbook Number 703 (Renard et al., 1997), and

were averaged among the four plots per study site. In this study, C was assumed to be 1 because there was no vegetative cover, though this study deviated somewhat from Unit Plot conditions because there was no tillage. Also, P = 1 because no erosion control practice was utilized.

5.2.3 Particle Size Distribution

The particle size distribution (PSD) analysis was performed on oven-dried materials from the buckets (combination of coarse and fine material) and 500 ml bottles (fine sediments). For buckets, ASTM- D6913 was followed to determine particle size distribution of coarse eroded material using sieve analysis. ASTM sieve numbers 3/4", 1/2", 3/8", No. 4, No. 8, No. 16, No. 30, No. 50, No. 100 and No. 200 were used. For fine sediments (material passed a No. 200 [0.074-mm] sieve), the standard hydrometer test method D422-63 was followed.

Using the percentage of flow division at each divider, the weight of remaining material on each sieve, and the results from hydrometer test, the particle size distribution of eroded material for each sampling event can be determined. For flow divider buckets, weight of material that remained on each sieve was scaled up by the percentage of flow division (1/12 or 1/24) related to the flow divider in the series of flow dividers. Then weights of material on the sieves with the same number (size) were added. The results of hydrometer tests were also scaled up based on the percentage of flow division (1/12 or 1/24) in the former flow divider. Then the sieve portion and hydrometer portion of the particle size distribution were combined. The sieve portion and hydrometer portion of the tests may not exactly line up, so correction of values from the hydrometer test was performed to match the two portions with each other, following the procedure found in Holtz and Kovacs (1981).

5.2.4 Data Analysis

Data analysis consisted of estimating measured sediment yields (erosion rates) per unit erosivity and the slope factors (R・L・S) in order to observe the influence of rainfall intensity and sediment yields for different sub-periods within the entire monitoring period June 2009 through July 2010. Particular attention was given to the first three-month monitoring period (June, July, August 2009), in which rill development was rapid (Figures 14 to 16). In addition, the computed sampling period erodibility (time-varying K factor) was examined over different sub-periods within the entire monitoring period. Erodibility was also examined in comparison to the combined R・L・S factors to observe the influence of rainfall intensity and sediment yields and its relationship with cumulative erosivity.

To identify outliers, the first quantile (Q_1), third quantile (Q_3), and Inter Quartile Range (IQR) − the difference between first and third quantiles − for the measured sediment yield were computed. The Q_1 - 1.5 × (IQR) and Q_3 + 1.5 × (IQR) were used as the lower and upper thresholds, respectively. JMP 9.0 statistical software packages was used to test if mean erosion rates differed among study sites, and to perform linear regression.

5.3 Results

Rainfall depth and duration, and erosion estimates per study site and sampling date are summarized in Table 4. A total of 59 data points were compiled among the three study sites. From the 59 sampling data, 7 of them turned out to be outliers based on the test described above. The remaining 52 data points were used to compute rainfall erosivity (R) and erodibility (K), and to complete the analysis to characterize measured erosion per erosivity, and erodibility.

Table 4. Sampling Date, Cumulative rainfall depth and duration, Maximum 5-minute rainfall intensity, measured erosion, calculated erosivity, and erodibility.

Site	Sampling Date	Cum. Rainfall Depth, (mm)	Cum. Rainfall Duration, (h.)	Max 5 min. Intensity, ($mm \cdot h^{-1}$)	R $MJ \cdot mm \cdot (ha \cdot h)^{-1}$	Erosion ($t \cdot ha^{-1}$)	K factor* Mg. ha. h. $(ha\ MJ\ mm)^{-1}$
National	June 25, 2009	96.1	12.8	114	587.12	261.79	0.496
	July 7, 2009	60.7	35.5	58.5	266.64	112.54	0.469
	July 15, 2009	72.6	11.0	100.4	897.92	201.21	0.249
	August 3, 2009	198.4	86.4	76.5	765.86	78.80	0.283
	August 14, 2009	47.6	11.0	111.0	281.78	25.91	0.253
	September 25, 2009	138.8	104.4	43.5	480.29	11.21	0.064
	September 29, 2009	49.5	14.9	36.0	127.01	3.46	0.075
	October 8, 2009	41.3	33.5	45.0	115.66	3.17	0.075
	October 22, 2009	106.3	94.6	81.0	423.94	9.36	0.061
	October 29, 2009	22.1	15.3	9.0	10.09	0.21	0.058
	November 5, 2009	31.3	16.8	21.0	47.95	0.59	0.033
	November 12, 2009	16.9	13.6	7.5	12.62	0.17	0.038
	December 1, 2009	44.9	35.6	16.5	63.51	0.79	0.034
	December 14, 2009	130.6	52.7	33.0	184.21	2.69	0.040
	April 13, 2010	72.25	26.1	52.5	205.24	7.97	0.107
	May 7, 2010	193	59.7	49.5	621.61	21.26	0.094
	May 19, 2010	41	5.8	111.0	294.40	9.96	0.093
	June 23, 2010	79.5	14.5	87.0	168.65	5.89	0.096
	June 29, 2010	28.5	4.3	72.0	95.05	3.69	0.107
	July 16, 2010	93.245	10.4	109.4	554.74	16.48	0.082
Premium	June 24, 2009	38.1	17.5	31.5	727.17	48.98	0.102
	July 17, 2009	127.3	44.9	75.0	986.24	66.26	0.101
	August 3, 2009	106.1	48.0	39.0	268.75	4.38	0.06
	August 13, 2009	20.8	5.6	37.5	111.03	1.72	0.06
	August 24, 2009	75.9	28.0	82.5	458.42	34.94	0.115
	September 22, 2009	162.9	99.0	67.5	584.60	12.22	0.08
	October 1, 2009	96.0	25.0	79.5	783.53	20.23	0.10
	October 20, 2009	73.4	48.2	19.5	102.20	1.61	0.06
	October 27, 2009	37.3	21.5	18.0	35.75	0.43	0.04
	November 3, 2009	14.6	17.8	9.0	10.09	0.18	0.07
	November 24, 2009	49.8	43.8	10.5	29.44	0.41	0.05
	December 3, 2009	39.3	30.8	27.0	40.80	0.49	0.04
	December 17, 2009	139.8	31.3	42.0	450.43	7.93	0.07
	May 7, 2010	131.5	64.4	105.0	496.70	7.33	0.05
	May 18, 2010	27.375	4.4	43.5	93.79	1.11	0.04
	June 8, 2010	60.625	14.2	54.0	256.97	2.51	0.04
	July 20, 2010	79.125	17.8	52.5	224.59	3.77	0.06

Table 4. Continued

Mountainside	July 2, 2009	132.8	3.6	54.4	33.65 (+1225.35**)	3.19	0.313
	July 14, 2009	62.6	21.9	75.6	454.22	118.20	0.347
	September 22, 2009	120.7	75.8	86.2	527.40	9.46	0.059
	October 1, 2009	98.5	37.9	13.6	683.01	18.97	0.091
	October 13, 2009	59.6	33.8	65.0	210.71	4.48	0.070
	October 20, 2009	51.7	70.6	33.3	79.07	1.82	0.076
	November 3, 2009	36.0	21.3	13.6	44.16	0.67	0.050
	December 1, 2009	18.1	14.6	10.6	16.40	0.21	0.043
	December 10, 2009	99.3	35.3	24.2	145.52	1.60	0.036
	December 14, 2009	35.0	8.8	10.6	45.84	0.67	0.048
	March 26, 2010	77.1	37.1	54.4	146.36	2.28	0.051
	May 13, 2010	242.6	57.3	66.5	612.35	8.66	0.047
	May 18, 2010	47.5	7.3	98.3	315.43	4.46	0.047
	June 8, 2010	52.7	7.8	83.2	303.65	3.81	0.041
	June 25, 2010	50.5	6.8	133.1	264.12	3.56	0.044

*USLE K factor as defined by Mitchell and Bubenzer (1980) where A= 0.224 RKLSCP, for each sampling date

** Cumulative erosivity that study site experienced before this date (previouse sampling events are not reported due to outlier sediment yileds)

Table 5. Constructed characteristics of field plots per Mountainside, National, and Premium study sites including length and width, slope, and spoil unit weights.

	D_{50} (mm)				D_{84} (mm)			
Site	a*	b**	c +	d ++	a*	b**	c +	d ++
Premium	4	0.05	0.22	2.5	18	0.4	5	14
Mountainside	2	0.06	0.08	0.75	17	0.7	3	11
National	2	0.08	0.15	0.55	17	4	3	10
Avg.	2.67	0.06	0.15	1.27	17.33	1.70	3.67	11.67

* June, July, and August 2009 + March, April, and May 2010

** September through Dec. 2009 ++ June, July 2010

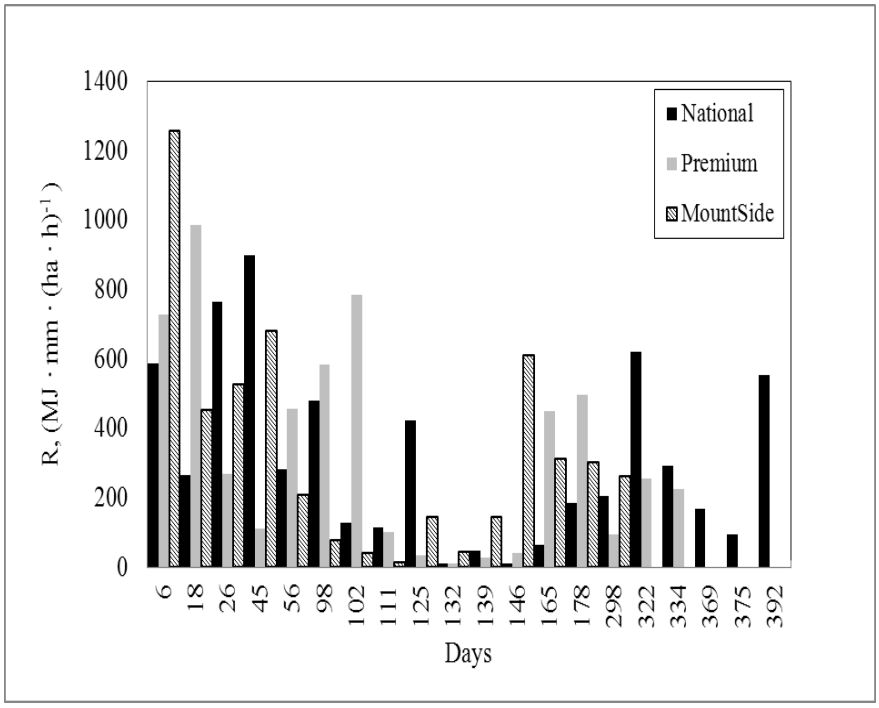

Figure 17. Erosivity (R) in MJ·mm·(ha·h)$^{-1}$ related to each sampling event, for the Premium, National, and Mountainside sites, with the x-axis representing days from beginning of the monitoring period.

5.3.1 Measured Erosion per Erosivity

Rainfall erosivity experienced at the study sites (the cumulative rainfall erosivity between two sampling events) during the monitoring period from June 2009 through July 2010 ranged widely from 10.09 to 986.2 MJ·mm·(ha·h)$^{-1}$ (Figure 17, Table 4). The rainfall erosivity (R factor) for the entire monitoring period averaged over all three sites was 5249 MJ·mm·(ha·h)$^{-1}$.

The measured erosion rates for each sampling period were paired with the corresponding calculated rainfall erosivity (R factor), and these data were used in the sediment yield analysis (Table 4). According to t-test calculations, there were no significant differences between erosion rates on the three sties ($p = 0.1 > \alpha = 0.05$, H_0: differences exist among means). Combining data from all three sites, the average total erosion rate was 391 t·ha^{-1} during the entire monitoring

period. The distribution of sampling period erosion rates is slightly right skewed, with the 90% percentile at 75 $t \cdot ha^{-1}$. Based on 52 sampling points, the average erosion rate per sampling event was 22.6 $t \cdot ha^{-1}$. The average erosion rate for the first three months of the study (during rill development) was 116 $t \cdot ha^{-1}$, while for the remaining period from July 2009- July 2010, it was 8.0 $t \cdot ha^{-1}$.

Measured erosion rates were plotted versus the product of rainfall erosivity and slope-steepness factor ($R \cdot L \cdot S$) for all three study sites and the 14-month monitoring period June 2009 through July 2010 (Figure 18). Erosion rates during the period June, July, and August 2009 were much greater than other sub-periods in the entire monitoring period, and 4.4 times greater than the erosion rates estimated for the remaining portion of monitoring period, September 2009 through July 2010. About 75% of the total eroded material was delivered during this initial three months. Rill development was rapid during this period, with relatively uniformly spaced rills across the study plots, deeper at the slope bottom (Figures 14 to 16). Erosion rates for the first three months were seven times the rates for the same months in the following year (June, July, and August 2010) (Figure 19). Though not significant at the chosen $\alpha = 0.05$, during the first three months of monitoring, erosion rates from the National site were generally greater than the Premium and Mountainside sites. Erosion rates were highly variable among the three sites during the first three-month monitoring period ($R^2 = 0.40$; $p < 0.001$).

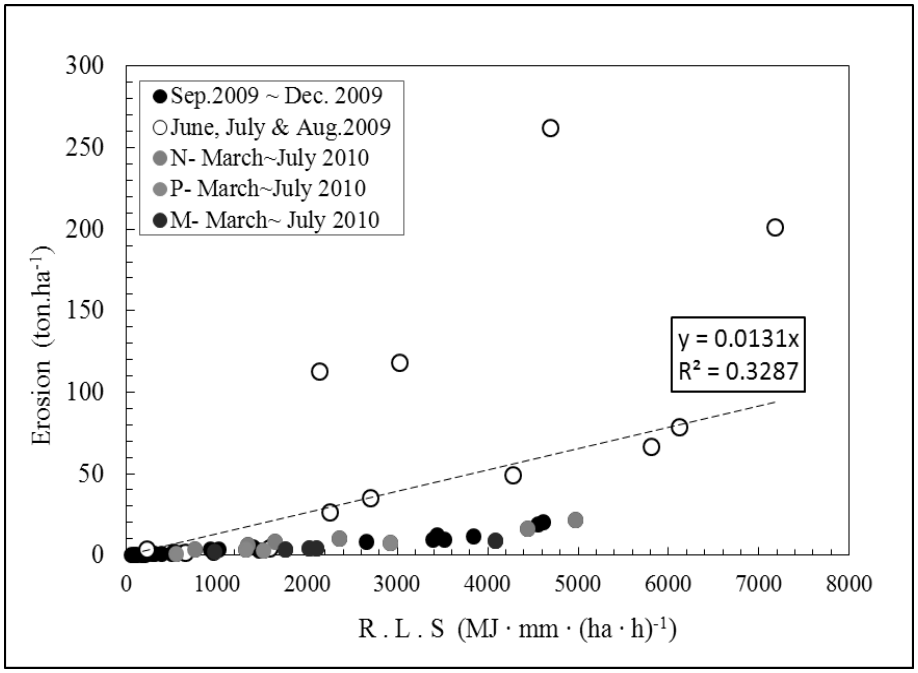

Figure 18. Observed erosion rates ($t \cdot ha^{-1}$) related to each sampling event, for each study site from June 2009 through July 2010 (N = National, P = Premium, and M = Mountainside).

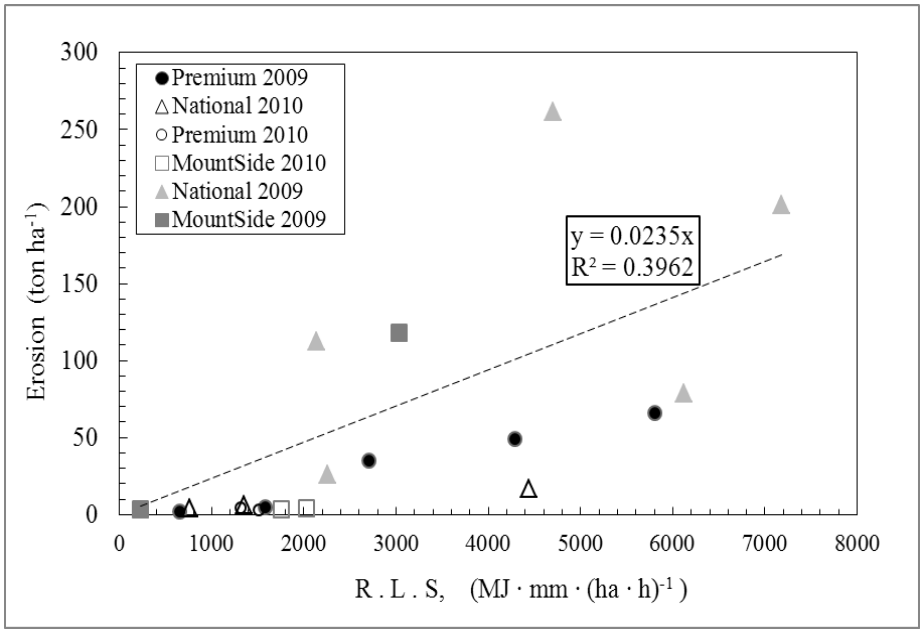

Figure 19. Observed erosion rates ($t \cdot ha^{-1}$) related to each sampling event, for each site during two periods: June to August 2009 and June to August 2010. The regression line fits just 2009 data.

After September 2009, once rill development apparently stabilized, erosion rates were strongly correlated with rainfall erosivity and slope-length factors (R・L・S) for all three study sites (R^2 = 0.85; p = 0.03) (Figure 20). Variation of erosion rates with rainfall erosivity for this period September 2009 through July 2010 was much less than the period prior to September 2009. Again, though not significant at the chosen α = 0.05, the National site had slightly more erosion than the other sites across similar ranges of rainfall erosivity.

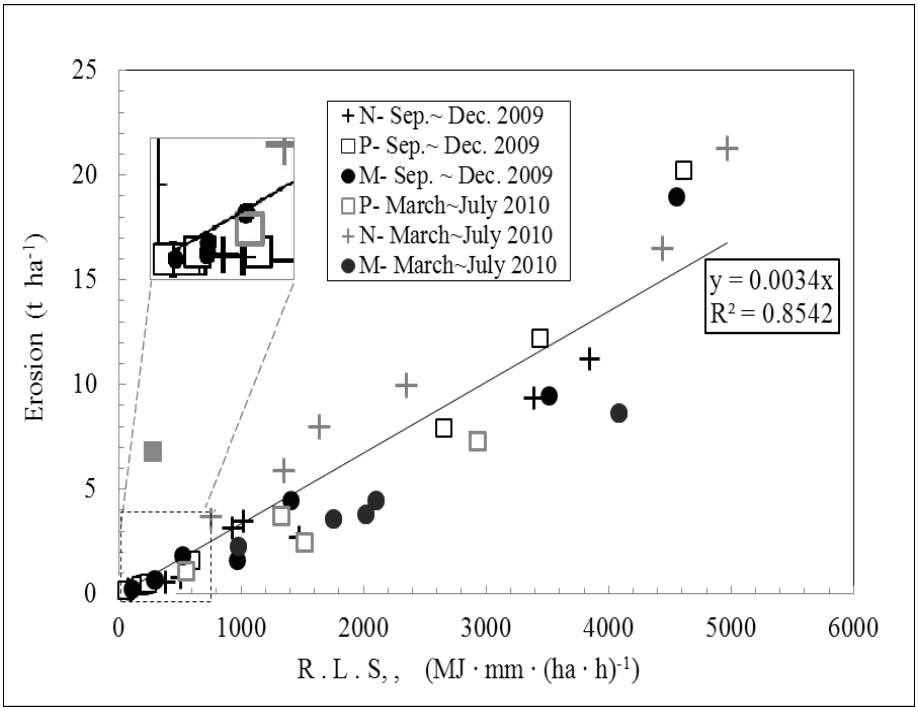

Figure 20. Observed erosion rates (t・ha^{-1}) related to each sampling event, for each study site (N = National, P = Premium, and M = Mountainside) for different monitoring periods (September through December 2009; and March through July 2010).

5.3.2 Erodibility

Calculated erodibility (K factors) based on the measured erosion and erosivity ranged from 0.03-0.50 t・ha・h・(ha・MJ・mm)$^{-1}$ during the entire monitoring period June 2009 through July 2010 (Figure 21, Table 4). The general pattern of erodibility per unit of erosivity in Figure

21 is similar to the patterns of erosion rates observed in Figure 18. Erodibility was greatest during the first three months of the monitoring period (June, July and August 2009), a period in which rill development was rapid. During June to August 2009, erodibility was not correlated with erosivity, and each study site appeared to have its general response (Figure 22). As shown in Figure 22, K factors ranged from about 0.25 to 0.50 $t \cdot ha \cdot h \cdot (ha \cdot MJ \cdot mm)^{-1}$ for National and Mountainside sites, whereas Premium site ranged from 0.05 to 0.12 $t \cdot ha \cdot h \cdot (ha \cdot MJ \cdot mm)^{-1}$.

After September 2009, erodibility (K factors) for all study sites were below 0.12 $t \cdot ha \cdot h \cdot (ha \cdot MJ \cdot mm)^{-1}$, with a median of 0.06 $t \cdot ha \cdot h \cdot (ha \cdot MJ \cdot mm)^{-1}$ (Table 4). In general, lower intensity storm events occurred between August and December 2009, and K factors appear to cluster about 0.065 $t \cdot ha \cdot h \cdot (ha \cdot MJ \cdot mm)^{-1}$ (Figure 23). While Premium and Mountainside

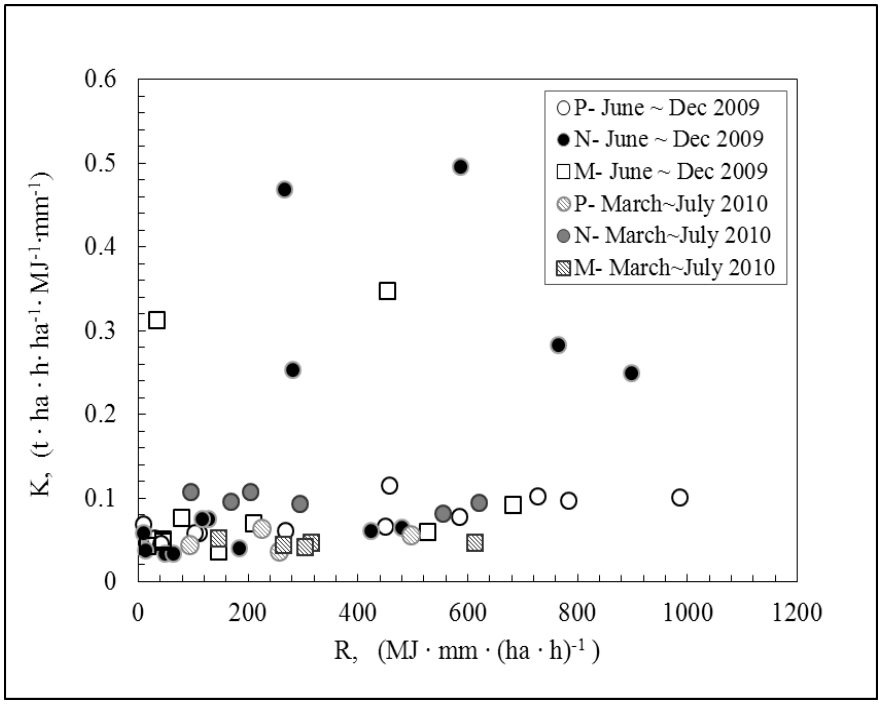

Figure 21. Erodibility (K factors) ($t \cdot ha \cdot h \cdot ha^{-1} \cdot MJ^{-1} \cdot mm^{-1}$) related to each sampling event, for each study site (N = National, P = Premium, and M = Mountainside) for the entire monitoring period from June 2009 to July 2010.

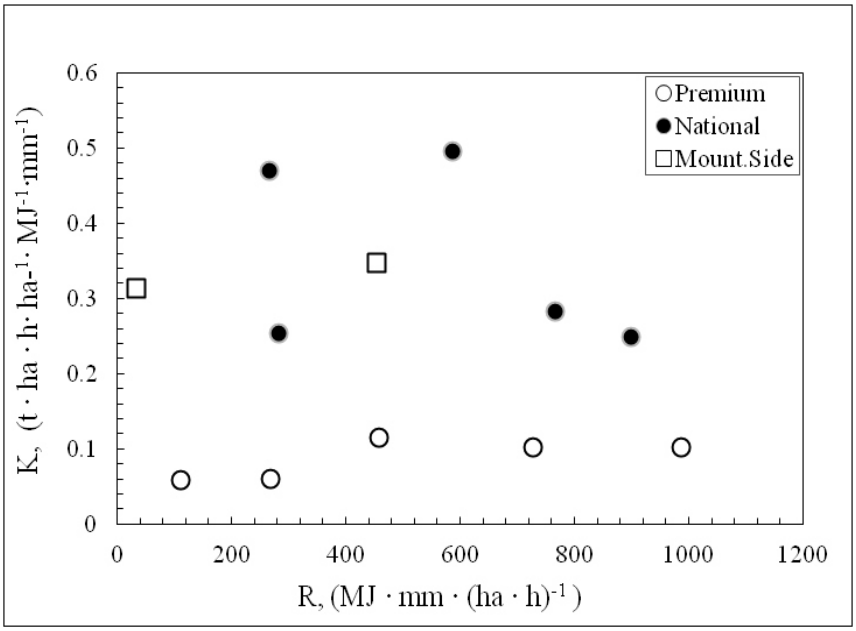

Figure 22. Erodibility (K-factors) ($t \cdot ha \cdot h \cdot ha^{-1} \cdot MJ^{-1} \cdot mm^{-1}$) related to each sampling event, for Premium, National, and Mountainside study sites from June to August 2009.

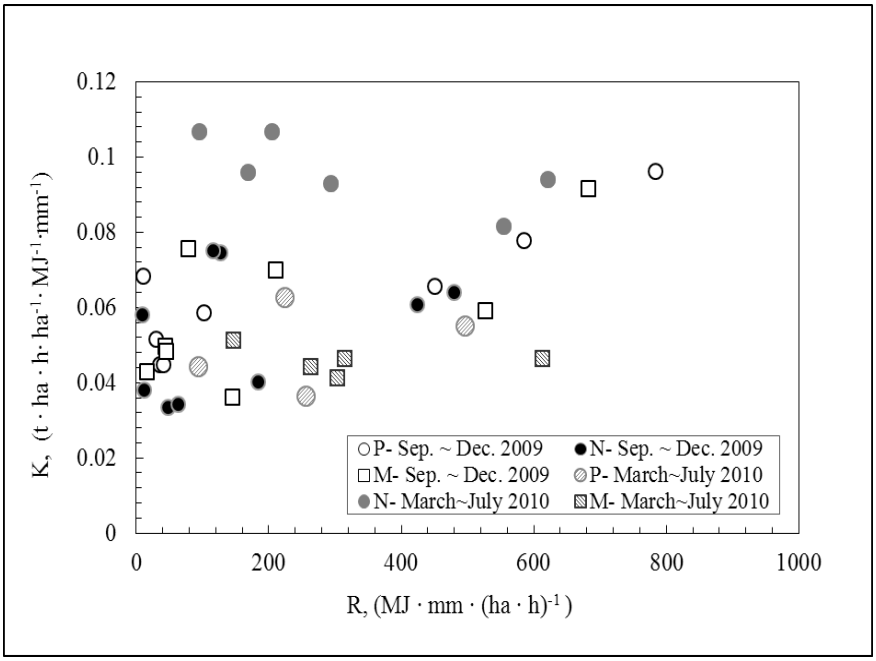

Figure 23. Erodibility (K-factors) ($t \cdot ha \cdot h \cdot ha^{-1} \cdot MJ^{-1} \cdot mm^{-1}$) related to each sampling event, for each study site (N = National, P = Premium, and M = Mountainside) from September 2009 to July 2010.

sites retained this K factor into the next year (March to July 2010), the National site exhibited a greater K factor between 0.08 and 0.11 $t \cdot ha \cdot h \cdot (ha \cdot MJ \cdot mm)^{-1}$ during this period.

Apparently due to rapid rill development, the K factor declined from values of >0.3 to values < 0.1 $t \cdot ha \cdot h \cdot (ha \cdot MJ \cdot mm)^{-1}$ over the first three months of the monitoring period for the National and Mountainside study sites, with this period representing approximately 2,500 to 3,500 $MJ \cdot mm \cdot (ha \cdot h)^{-1}$ of cumulative erosivity (Figure 24). This shows that K values dropped significantly but ultimately reached almost steady state, settling near 0.06 $t \cdot ha \cdot h \cdot (ha \cdot MJ \cdot mm)^{-1}$ at the end of monitoring period (Figure 24). Erodibility of the National site at the end of the monitoring period was 17% of the initial value, and the Mountainside site was 13%. The K factor on the Premium site was 60% of the initial value.

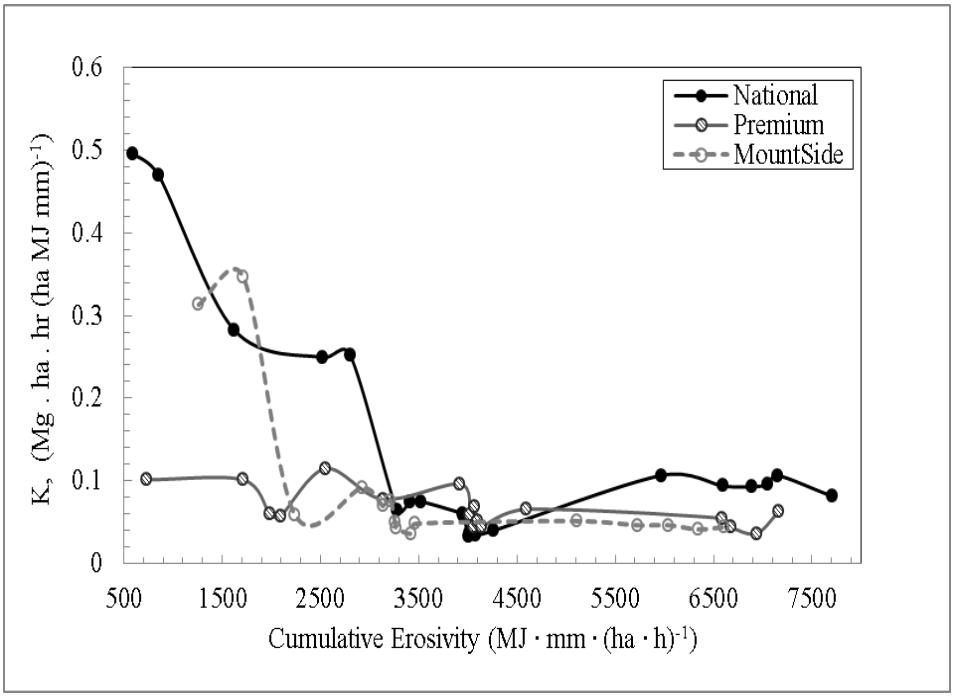

Figure 24. Erodibility (K-factors) ($t \cdot ha \cdot h \cdot ha^{-1} \cdot MJ^{-1} \cdot mm^{-1}$) related to each sampling event versus cumulative erosivity (R-factor) ($MJ \cdot mm \cdot (ha \cdot h)^{-1}$) over the 14-month monitoring period from June 2009 through July 2010 for Premium, National, and Mountainside study sites.

5.3.3 Particle Size Distribution

Particle size distributions for all three sites were generally similar during the entire monitoring period (June 2009 to July 2010), although Premium had slightly more coarse eroded material (Figure 25 and Table 5). The results show that from September till December 2009, between 50% and 60% of eroded material was silt and clay. This is the period during which rainfall events had low intensities. For the rest of monitoring period, between 15% and 40% of the eroded material was silt and clay. During June, July, and August 2009, the eroded material was coarser (D_{50}= 2.7 mm; D_{84}= 17.3 mm) than the rest of monitoring period (D_{50}< 1.3 mm; D_{84}< 11.7 mm). Particle size of eroded material got finer as time passed, with June 2009 - May 2010 having D_{50}: 2.7 mm to 0.15 mm; D_{84}: 17.3 mm to 3.7 mm, but near the end of monitoring period (June and July 2010) there was a trend toward more coarse material (D_{50}: 0.15 mm to 1.3 mm; D_{84}: 3.7 mm to 11.7 mm) (Table 5 and Figure 25).

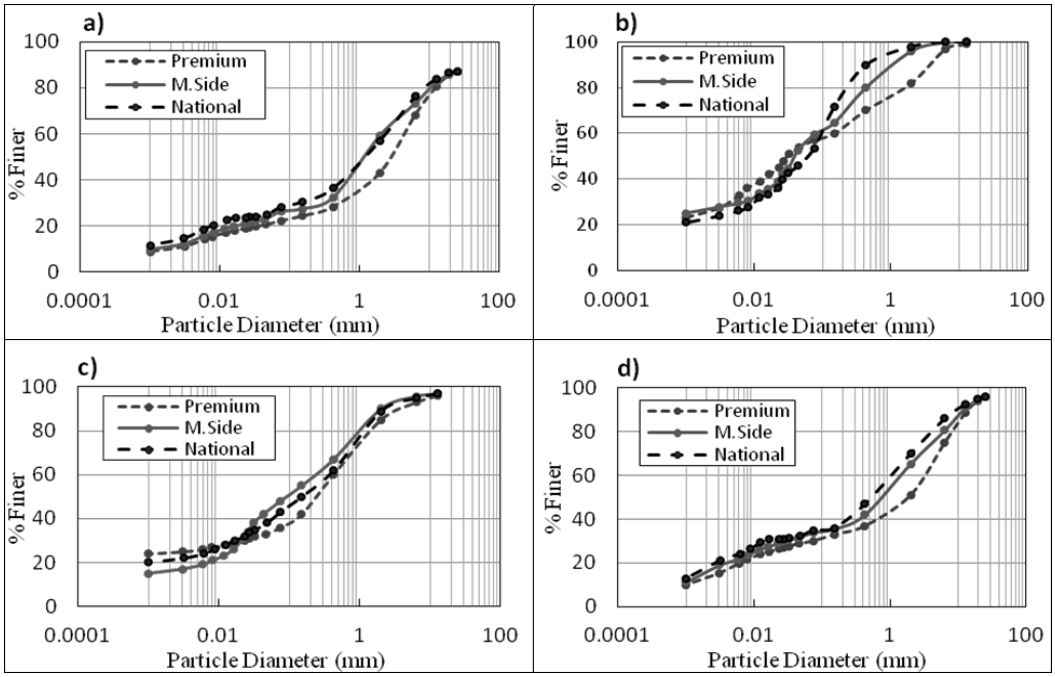

Figure 25. Typical particle size distributions of eroded material for a) June, July, and August 2009; b) September through Dec. 2009; c) March, April, and May 2010; and d) June, July 2010.

5.4 Discussion

This study estimated the erodibility K factor for low-compaction, steep-sloped reclaimed mine lands without vegetative cover. K factors were quantified as a function of rainfall erosivity, and observed periods of rapid rill development were followed by rill stabilization. Several studies have illustrated the importance of quantifying K in terms of erosivity as a surrogate measure for rainfall intensity, and rill formation (Nearing et al., 1997; Foltz et al., 2008; Yao et al., 2008; Berger et al., 2010). As a point of reference, the average annual erosivity for these study sites was 1.5 times greater than the long-term regional annual average of 3,404 $MJ \cdot mm \cdot ha^{-1} \cdot h^{-1} \cdot year^{-1}$ reported by Renard et al. (1997). The highest rainfall intensities and erosivities occurred during the initial project period from June 2009 through August 2009. About 45% of the total erosivity measured in this study was during these first three months, immediately following reclamation site construction. Similarly, Berger et al. (2010) observed rill development on steep-sloped mine lands immediately following construction, indicating rainfall intensity was a driving factor in their rapid development on bare spoils.

During the period June through August 2009, in which rill formation and development occurred in this study, sediment yields from surface erosion averaged 116 $t \cdot ha^{-1}$.Total sediment yields for the entire period averaged 391 $t \cdot ha^{-1}$, which compared to that reported by Carroll et al. (2000) for spoils on 20% slope with annual erosion rates of 314, 318, and 1,120 $t \cdot ha^{-1}$. Curtis and Superfesky (1977) estimated yield to be 526 t·ha-1 for a 20-month period. Both studies by Curtis and Superfesky (1977) and Carroll et al. (2000) experienced initial rill development similar to that found in this study. Noting a smaller erosivity of 2,160 $MJ \cdot mm \cdot (ha \cdot h \cdot year)^{-1}$ and a smaller slope steepness of 9% compared with this study, McIntosh and Barnhisel (1993) measured sediment yields on mine spoils of 91.5 $t \cdot ha^{-1}$, illustrating the potential influence of

reduced rainfall intensity and slope steepness on erosion. During this study's period when rills were developing rapidly, sediment particle sizes consisted of more coarse material (D_{84} = 17.3 mm) compared to following periods in which rills stabilized (D_{84} < 11.7 mm). As illustrated in Figures 18 through 20, sediment yields dropped by 93 percent for the three study sites for the period after July 2009, when rills apparently stabilized, though total rainfall erosivities were approximately the same. Other studies have observed rill development immediately following construction of the reclaimed slopes and the stabilization of the rills within one year (Dickens et al., 1985; Hahn et al., 1985; Nicolau, 2002; Hancock et al., 2008).

In this study of loose spoils, and as observed by others, runoff generation on slopes indicates that overland flow govern hydrologically over infiltration for steep slopes over 20% (Sheridan et al., 2000; Cerda, 2001; Guebert and Gardner, 2001; Smets et al., 2008). Taylor et al. (2009) reported no overland flow in an experiment utilizing loose spoils on slopes ranging from 2 to 10% in eastern Kentucky. Sufficient hydraulic shear stress initiates erosion from overland flow, and over a rapid period of time, flows will concentrate in channels and accelerate rill development (Nearing et al., 1997; Govers et al., 1987; Foltz et al., 2008; Yao et al., 2008). On steep slopes, other key factors promoting overland flow include percent rock fragments and soil moisture (Jean et al., 2000; Nicolau, 2002). Harms and Chanasyk (2000) note overland flow from infiltration excess is highly dependent on the spoil compaction and sorting during the reclamation process. Studies vary with regard to percent rock fragments, where in some cases a high percentage of rock fragments (> 10% by area) promotes infiltration, and in other cases it does not. The Premium study site produced lower sediment yields compared to the National and Mountainside sites, although it wasn't statistically significant at $\alpha = 0.05$. Premium experienced similar erosivities as the other sites, but had a lower (wet) bulk density of 18.5 $KN \cdot m^{-3}$

compared to 20.3 $KN \cdot m^{-3}$, and had more large rock fragments on the surface. The use of lower bulk density for steep-sloped reclaimed mine lands for engineering specifications may be valuable, if this finding is confirmed with additional research.

The K factor ranged between 0.03 and 0.5 $t \cdot ha \cdot h \cdot (ha \cdot MJ \cdot mm)^{-1}$ for low compaction steep-sloped reclaimed mine lands. During the rill development period, the K factor averaged 0.34 $t \cdot ha \cdot h \cdot (ha \cdot MJ \cdot mm)^{-1}$ for the National and Mountainside sites. Once the rills stabilized, the K factor averaged 0.062 $t \cdot ha \cdot h \cdot (ha \cdot MJ \cdot mm)^{-1}$ for the study sites. Uniquely, this study quantified the change in erodibility over time through rill development to a more stable morphology (Figure 24). The K factor for the Premium site for the entire monitoring period was below 0.12 $t \cdot ha \cdot h \cdot (ha \cdot MJ \cdot mm)^{-1}$, and this result may be due to compaction that was slightly less than the other two sites as measured by the bulk densities. In general, the K factors measured in this study compared well with other studies on low to moderately compacted spoils, ranging from 0.04 to 0.65 $t \cdot ha \cdot h \cdot (ha \cdot MJ \cdot mm)^{-1}$ (Mitchell et al. 1983; McIntosh and Barnhisel, 1993; Torri et al., 1997). McIntosh and Barnhisel (1993) reported a K factor for mine spoils of 0.051 $t \cdot ha \cdot h \cdot (ha \cdot MJ \cdot mm)^{-1}$ less than 0.067 for subsoils, and attributed it to physical weathering. This study did find median particle size (D_{50}) to decrease from about 2.67 mm to less than 1.27 mm after rill development, indicating the possible effect of armoring, as the K factor decreased over time concurrently with the fining of the spoil materials.

It is possible that the fining of particle sizes over time is a result of surface armoring and of rill stabilization. Armoring appears to reduce erosion and sediment yields on bare mine spoil material in the first year after reclamation (Curtis, 1971; Dickens et al., 1985). In considering rill stabilization, Foster and Lane (1983) proposed a model describing hydrogeomorphic processes associated with rill stabilization. Based on the Foster and Lane (1983) model, shear stress is not

evenly distributed across the channel, but rather tends to be concentrated in high velocity areas. The maximum shear stress is at the bottom center of the channel, so the maximum erosion tends at that location, ultimately forming a triangular cross section. This process continues until the shear stress on the sidewalls is not enough to cause soil detachment, caused partly by the hydraulic radius of the rill decreasing as the rill becomes deep and narrow. The Manning's n may increase during rill formation as well, as a higher percentage of large rocks in the spoils would increase hydraulic roughness, potentially accelerating rill stabilization. This combination of decreasing hydraulic radius and increasing roughness cause a substantial decrease in Manning's velocity, decreasing shear stress on the soil in the rill. After rills stabilize such that they can carry runoff generated from the sites, the main source of sediment yield will be sheet erosion between the rills (Haan et al., 1994). On land surfaces with stable rill morphology, erodibility and erosion is a function of soil susceptibility to the rainfall impact and erosivity.

In this study, the assumption that the management factor equals one (C = 1) is consistent with other studies computing erodibility (K factor) on bare mine spoils (Hartley, 1982; Mitchell et al., 1983; McIntosh and Barnhistel, 1993; Torri et al., 1997; Toy et al., 1999), though this does not meet the strict definition of Unit Plot conditions, which requires no cover and repeated tillage (Renard et. al., 1997). Although our study plots had no effective cover, the repeated tillage requirement was not met. Barfield et al. (1988) computed C factors for different mining surface treatments on experimental spoil plots with rainfall simulators where a K factor was estimated per the RUSLE standard procedure. C factors were then computed by A / (R • K). Without regular tillage, surface roughness diminishes fairly quickly, reducing the Surface Roughness subfactor (SR), where the C factor becomes less than 1. On mild slopes, roughness slows runoff velocities and increases ponding, thereby reducing the erosion rate potential (Haan et al., 1994).

Among experimental plots by Wu (2001), when 45% of the surface is covered with rock fragments (gravel), the C factor was approximately equal to 0.5. Because the experimental plots in this study were on reclaimed mines lands regular tillage was not reasonable, so it is not completely clear where the impact of rill stabilization and surface armoring should reside. Should this dynamic property be taken as an inherent soil property and seen as a change in K, or should it be taken as a management effect different from Unit Plot management conditions and included in the C factor? The K factor derived in this study and other similar on-site experimental designs generally assume a C factor of 1, suggesting that the change is included in K, but the estimated K factor in this study is actually a KC factor. To develop a "real" K factor that would allow a "real" C factor development for other managements, long-term studies (using either real study plots or rainfall simulator) under Unit Plot conditions are required. The study plots in future studies should be tilled repeatedly and cover management should be placed soon enough to have the expected effect in reducing erosion. This is important for estimating the C factor because in this study it is not clear how much C factor exists just by not disturbing the plots. If "real" K values were quantified as described above, tests could be run to determine the C factor for lack of disturbance, and that part of C factor could be separated from the C effect from other practices. Without that "real" K factor, this separation is simply not possible. Practitioners estimating sediment yields with RUSLE or SEDCAD™ apply the K factor assuming a C factor of 1 for bare spoils. Vegetative cover will reduce erosion and sediment yield, and a C factor for these conditions must be applied accordingly.

Establishing vegetative cover immediately following reclamation construction of steep-sloped mine lands is critical in reducing erosion and sediment yields, and in ensuring ground cover growth and tree survival (Espigares et al., 2011). The success of OSM's FRA is dependent

on this establishment (Sweigard et al., 2007). As observed with this study and others on steep-sloped reclaimed mine lands, seed for ground cover not properly applied will be washed from the surface during high intensity storms (Dickens et al., 1985; Carroll et al., 2000; Smets et al., 2008). Espigares et al. (2011) report rill erosion rates of 17 $t \cdot ha^{-1} \cdot yr^{-1}$ when plant cover is less than 30%. These studies note that rill development severely hinders ground cover establishment. Rill development not only removes seeds but affects soil moisture and ultimately plant survival and growth. Ground cover is especially necessary at the upper slope areas to prevent rill initiation because unprotected bare spoils on long slopes over 11 m are prone to rill development (Smet et al., 2008). Because ground cover is critical for erosion control, timing of seeding for best germination and growth based on seasons per regional specifications should be followed for successful application of FRA.

Design of erosion control BMPs for low compaction steep-sloped (> 20%) mining reclamation sites are supported by the data generated in this study. Data include K factors for different physical conditions associated with rills, and the particle size distributions. In addition, Hoomehr et al. (2012) generated runoff curve numbers in the range of 58.5 to 60.0. The SEDCAD™ model utilized all these data for design of erosion control BMPs, which is standard in surface coal mining practice.

5.5 Conclusion

Erodibility on bare, loose spoils on steep slopes greater than 20% is highly susceptible to rill development, where during periods of rill development K factors were estimated to range between 0.2 to 0.5 $t \cdot ha \cdot h \cdot (ha \cdot MJ \cdot mm)^{-1}$. Development of rills immediately following site slope construction coincided with intense rainfall events, with erosivity estimates as high as 986 $MJ \cdot mm \cdot (ha \cdot h)^{-1}$. Once rills apparently stabilized on these sites, estimated K factors were below

0.12 t·ha·h·(ha·MJ·mm)$^{-1}$, with a median of 0.06 t·ha·h·(ha·MJ·mm)$^{-1}$. Sediment yields from erosion were similarly impacted by rill development, averaging 391 t·ha^{-1} during the entire monitoring period for all three sites. The average erosion rate per sampling event was 22.6 t·ha^{-1}. In contrast to other studies that measured little or no runoff on low-gradient slopes with loose spoils, this study measured runoff easily sufficient to form rills. Both coarse and fine sediments erode from these sites, and the D_{50} estimates ranged from 0.06 to 2.67 mm during the study period. The above information provides valuable model input data for SEDCAD™, the model commonly used in the United States to plan BMPs to mitigate impacts from probable hydrological consequences, and generally supports surface coal mining reclamation practices.

Chapter 6

SEDCAD Performance on Reclaimed Mine Lands

Hoomehr S., J.S. Schwartz. "Evaluating SEDCAD model performance on reclaimed coal mine lands in East Tennessee." *ASCE Journal of Irrigation and Drainage Engineering*. Under Review.

6.1 Introduction

In the surface coal mining industry, the Sediment, Erosion, Discharge by Computer Aided Design (SEDCAD) program is extensively used for developing engineered plans with best management practices (BMPs) for erosion control (USDI 2010). As required by the Surface Mining Control and Reclamation Act of 1977 (SMCRA), mining permit applications consist of site layout designs that embrace reclamation practices where back-to-contour spoil placement approximates natural slopes. In addition to slope reclamation, BMPs for erosion control are designed into layout plans to minimize environmental impacts from probable hydrological consequences. Mining and consulting engineers submit SEDCAD program outputs with their mining permits, and outputs are reviewed by US Office of Surface Mining (OSM) engineers. OSM provides SEDCAD to the 24 states with primacy under SMCRA for use with permit review and remediation project design at bond forfeiture sites. Although SEDCAD is the primary BMP design tool used in this industry, very limited published information is available on its performance in estimating site runoff and sediment yields.

SEDCAD is an event-based distributed hydrology model using curve number (CN) rainfall-runoff relationships, and integrates runoff routing with the Revised Universal Soil Loss Equation (RUSLE) to estimate sediment yields (Warner et al. 1998). It was developed at the University of Kentucky, Lexington, and is now maintained by Civil Software Design©, Ames, Iowa. Specifically, SEDCAD evaluates: 1) hydrologic capacity of a system of drainage channels, and hydraulic and sediment control structures; 2) channel stability for designs using riprap and

grassy vegetation; and 3) effectiveness of sediment control structures, i.e., detention ponds, check dams, grassy swales, and silt fences, with respect to sediment trap efficiency and effluent sediment concentration prediction.

The study objective was to evaluate SEDCAD performance predicting runoff and sediment yield from a hillslope by comparing model outputs with measured values at active surface coal mining sites. In addition, a sensitivity analysis was conducted for SEDCAD's hydrologic CN and erodibility K factor input parameters. Understanding confidence ranges with SEDCAD model predictions is important so that BMPs can adequately protect surface waters from sediment impairment, where in the Appalachian Coal Region more than 600,000 ha have been surface mined and currently about 10,000 ha are mined each year (Zipper et al. 2011). This study also assesses SEDCAD performance on mine sites that use the Forest Reclamation Approach (FRA) for natural contour reconstructions where spoils remain loose for enhancing tree regeneration (Angel et al. 2006; Sweigard et al. 2007; Taylor et al. 2009). OSM is currently promoting FRA at mine sites. Natural slopes in the Appalachia can exceed 20%, and commonly are in the order of 30 to 35%, and loose spoils are more prone to erosion (Hoomehr et al. 2012a,b). SEDCAD performance has not been evaluated for FRA site conditions.

6.2 Methods and Material

6.2.1 Study Design

In order to compare measured versus model estimates for runoff and sediment yield, three active coal mining sites north of the city of Knoxville in East Tennessee were selected for study. Named per mining company ownership, the three study sites were: 1) *Premium*, located in Anderson County at N 36^{o} 6' 36", W 84^{o} 19' 30"; 2) *National*, located in Campbell County at N 36^{o} 30' 30", W 84^{o} 16' 12"; and 3) Mountainside, located in Claiborne County at N 36^{o} 31' 30",

W 83^{o} 57’ 23”. In general, mine spoils consisted of silty-clay soils mixed with larger gray shale and brown sandstone rocks. Specific CN and K factor values were generated for these sites over a 14-month monitoring period from June 2009 through July 2010, which during this period the sites were essentially devoid of vegetation (Hoomehr et al. 2010, 2012a,b). Rill development was most active during the first three months of this period. It was this 3-month period that was used in this study because of the active site erosion. In order to meet the study objectives, the following tasks were conducted:

1. Rainfall depths, basin hydrology (CN) , and erodibility (K) parameters based on the site monitoring data were entered as SEDCAD inputs; other hydrologic and RUSLE model input parameters were estimated using standard methodologies, or they were automatically computed in SEDCAD;
2. Per study site, sediment yields were computed for a series of model runs by varying rainfall depths to get erosivity values (R) from SEDCAD that matches the range of observed R values. Based on a computed erosivity by SEDCAD, sediment yields grouped by R classes (782.9, 548.0, 479.8, 286.4, and 128.8 $MJ \cdot mm \cdot h^{-1} \cdot ha^{-1}$), and measured sediment yields within these R classes were compiled in order to compare measured and modeled yields with similar erosivities; and
3. SEDCAD model output, sediment yield, was assessed as to its sensitivity to CN and RUSLE K factor input values. Estimated values for these two parameters, which are based on monitoring data, were used as a baseline for input parameters, and then change in model outputs due to deviation from this baseline was recorded.

6.2.2 SEDCAD Model Setup

To estimate sediment yields at a designated catchment outlet, SEDCAD input parameters include catchment size, slope length and gradient, channel slopes and roughness, storm frequency, catchment hydrology, erodibility, and type of control practices (Warner et al. 1998). The catchment area used in modeling for this study was the average of four field plots per site (Table 6). The NRCS Storm Type II with 241 point distribution was used for this study, and the design storm frequency (years) and duration (hours) was chosen by setting rainfall depth and hyetograph duration equal to observed values for the range observed during site monitoring.

6.2.2.1 *Catchment Hydrology*

Runoff volume and peak flow are calculated by the curve number methodology using the Soil Conservation Service TR-55 Emulator. SEDCAD is event-based and limited to the production of a 50-hour hydrograph, which is sufficient for catchments of less than 100 ha. The hydrology module in SEDCAD requires the following parameters: CN, time of concentration, and selection of a dimensionless unit hydrograph shape. A CN of 59 was used for the SEDCAD model input to test performance (Table 6), based on a study by Hoomehr et al. (2012a) that estimated CN values between 58.5 and 60 for low-compaction, steep sloped reclaimed surfaces using the rainfall-runoff depth (P-Q) frequency match approach. SECAD assumes an initial abstraction coefficient of 0.20 ($\lambda = 0.2$). SEDCAD calculates time of concentration using the input values for land cover, slope steepness, and length of catchment. For this study "*Nearly bare and untilled*" condition was selected from the list of default Land Flow Conditions within SEDCAD. Average slope steepness and plot length for the four plots per study site were used as input values (Table 6). The selected dimensionless unit hydrograph shape was fast hydrograph response.

6.2.2.2 Soil Erodibility

SEDCAD estimates sediment yields by surface erosion using RUSLE by:

$$A = R \cdot K \cdot LS \cdot C \cdot P$$

where, A = amount of soil loss or yield (kg/m^2); R = rainfall and runoff erosivity factor; K = soil erodibility factor, which is a soil loss rate per erosivity index unit for a specified soil as measured on a standard plot (22.13 m length and 9% slope) under annual tilled management conditions; LS = combined length-slope factor; C= cover management factor; and P = erosion control practice factor (Wischmeier and Smith 1978, SWCS 1993). SEDCAD automatically calculates rainfall-runoff erosivity factor (R) based on the hydrological inputs. R factors were also computed from measured precipitation data, where they ranged between 10.09 and 986.2 $MJ \cdot mm \cdot (ha \cdot h)^{-1}$ (Hoomehr et al. 2012a). The site average K-factor values for the first 3-months of the monitoring periods were used, which were 0.10, 0.33, and 0.35 $Mg \cdot ha \cdot h \cdot ha^{-1} \cdot MJ^{-1} \cdot mm^{-1}$ for Premium, Mountainside and National sites, respectively (Table 6). The model computes LS factors based on tabulated values in the USDA Agricultural Handbook Number 703 (Renard et al., 1997). Slopes' length and steepness are reported per site in Table 6.

Table 6. SEDCAD input values for erodibility (K) factor, CN, average slope steepness and length for National, Premium, and Mountainside study sites and Basin area.

Study Sites														
National					*Premium*					*Mountainside*				
K*	CN	Avg. Slope Length (m)	Avg. Slope (Degree)	Area (m^2)	K*	CN	Avg. Slope Length (m)	Avg. Slope (Degree)	Area (m^2)	K*	CN	Avg. Slope Length (m)	Avg. Slope (Degree)	Area (m^2)
0.35	59	48.35	20.3	1156	0.1	59	32.15	28.5	850	0.33	59	45.4	27.8	1054

* K unit is Mg. ha. h. (ha MJ mm)$^{-1}$; For National and Mountainside K = 0.34 (avg. of both sites) were used for simulation in Figure 26.

Because there was no vegetative cover on the study plots and no erosion control practices, C and P were set equal to 1 in the SEDCAD model runs.

6.3 Results and Discussion

Based on condition specific CN and K factors developed in Hoomehr et al. (2012a,b) for loose companion steep-sloped reclaimed surface mining sites, sediment yields generated by SEDCAD increased with increase in erosivity relative to measured yields (Figure 26). SEDCAD tended to overestimate sediment yields compared with all measured values, although those varied greatly among the three study sites. For example, within the 548 $MJ \cdot mm \cdot h^{-1} \cdot ha^{-1}$ R class, the SEDCAD sediment delivery estimate was 2.5 times that seen on the National site, 1.6 times that measured on the Premium site, and 1.4 times that measured on the Mountainside site. Although the K factors used in the SEDCAD model runs included the effect of rill development on erodibility, the variability of measured sediment yields among the three study sites was likely due to various factors that influence rill development (Yao et al. 2008, Zhang et al. 2009, Berger et al. 2010). These factors include spoil bulk density and % surface exposed large rock, soil moisture, and hydraulic roughness. Selection of the K factor affects computed sediment yields linearly, therefore percent differences between computed and measured are directly proportional.

Traditionally, the K factor would be constant per soil type and standard RUSLE unit plot conditions, and the C factor would be adjusted (Barfield et al. 1988; Haan et al. 1994). However, in the mining industry K has been used to reflect site erodibility before establishment of vegetative cover (McIntosh and Banhisel 1993, Toy et al. 1999). Hoomehr et al. (2012b) observed erodibility reductions over a 14-month period from a period of rill development to rill stabilization, where K dropped from about 0.35 to 0.1 $t \cdot ha \cdot h \cdot ha^{-1} \cdot MJ^{-1} \cdot mm^{-1}$. This study

focused on the period of rill development since it is the period that would generate the largest sediment yields needed for BMP design.

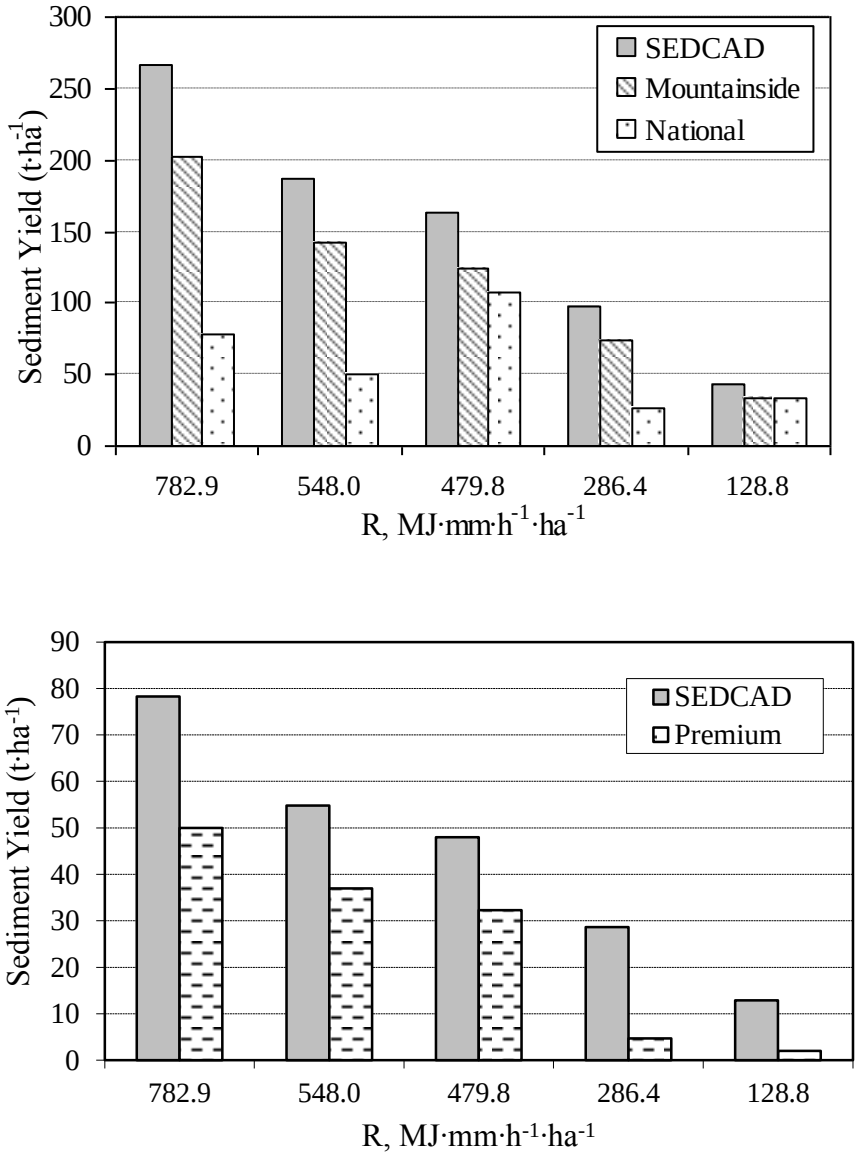

Figure 26. Sediment yields in $t \cdot ha^{-1}$ from measured amounts at National, Premium, and Mountainside study sites, and SEDCAD calculated amounts, grouped by erosivity (R) classes: 782.9, 548.0, 479.8, 286.4, and 128.8 $MJ \cdot mm \cdot h^{-1} \cdot ha^{-1}$.

Sensitivity of CN selection on sediment yields computed from SEDCAD was investigated using a base CN of 59, with deviations from this used for this analysis. A CN of 59 is the best estimate for the surface mining reclamation sites consisting of loose spoils on steep slopes (Hoomehr et al. 2012a). The percent change in sediment yields computed by SEDCAD due to the departure from a CN of 59 was estimated, and results are shown in Figure 27. SEDCAD appears to be sensitive to CN selection, where small changes in CN selection generate large changes in sediment yield. For example, a 40% deviation in selecting a CN will double the computed sediment yield. In order to examine the level of uncertainty for CN selection, complimentary curves for +/- 5% confidence intervals are also shown in Figure 27. Table 7 summarizes values used to construct Figure 27. The range in CN selection was determined by considering the range of CN values obtained from monitoring study sites, and the SEDCAD ability to reflect that change in its outputs.

Table 7. Percent difference in estimated sediment yields from the SEDCAD model relative to CN selection deviating from an average estimate of 59.

CN	Sed. Yield t/ha	CN Deviation			% Difference in Sediment Yields		
		CN = 59 *	+ 5% **	- 5% ***	CN=59 *	+ 5% **	- 5% ***
40	1.1	-0.33	-0.38	-0.27	-0.92	-0.94	-0.88
45	3.5	-0.25	-0.31	-0.18	-0.74	-0.81	-0.63
50	6.2	-0.17	-0.23	-0.09	-0.54	-0.66	-0.34
55	9.4	-0.08	-0.15	0.00	-0.31	-0.48	0.00
59	13.6	0.00	-0.08	0.09	0.00	-0.25	0.45
65	18.2	0.08	0.00	0.18	0.34	0.00	0.94
70	23.2	0.17	0.08	0.27	0.71	0.27	1.47
75	28.6	0.25	0.15	0.36	1.10	0.57	2.04
80	34.2	0.33	0.23	0.45	1.51	0.88	2.64
85	40.1	0.42	0.31	0.55	1.95	1.20	3.27
90	46	0.50	0.38	0.64	2.38	1.53	3.89
95	51.6	0.58	0.46	0.73	2.79	1.84	4.49
100	56.2	0.67	0.54	0.82	3.13	2.09	4.98

* The CN of 59 was estimated from site measurements using the asymptotic method (Hoomehr et al. 2012a)
** + 5% increase in estimating value of CN from 59.
*** - 5% increase in estimating value of CN from 59.

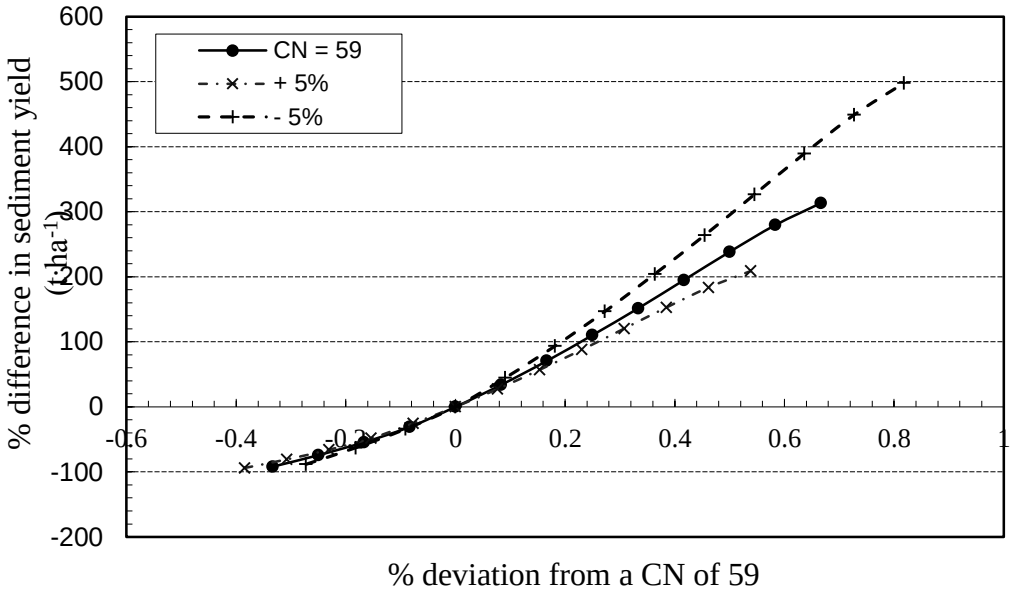

Figure 27. Percent difference in amount of estimated sediment yields ($t \cdot ha^{-1}$) relative to a percent deviation in CN selection from the measured estimate of 59 for loose compaction spoils on reclaimed surface coal mining sites.

6.4 Conclusions

SEDCAD performed reasonably in predicting sediment yield, but it should be noted that this test used just the hillslope erosion portion of SEDCAD and not the channel transport and the sediment basin settling routines, which are likely to add greater uncertainty. In spite of that limitation, the results are reasonable for low-compaction reclaimed surface coal mining sites considering the general predictive capabilities of sediment yield models based on RUSLE. This paper illustrates the importance of selecting CN and K factors that reflect site conditions. Specific to this study, reclaimed surface mining sites reflected FRA, loose compaction spoils on steep slopes, where a CN of 59 is reasonable, and a K factor of 0.35 $t \cdot ha \cdot h \cdot ha^{-1} \cdot MJ^{-1} \cdot mm^{-1}$ is acceptable during rill development (Hoomehr et al. 2012a.b). SEDCAD tended to overestimate sediment yields, up to 57% greater than the maximally measured yields as a function of erosivity.

It was also relatively sensitive to CN selection when CN increased from 59. This study provides SEDCAD users critical information of interpretation of model outputs for designing runoff and sediment control structures on reclaimed surface mining sites.

Chapter 7

Climate Change and Erosivity

7.1 Introduction

Climate change will effect soil erosion by changing the amount, pattern and erosivity of future rainfall events. In a broader perspective, it will influence soil erosion by causing shifts in land use necessary to meet the limitations of cropping under a new climatic system, and by changing plant biomass production, residue decomposition rates, soil microbial activity, evapotranspiration rates, and soil surface sealing and crusting (Williams et al., 1996). Variations in rainfall erosivity can have more significant impact on ecosystems than will the general global warming due to its wide domain of influence (Sauerborn et al., 1999; Allen and Ingram, 2002; Diodato et al. 2009). Based on the historical weather records, over the last century, the number of rainfall events and the event intensities are both increasing across U.S. (IPCC 2007; Nearing 2001). In a warmer climate, extreme precipitations and temperatures will increase more significantly than their related means (Hegerl et al. 2004). The global average soil erosion is projected to increase approximately 9% by 2090 due to climate changes (Yang et al. 2003).

The potential effects of climate change on erosion have been studied by scientists using different approaches. Favis-Mortlock and Boardman (1995) investigated changes in erosion rates due to the effect of climate change by using Erosion Productivity Impact Calculator (EPIC) model at the South Downs, United Kingdom. Their model, EPIC, was limited in its ability to model the complicated interactions in the erosional system as the climate changes (Pruski and Nearing 2002). The Water Erosion Prediction Project (WEPP) model was used by Favis-Mortlock and Savabi (1996) to determine the effects of change in CO_2 concentrations on water

balances, and crop biomass production rates. Sensitivity of erosion to changes in CO_2 concentration and temperature was investigated by Savabi and Stockle (2001), but no further evaluation was performed on the potential impact of precipitation changes on erosion. Using three different GCMs, soil erosion changes due to climate change effect in Mato Grosso State of Brazil were investigated using a CO_2-sensitive version of WEPP, which showed 27% to 55% increase in soil erosion (Savabi and Stockle 2001). Nearing (2001) used results of climate change scenarios from two GCMs to study potential changes in rainfall erosivity due to climate change across the United States for the 21st century. Study results showed a potential for erosivity change across much of the U.S. during 21st century, with a magnitude of change in the range of 16-58% (positive or negative). Based on Nearing's study, using the U.K. Meteorological Office's Hadley Centre HadCM3 coupled GCM, a 25-50% average increase in rainfall erosivity was projected for East Tennessee from 2000-2019 to 2080-2099. Pruski and Nearing (2002) used simulated climate data from the HadCM3 GCM to study potential impacts of climate change on soil erosion by water. They modeled erosion at eight locations within the U.S. using a modified version of the WEPP model to consider the effects of change in CO_2 concentrations on plant growth. Their investigation showed an increase in erosion rate when there is a significant increase in precipitation amount/intensity, while for decreases in precipitation amount/intensity the overall erosion can either increase or decrease, due to interactions between plant biomass, runoff, and erosion. Also, changes in rainfall intensity have a more significant impact on erosion rates than do changes in the number of rainy days, but this study concluded that future erosional studies under climate change should incorporate both factors. Finally, the study revealed that each 1% change in precipitation would result in a 2% change in runoff and approximately 1.7%

change in erosion, assuming that other environmental factors (CO_2 concentration, temperature, etc.) remain constant in future.

Data from most GCMs can provide scenarios of monthly and annual changes in total precipitation around the world (Nearing et al. 1990), but they do not have enough precipitation details (such as daily climate data at specific locations) in order to directly enable computation of the R factor for physically-based erosion models like RUSLE (McFarlane et al. 1992; Johns et al.1997; Nearing M.A, 2001; Zhang et al. 2010). Even GCMs that provide daily values at their grid scales still require spatial downscaling to generate climate data for a specific location of interest. If monthly projections from GCMs are to be used in erosion modeling–which is the case in most erosion studies–then both spatial and temporal downscaling are required (Zhang 2007).Generally, downscaling refers to techniques that have been used to fill the information gap between what the climate modeling community can provide and the information need by the impact research community (Wilby and Wigley, 1997).

Downscaling is generally divided into spatial and temporal techniques. Spatial downscaling derives finer resolution climate information from coarser resolution GCM outputs, as GCM resolution does not represent factors like topography and land cover that affect local climate. Spatial downscaling assumes that there are significant statistical relationships between local and large-scale climate that will remain valid under future climate conditions. Temporal downscaling derives fine-scale temporal data from coarser-scale temporal information, like derivation of daily data from monthly or seasonal information. The popular way of generating daily weather data from monthly information is through use of stochastic weather generator. The stochastic weather generator is a statistical model that generates time series of artificial weather data with the same statistical characteristics as the observations for the study region (Wilks and

Wilby, 1999). Daily weather series generated by different downscaling methods usually are statistically different and result in different soil erosion and runoff predictions for a specific climate change scenario (Zhang 2007).

Statistical downscaling methods have been used as a tool to investigate the effect of change in R factor (by change in monthly and annual precipitation amounts obtained from GCM outputs), on soil erosion (Zhang et al. 2010; Nearing, 2001; Renard and Freidmund, 1994), but these relationships have limitations, primarily with regard to snow dominated areas, and do not consider the impact of large changes in the storm intensity or duration on rainfall erosivity (Zhang et al. 2010). Because of these limitations to statistical downscaling, stochastic weather generators have been widely used to statistically downscale Regional Climate Models (RCMs), or GCMs projections to the location of interest (Wilks 1992; Semenov and Barrow 1997; Katz 1996; Mearns et al. 1997; Mavromatis and Jones 1998; Hansen and Ines 2005; Tisseuil et al. 2010; Zhang et al. 2010). In this method, present-date stochastic climate parameters are adjusted for GCM projected relative climate changes, then future climate series are generated using those perturbed parameter values (Zhang 2007). This method utilizes two spatial downscaling methods, termed implicit and explicit methods. More information can be found in Zhang (2007). The CLIGEN model (Nicks and Gander 1994) is a stochastic daily weather generator that uses a first-order two-state Markov chain to produce daily precipitation occurrence. The Markov chain is constructed per transition probabilities of a wet day following a wet day ($P_{w/w}$) and a wet day following a dry day ($P_{w/d}$). The daily mean precipitation is generated using a transformed, skewed, normal distribution while the daily maximum and minimum temperatures are generated using normal distributions (Zhang 2007). Previous studies showed that generated R-factors by CLIGEN are highly correlated with the measured R-factors (Yu 2002, 2003; Zhang et al. 2010).

Thus CLIGEN–together with the calibration formulas to adjust the generated R factor–is able to adequately generate R-factor values for RUSLE (Zhang et al. 2010).

Zhang et al. (2010) investigated rainfall erosivity changes under climate change using six GCM models under three emissions scenarios (A2, A1B, and B1). They computed downscaled mean annual precipitation and USLE rainfall erosivity (R factor) for the time periods 2030 through 2059 and 2070 through 2099 for northeast China. They established a new approach that combines the methods developed by Zhang (2005, 2007) to downscale monthly precipitation data from GCMs at time scales meaningful for modeling erosion processes, and the method developed by Yu (2002, 2003) that uses a weather generator (CLI GEN) to generate accurate RUSLE erosivity factors. Their study revealed that changes in rainfall erosivity under the higher greenhouse gas emissions scenarios (A1B and A2) show the highest projected changes, and those changes in erosivity do not spatially correspond to changes in total annual rainfall depths.

The objectives of this study were to assess potential future changes in rainfall erosivity under climate change in New River basin of East Tennessee, to correspond these changes to geographic location, and to match projected erosivity with historic erosivity at other parts of US. The Zhang et al. (2010) approach was utilized in this study to estimate future R-factor values for the New River basin at East Tennessee. Results from this study can widely be used to assess future soil erosion in this area, and to determine how effective current best management practices (BMPs) may be in reducing soil erosion and sediment delivery. The same method and technique is also applicable for other regions of interest.

7.2 Study area

The study area is located in the mountainous Cumberland Plateau region of Tennessee, within the New River basin. It covers a drainage area of 1026 km^2 and is contained in Anderson, Campbell, Morgan, and Scott counties of Tennessee (Carey, 1984) (Figures 28, 29, and 30). The New River basin has gone through a long history of logging and coal mining since the late 1800's (Gardner, 2006). Disturbances from coal mining and timber harvest on steep sloped terrain are still problematic in terms of erosion and sediment delivery (Massey 2008).

The New River basin originates near the Frozen Head State Park of Tennessee, north of Oliver Springs and east of Wartburg, and its intersection with the Clear Fork stream forms the basin's outlet (Figures 29 and 30). At the New River and Clear Fork confluence, the South Fork Cumberland River begins near the 497 km^2 (192 mi^2) Big South Fork National River and Recreation Area. It is a subbasin of the South Fork Cumberland Basin (HUC 05130104), which

Figure 28. Overlooking the New River Basin.

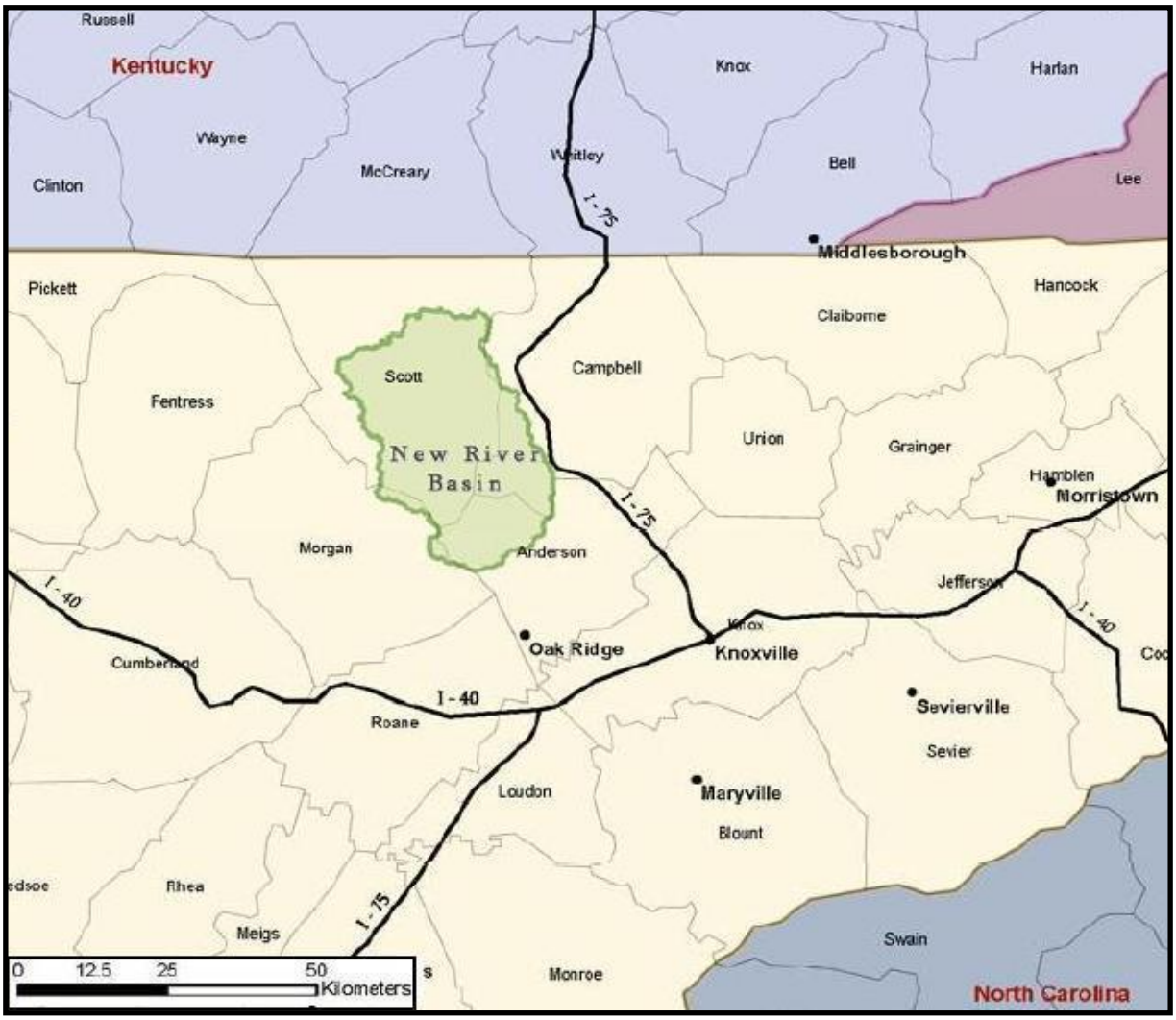

Figure 29. Location map of the New River Basin, TN (Massey 2008).

is part of the Ohio Water Resource Region (HUC 05). It contains a rugged terrain ranging in elevation from 335 m to 1006 m with an average hillslope of 25% (Overton, 1980, Massey 2008). The New River Basin is located in the humid climatic regions and has a moderate average annual temperature of 12.3°C (54.2 °F) and an abundant 1358 mm (53.4 inches) of annual rainfall. The area's climate tends to be the warmest in the

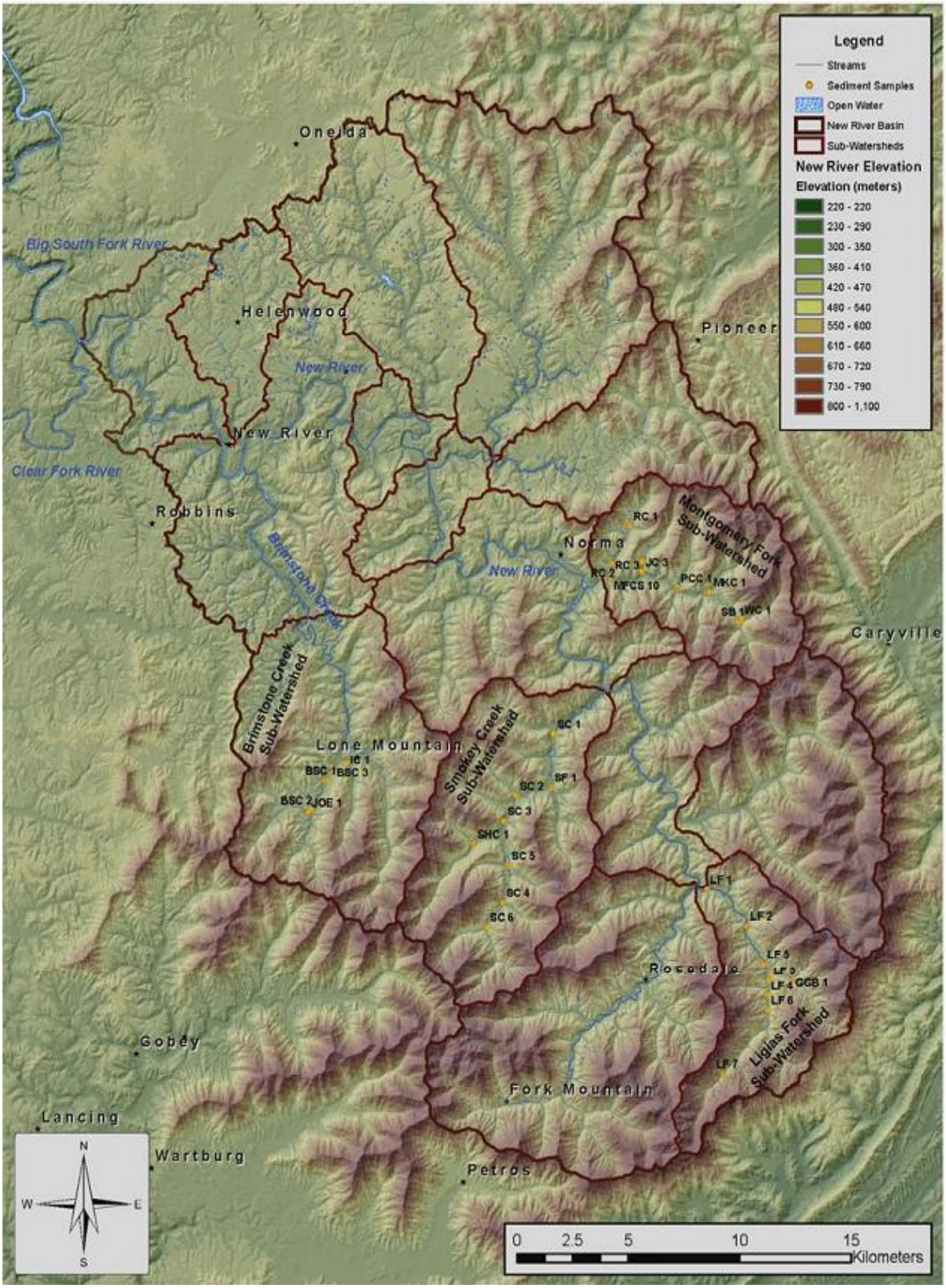

Figure 30. New River Basin, TN (Massey 2008).

month of July with an average temperature of 23.3°C (73.9 °F), while the coldest time of the year occurs in January with an average temperature of 1.0°C (33.8 °F) (NOAA, 2002). Therefore, this area observes warm to hot summers and mild winters (Massey 2008). The most rainfall occurs in March with nearly 133.35 mm (5.25 inches) of rain, but the rain continues throughout the summer months with monthly precipitation values near 127.0 mm (5.0 inches). The autumn season of September through October usually contains the least rainfall, with only 76.2 mm (3.0 inches) of rain during that period. Usually this area will see about an annual average of 1,270 mm (50 inches) of rainfall and 432 mm (17 inches) of snowfall in the mountains (Overton, 1980; Massey 2008).

7.3 Method

7.3.1 Climate change scenarios

The IPCC AR4 (IPCC 2007) coupled ocean-atmosphere GCM-CCSM simulation was used to estimate potential future change for erosivity (R-factor). To consider the different greenhouse gas (GHG) emission scenarios, three non-mitigated IPCC Special Report on Emission Scenarios (B1, A1B, and A1FI) were selected (IPCC 2007). To calibrate the GCM results, the observed historic data for New River Basin was gathered from National Ocean and Atmospheric Administration (NOAA), for the Oneida, TN weather station (Lat/Lon: 36°30'N / 84°32'W) for 1959-1999, and these data were used as the baseline period. In order to meet the study objectives, the following tasks were conducted:

1- A special-temporal downscaling method developed by Zhang (2005, 2007) was used to downscale the monthly precipitation data of GCM-projections from GCM-grid scale to the scale of the Oneida weather station.

2- Using observed daily weather data from Oneida local station, for 1959-1999, the baseline CLIGEN input parameters (R_d, σ^2_d, $P_{w/d}$, $P_{w/w}$) were determined.

3- Linear relationships between $P_{w/w}$ and mean monthly precipitation (R_m) and between $P_{w/d}$ and R_m were developed. Future conditional transition probabilities of precipitation were estimated from these linear relationships. Adjusted mean daily precipitation per wet day, R_d, and new daily precipitation variance related to monthly precipitation variance at the station, σ^2_d, were calculated using future conditional transition probabilities.

4- Using adjusted parameters (R_d and σ^2_d) along with future conditional transition probabilities as input parameters for CLIGEN, 100 years of daily series data, 2010-2099, were generated for the station for each climate change scenario.

5- Outputs for 100 years of daily series at each station from CLIGEN were used to calculate storm energy (E) and 30-minute maximum rainfall intensity (I_{30}) for each future storm, and R-factors were calculated based on them for each GHG scenario.

6- In order to correspond future change in rainfall erosivity in New River basin with geographic location and to match projected erosivity with historic erosivity for other parts of US, the erosivity map of the Eastern United States developed by Renard et al. (1993) was used as a frame of reference, and related erosivities were compared to that.

7.3.2 Downscaling and R-factor calculations

The special-temporal downscaling method developed by Zhang (2005, 2007) was used to downscale the monthly precipitation data of GCM-projections from GCM-grid scale to scale of Oneida weather station.

Spatial downscaling

Q-Q plots of the observed monthly precipitation from local gage and CCSM model data, were produced for the time period 1959-1999, with each dataset ranked first, in order of magnitude. For each month, both linear and non-linear regression functions between the two sets of ranked values were developed. To downscale GCM-projected future monthly precipitations, for the values within the data range for which the regression function was built, a nonlinear function was used, while in order to generate a conservative first-order approximation the linear function was used for the values outside of the initial range. For each month, 2010-2099 downscaled monthly precipitation values (with their means and variance) were obtained for the station.

Temporal downscaling

To estimate CLIGEN input parameters, temporal downscaling followed the Zhang (2005, 2007) method, so a brief description of that procedure is included here. More details and complete description can be found in the original literature. Basically, CLIGEN was used as a tool to generate daily weather series representing the future climates. To begin, using observed daily weather data from Oneida local station for 1959-1999, the baseline CLIGEN input parameters were determined. CLIGEN requires four precipitation parameters in order to generate weather series, which are the following: R_d, daily mean precipitation; σ^2_d, variance of daily precipitation for wet years (days with non-zero precipitation); $P_{w/d}$, Markov chain's conditional transition probabilities of a wet day following a dry day; $P_{w/w}$, Markov chain's conditional transition probabilities of a wet day following a wet day.

Based on the daily precipitation amounts of observed data (1959-1999), $P_{w/w}$ and $P_{w/d}$ were computed and used to develop a linear relationship between $P_{w/w}$ and mean monthly

precipitation (R_m), as well as relationships between $P_{w/d}$ and R_m. Future conditional transition probabilities of precipitation were estimated from these linear relationships (Zhang et al. 2010), as

$$\pi = (P_{w/d})/ (1+ P_{w/d} - P_{w/w}) \quad (15)$$

$$r = P_{w/w} - P_{w/d} \quad (16)$$

$$R_d = R_m / (N_d \pi) \quad (17)$$

$$\sigma^2_d = \sigma^2_m / (N_d \pi) – (1- \pi) \cdot (1+ r) R_d^2 / (1-r) \quad (18)$$

where R_d is adjusted mean daily precipitation per wet day, N_d is the number of days in the month, and σ^2_d is the new daily precipitation variance related to monthly precipitation variance at the station. Using these adjusted parameters as input parameters for CLIGEN, 100 years of daily series data was generated for station for each climate change scenario.

R-factor calculation

The outputs of 100 years of daily series at each station from CLIGEN were used to extract precipitation depth P (mm), storm duration D (h), time to peak as a fraction of storm duration t_p, and the ratio of peak intensity over the average intensity i_p, in order to calculate R factors (Nicks and Gander, 1994). A fuller description of the algorithm and steps in the calculations can be found in Yu (2002, 2003).

All storms on wet days that had a mean air temperature greater than zero were used. The peak I_{30} for each storm was calculated using Eqs. 19 and 20:

$$I_{30} = 2P \text{ for } D \leq 30 \text{ min} \quad (19)$$

$$I_{30} = \frac{2Pi_p}{bt_p} \left(1 - \exp\left(\frac{bt_p}{2D}\right)\right) \quad (20)$$

where b is a parameter describing the storm pattern (more details are in Zhang et al. 2010).

The storm energy (E) for each chosen storm was calculated as the integration of unit energy (e) over the double exponential storm pattern in CLIGEN:

$$E = P e_0 [1 - \frac{\propto i_p}{b t_p} \frac{I_0}{I_p} \left(e^{\frac{I_p}{I_0} e^{-b t_p}} - e^{-\frac{I_p}{I_0}} \right)] \quad (21)$$

where I_p is peak intensity ($mm \cdot h^{-1}$) and e is the unit energy calculated using the erosivity equation in RUSLE (Renard et al., 1997):

$$e(i) = e_0(1-\alpha e^{-I/I_0}) \quad (22)$$

where e_0 = 0.29 MJ ha^{-1} mm^{-1}, α = 0.72, and I_0 = 20 $mm \cdot h^{-1}$ (Brown and Foster, 1987). Storm rainfall erosivity (EI), defined as the product of I_{30} and E, was calculated for each storm and then the monthly mean EI values were obtained to compute the R factor, which is the sum of monthly mean EI values (Zhang et al. 2010).

7.4 Results and Discussion

Values for the four main parameters R_d, σ^2_d, $P_{w/d}$, and $P_{w/w}$ were calculated based on the 40 years of observed data (1959-1999), and used to establish linear and nonlinear relationships between $P_{w/w}$ and mean monthly precipitation (R_m), as well as relationships between $P_{w/d}$ and R_m (Table 8 and Figure 31). Monthly distribution of the historic-$P_{w/w}$ shows higher probability during summer and early winter, with the maximum probability in June (Figure 31).

As anticipated, the monthly distribution of the historic-$P_{w/d}$ followed a nearly symmetric pattern to $P_{w/w}$, with an axis of symmetry around P= 0.38. The historic-$P_{w/w}$ and -$P_{w/d}$ almost converged on the same value during October, P= 0.38, which represents the minimum value for $P_{w/w}$ and the maximum value for $P_{w/d}$. Both distributions, $P_{w/w}$ and $P_{w/d}$, show a cosine pattern throughout the year, and conform (inversely for $P_{w/d}$) to the historic (1959-1999) average monthly rainfall distribution for the study region (see R_m in Table 8).

Table 8. Monthly values for $P_{w|w}$, $P_{w|d}$, R_m, R_d, and $б_d$ obtained from observed data, 1959-1999, at Oneida station.

Observed Data (Oneida), 1959-1999					
Month	$P_{w\|w}$	$P_{w\|d}$	R_m mm/month	R_d mm/day (rainy)	$б_d$ for precipitation. mm/month
Jan.	0.41	0.31	117.2	10.6	8.4
Feb.	0.40	0.33	110.5	10.9	8.4
Mar.	0.43	0.33	136.9	11.9	9.4
Apr.	0.44	0.29	113.6	11.1	8.1
May	0.48	0.28	128.5	11.4	8.9
Jun.	0.49	0.26	122.6	11.9	8.9
Jul.	0.43	0.31	136.9	12.4	9.6
Aug.	0.41	0.32	106.6	12.4	8.6
Sep.	0.40	0.32	97.50	12.1	8.4
Oct.	0.38	0.34	94.90	11.9	7.9
Nov.	0.45	0.30	109.0	11.2	8.4
Dec.	0.45	0.30	120.6	11.1	8.9

Table 9. CLIGEN input parameters from GCM-CCSM.

CCSM Data 2010-2099												
	B1				A1FI				A1B			
Month	$P_{w\|w}$	$P_{w\|d}$	R_d mm/d	$б_d$ mm/d	$P_{w\|w}$	$P_{w\|d}$	R_d mm/d	$б_d$ mm/d	$P_{w\|w}$	$P_{w\|d}$	R_d mm/d	$б_d$ mm/d
Jan.	0.46	0.30	11.90	13.96	0.48	0.28	12.01	15.15	0.46	0.30	12.20	17.98
Feb.	0.41	0.35	12.56	9.75	0.43	0.33	12.80	15.04	0.42	0.34	12.65	14.93
Mar.	0.45	0.31	12.07	11.24	0.49	0.27	12.20	13.48	0.47	0.29	11.97	13.02
Apr.	0.44	0.32	11.95	7.50	0.45	0.31	12.42	11.09	0.45	0.31	12.04	8.81
May	0.47	0.29	11.73	11.64	0.50	0.26	12.23	10.79	0.49	0.27	11.68	10.25
Jun.	0.52	0.24	12.01	8.64	0.58	0.18	12.50	14.55	0.54	0.22	12.16	10.67
Jul.	0.46	0.30	13.11	9.14	0.49	0.27	13.80	17.18	0.49	0.27	13.29	12.95
Aug.	0.45	0.31	13.20	5.08	0.46	0.30	13.61	10.82	0.47	0.29	13.31	8.89
Sep.	0.44	0.32	13.12	13.18	0.43	0.33	13.39	15.75	0.44	0.32	13.01	12.27
Oct.	0.40	0.36	12.70	8.64	0.38	0.38	12.85	7.80	0.39	0.37	12.51	7.91
Nov.	0.44	0.32	11.97	12.55	0.44	0.32	12.49	20.19	0.44	0.32	11.88	14.54
Dec.	0.45	0.31	11.84	12.77	0.47	0.29	12.21	17.87	0.49	0.27	11.89	18.59

The CLIGEN input parameters were computed for the period 2010-2099 for each GHG emission scenario and calendar month, based on the CCSM model output data (Table 9). These values were obtained using the linear and nonlinear relationships developed from the observed and historic data between $P_{w/w}$, $P_{w/d}$, and R_m (Table 8), and it was assumed that those relationships remain the same for all future years. The monthly patterns of projected $P_{w/w}$ and $P_{w/d}$ for each emission scenario are almost symmetric. Generally, the A1FI has the highest and B1 has the lowest $P_{w/w}$ value within a month. All the scenarios show equal or higher projected $P_{w/w}$ compared to historic values within a month (Figure 31). A higher projected $P_{w/w}$ value indicates a higher chance of rainfall and thus implicitly indicates higher future rainfall.

Adjusted mean daily precipitations per wet day, R_d, for the observed and projected period are shown in Figure 32. Generally, most emission scenarios show higher adjusted mean daily precipitation value in the future, compared to the historic data. A1B and B1 scenarios produce almost the same results, while A1FI looks more different than the other scenarios. Average changes in mean annual precipitation during the projection period (2010-2099) relative to the historic period (1959-1999) show 20%, 14%, and 9% increases in mean annual precipitation under the A1FI, A1B, and B1 scenarios, respectively (Figure 33).

Incorporating calculated values for input parameters into CLIGEN and using Eqs. (19) through (22), projected rainfall erosivity for the 2010-2099 period were estimated. Projected average monthly erosivities for the New River Basin, TN are tabulated in Table 10 and are shown in Figure 34. The average annual rainfall erosivity for New River Basin, TN during 1959-1999 period was 4085 MJ mm·h^{-1}·ha^{-1} (240 $\frac{hundreds\ of\ foot.tonf.inch}{acre.hour.year}$). The results of this study predict increases in monthly and annual rainfall erosivity at the New River Basin, for future

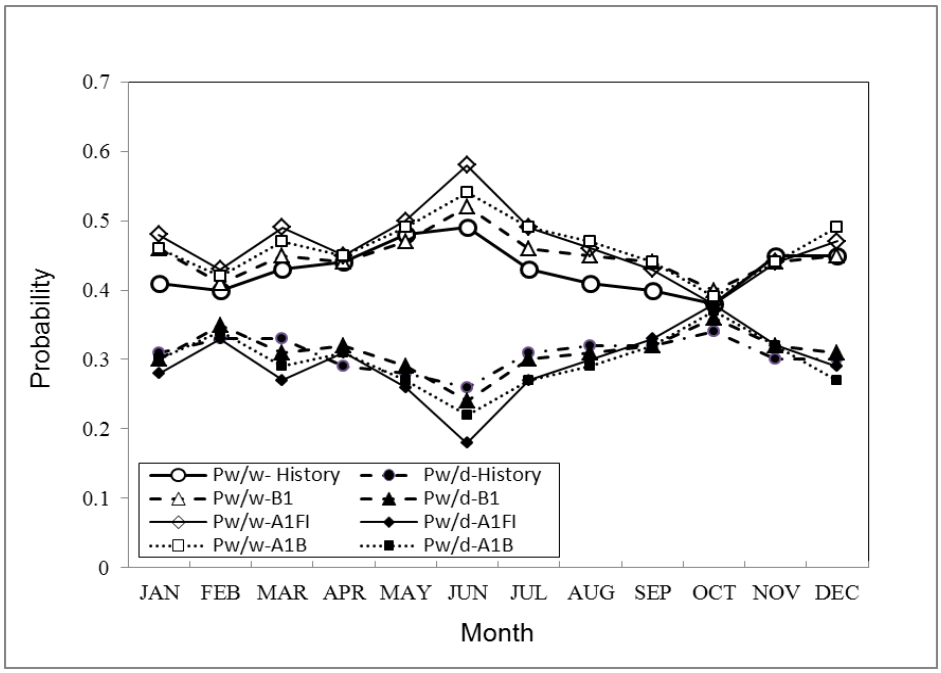

Figure 31. $P_{w/w}$ and $P_{w/d}$ calculated based on the 40 years of observed data, 1959-1999, and their projection for different GHG emission scenarios plotted against different months of year.

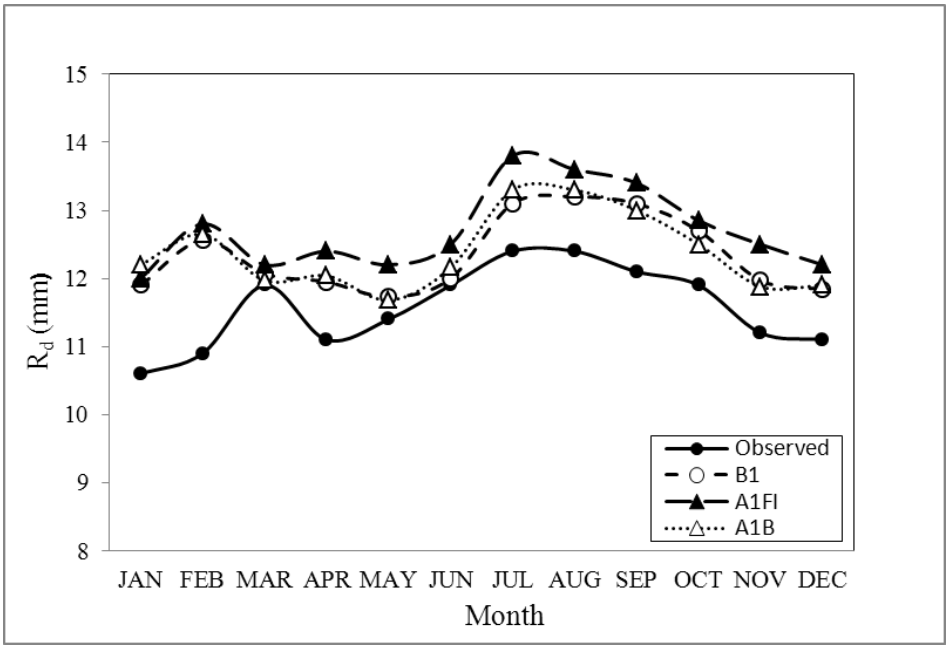

Figure 32. Adjusted mean daily precipitation per wet day, R_d, distributed during months of year for the observed, 1959-1999, and projected period, 2010-2099, under three GHG scenarios.

years (2010 – 2099) based on all three GHG emission scenarios. The average annual rainfall erosivity for the B1 scenario is 4525.5 $MJ \cdot mm \cdot h^{-1} \cdot ha^{-1}$, for the A1B scenario is 5376.2 $MJ \cdot mm \cdot h^{-1} \cdot ha^{-1}$, and for the A1FI scenario is 6281.3 $MJ \cdot mm \cdot h^{-1} \cdot ha^{-1}$. All three scenarios produce similar rainfall erosivity distributions during the projection period. Although the average projected rainfall erosivity reaches its maximum value with A1FI scenario and its minimum with B1, while the A1B is in between, this trend was not followed for each month. For instance, during September and October the B1 scenario shows higher values than the same period in the A1B scenario. This may indicate that as GHG concentration in atmosphere increases, these months of year will face lower precipitation. Projected mean annual erosivity (R factor) values show 49%, 28%, and 7% increases in comparison to the historic period (1959-1999), under A1FI, A1B, and B1 scenarios, respectively (Figure 35). Nearing (2001) results are consistent with the

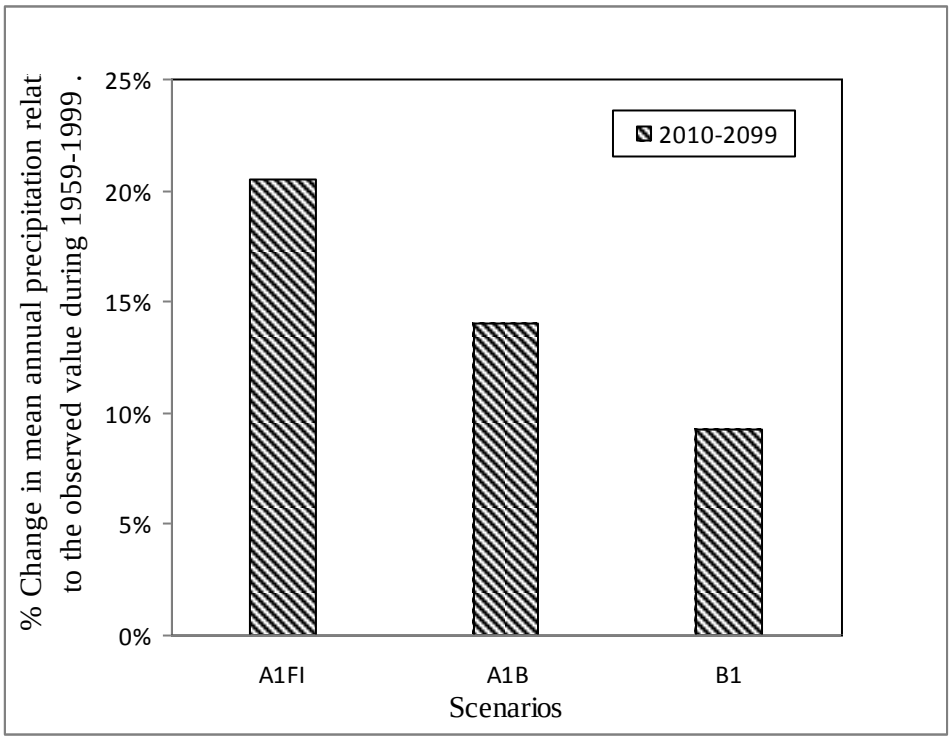

Figure 33. Average change in mean annual precipitation during projection period, 2010-2099, relative to the historic data, 1959-1999, presented in percentage (%).

Table 10. Monthly and yearly average rainfall erosivity values for 2010-2099.

GHG*	JAN	FEB	MAR	APR	MAY	JUN	JUL	AUG	SEP	OCT	NOV	DEC	Yr. R**
						MJ mm h^{-1} ha^{-1}							
A1FI	229	341	398	527	631	921	1182	570	507	207	424	342	6281
A1B	319	303	329	456	563	810	992	522	361	182	277	262	5376
B1	139	142	310	357	550	702	880	477	429	201	200	138	4525

* Greenhouse gas emission scenarios

**Yearly rainfall erosivity (divide by factor 17.02 to convert into ($\frac{hundreds\ of\ foot.tonf.inch}{acre.hour.year}$))

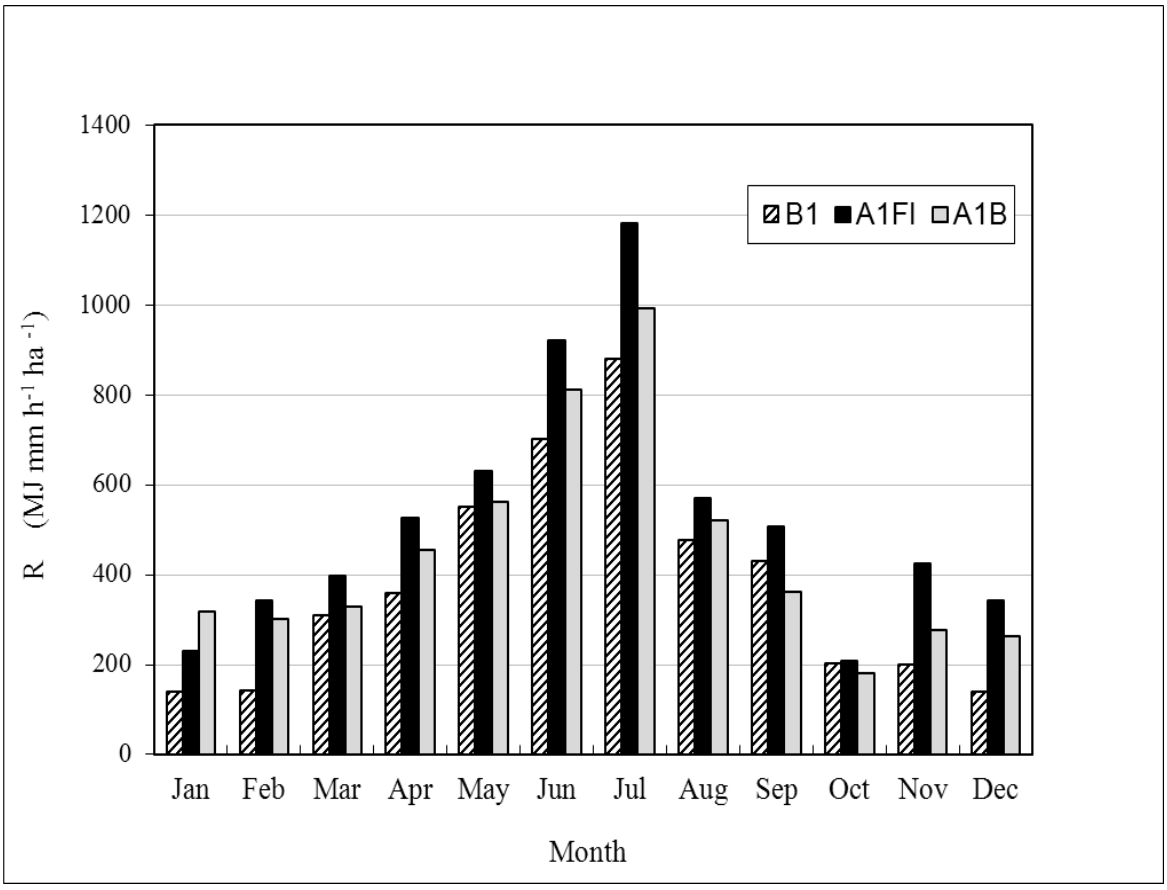

Figure 34. Rainfall erosivity for period 2010 – 2099 (New River Basin, TN).

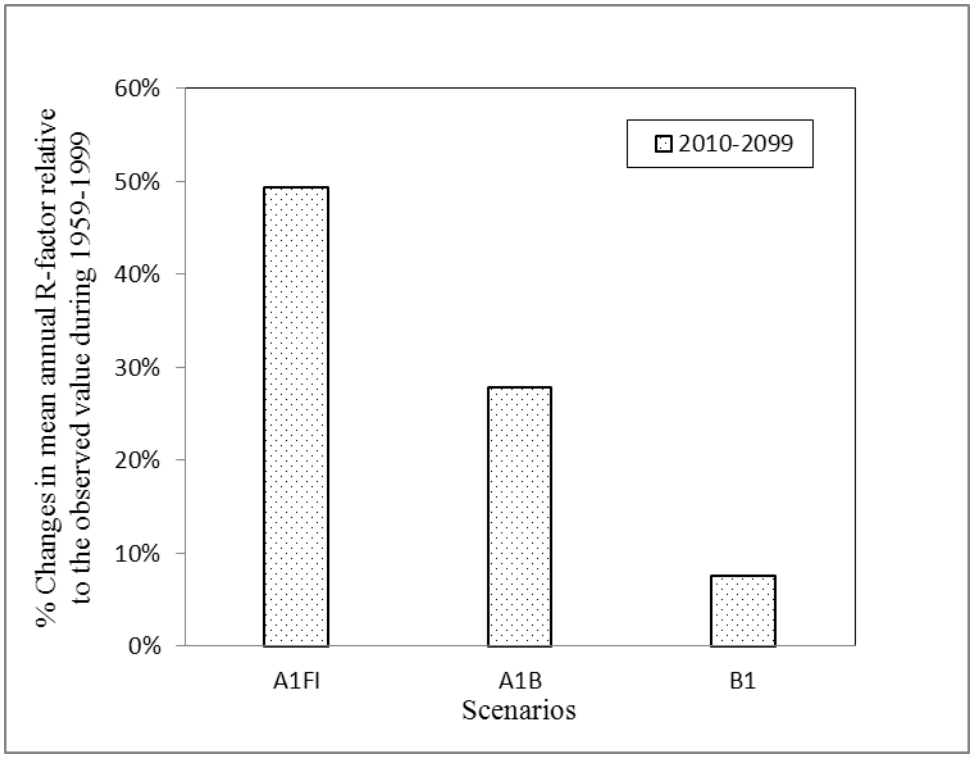

Figure 35. Changes in mean annual R-factor relative to the observed value during 1959-1999.

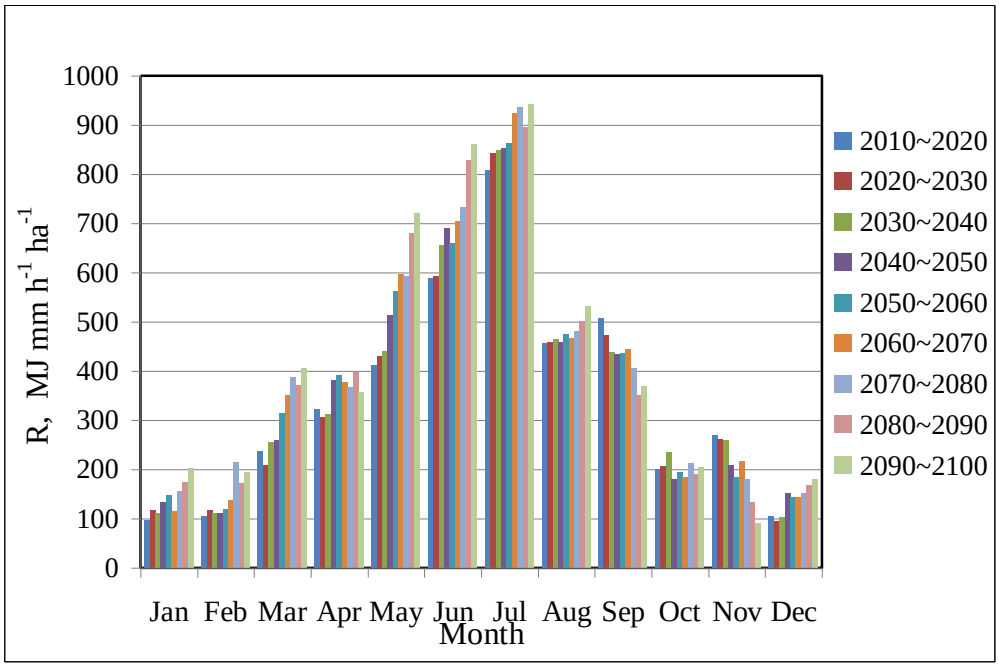

Figure 36. Rainfall erosivity ($MJ \cdot mm \cdot h^{-1} \cdot ha^{-1}$) distribution for B1 greenhouse gas emission scenario during projection period (2010~2099) and for different months.

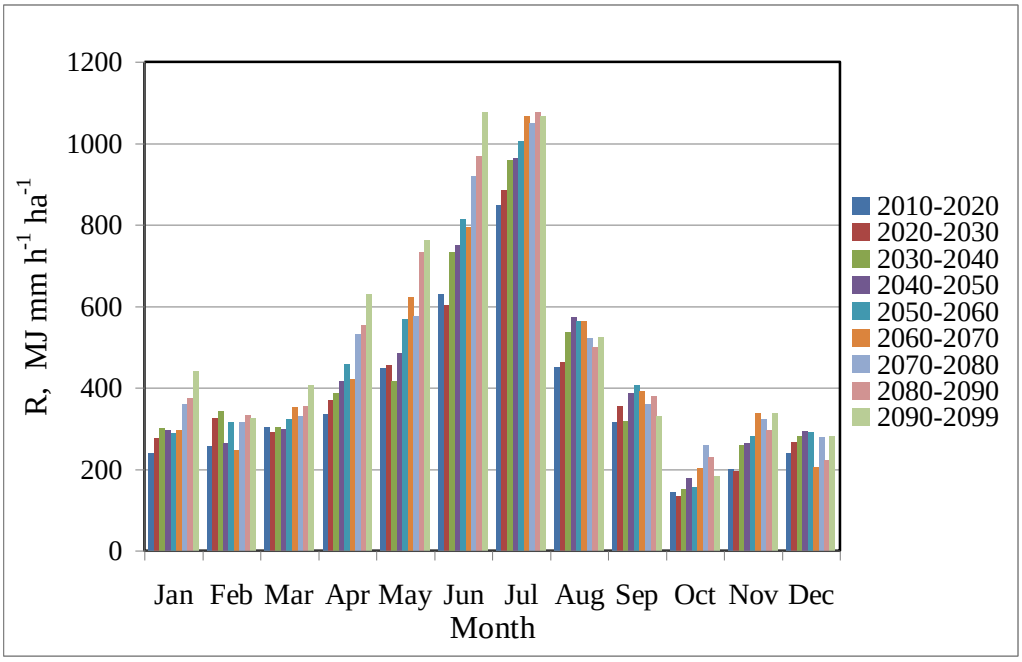

Figure 37. Rainfall erosivity ($MJ \cdot mm \cdot h^{-1} \cdot ha^{-1}$) distribution for A1B greenhouse gas emission scenario during projection period (2010~2099) and for different months.

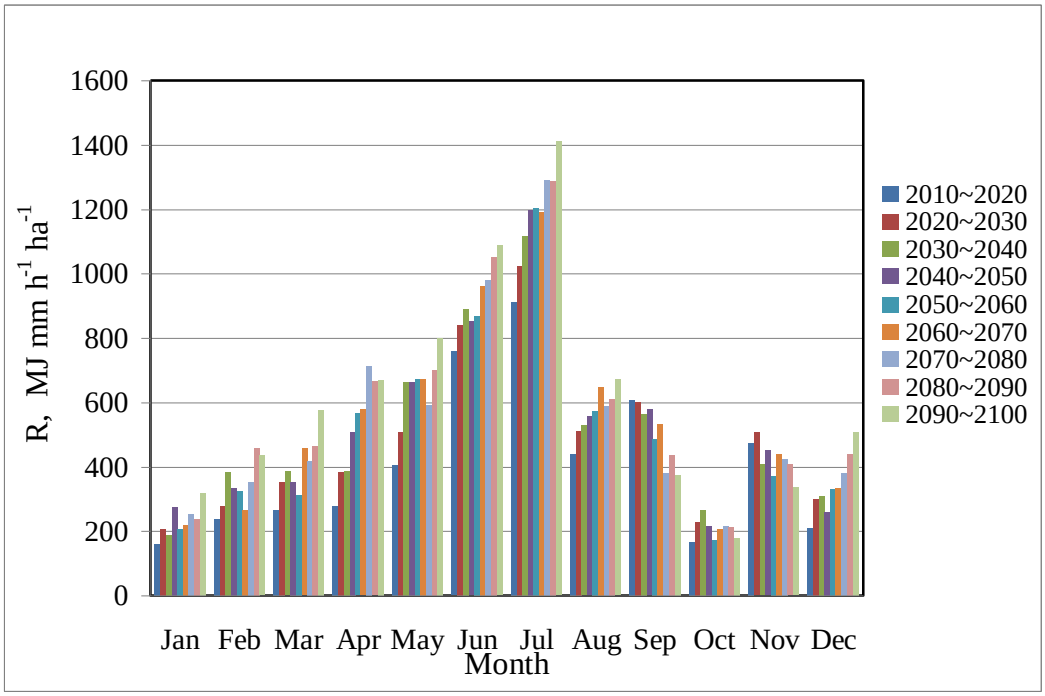

Figure 38. Rainfall erosivity ($MJ \cdot mm \cdot h^{-1} \cdot ha^{-1}$) distribution for A1FI greenhouse gas emission scenario during projection period (2010~2099) and for different months.

findings of this study.

To better investigate future potential changes in rainfall erosivity, computed erosivities for 2010 through 2099 were grouped and averaged over 10-year periods (Figures 36, 37, and 38). Generally, erosivity increases within each month throughout the projection period (2010 ~2099), except for September and November for the B1 and A1FI scenarios. In general, increases in erosivity for January through July are greater after 2050. May, June, and July show more sensitivity to climate change, and at least a 60% increase in erosivity is projected for each of these months by end of 2099.

7.4.1 Projected erosivities and U.S. erosivity map

To correspond change in future rainfall erosivity with geographic location and match projected erosivity for New River basin with current erosivity at other parts of US, the erosivity (R factor) map of Eastern United States developed by Renard et al., (1993) was used as a frame of reference. Average annual rainfall erosivities for 10-year periods and for each GHG scenario were plotted on the map (Figures 39, 40, and 41). Paths that represent increases in erosivity were plotted in a way that always remain perpendicular to erosivity isolines.

The erosivity map that developed by Renard et al., (1993) represents erosivity at Eastern United States for about 1990. The historic data at Oneida station, 1959-1999, shows about a 20% increase in erosivity by the beginning of 21st century, gaining erosivity like what Chattanooga, TN experienced by about 1990. Projected erosivity for all three GHG emission scenarios almost follow the same path on the erosivity map toward Alabama, while for A1B and A1FI scenarios study area will ultimately gain erosivity like what central to Southern Alabama experienced in about 1990. For B1 scenario, by the end of projection period at 2099, erosivity at the study area

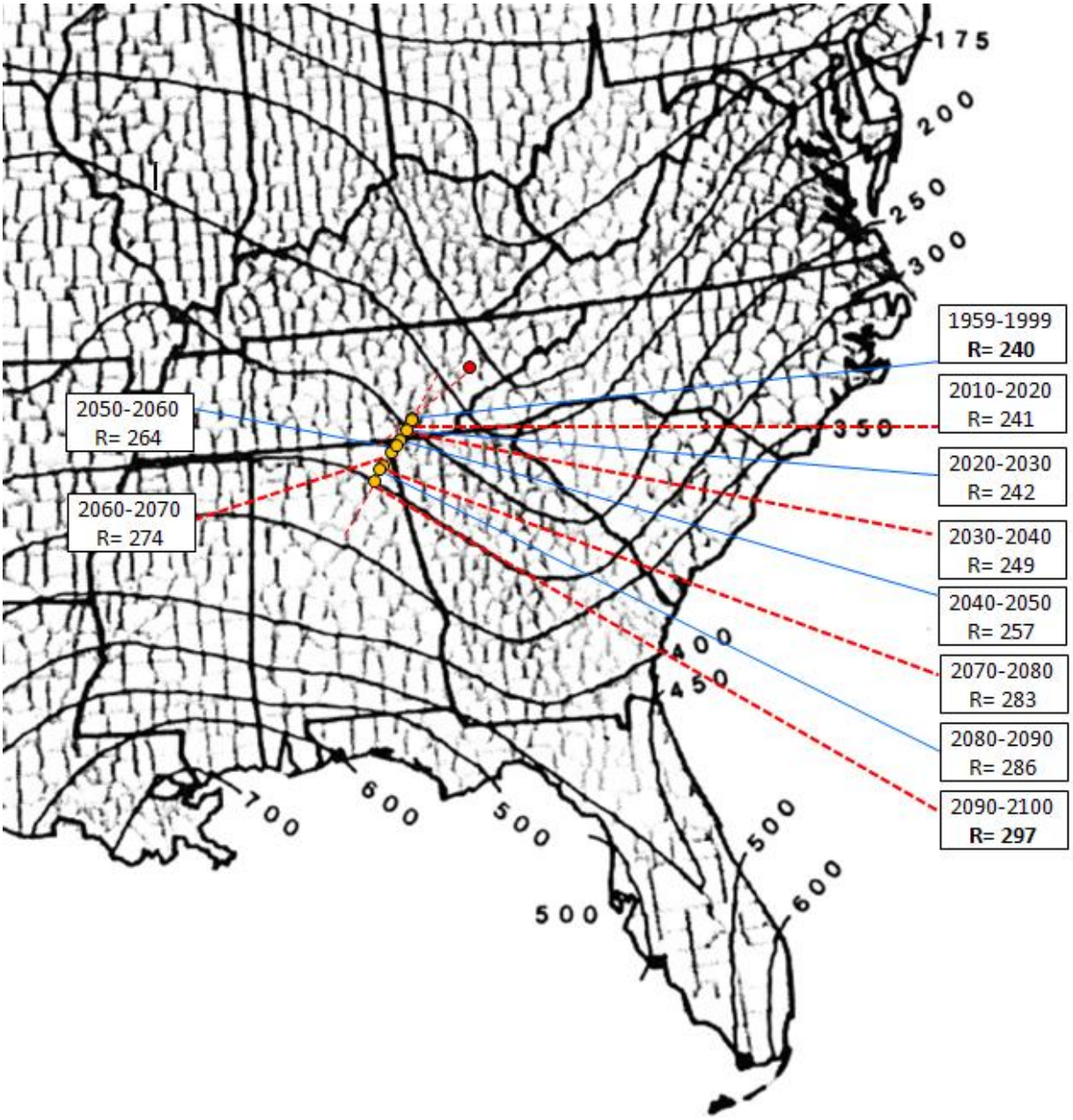

Figure 39. Historic rainfall erosivity (1959-1999) and projected erosivity for the B1 scenario (2010 ~2099) plotted on erosivity map of Eastern US. Isolines of annual erosivity (R factor) for the Eastern United States were developed by Renard et al., (1993); R factors are in ft·tonsf·in / (acre·hr·yr). Multiply by 17.02 to convert into MJ·mm·h^{-1}·ha^{-1}. The red point shows the location of the study area.

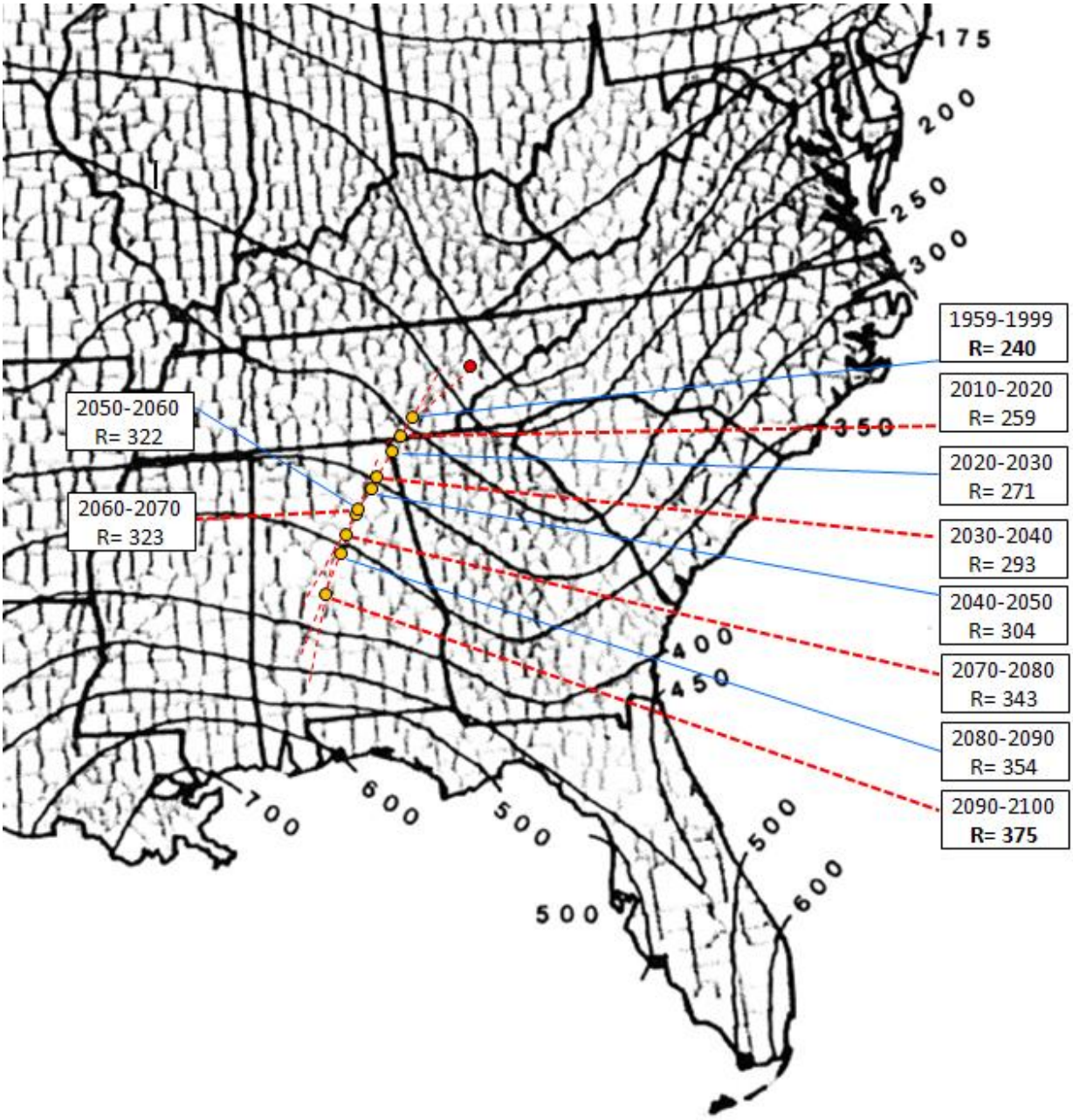

Figure 40. Historic rainfall erosivity (1959-1999) and projected erosivity for the A1B scenario (2010 ~2099) plotted on erosivity map of Eastern US. Isolines of annual erosivity (R factor) for the Eastern United States were developed by Renard et al., (1993); R factors are in ft·tonsf·in / (acre·hr·yr). Multiply by 17.02 to convert into $MJ \cdot mm \cdot h^{-1} \cdot ha^{-1}$. The red point shows the location of the study area.

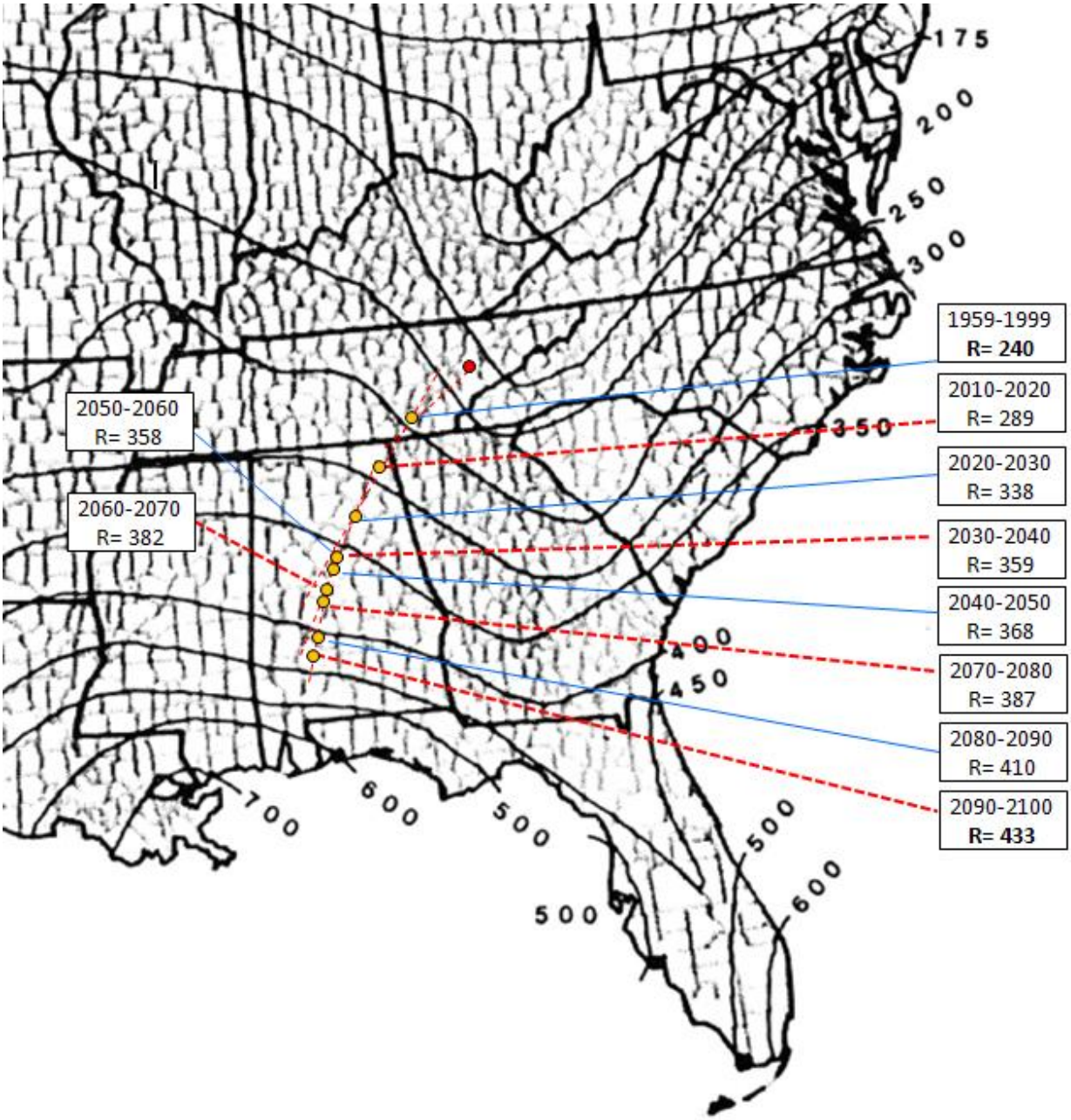

Figure 41. Historic rainfall erosivity (1959-1999) and projected erosivity for the A1FI scenario (2010 ~2099) plotted on erosivity map of Eastern US. Isolines of annual erosivity (R factor) for the Eastern United States were developed by Renard et al., (1993); R factors are in ft·tonsf·in / (acre·hr·yr). Multiply by 17.02 to convert into MJ·mm·h^{-1}·ha^{-1}. The red point shows the location of the study area.

will be almost the same as what Gadsden, AL experienced by about 1990. For A1B scenario projected erosivity at study area will be the same as Brent, AL for about 1990, and for A1FI erosivity will be like what experienced by Thomasville, AL for about 1990. These results show that rainfall erosivity at New River basin will increase between 10 to 50% by the end of 21st century, which will result in 10 to 50% increase in sediment yield, based on the linear relationship between erosivity and erosion rate in RUSLE, so current BMPs used in the study region will not adequately mitigate the effects of sediment yield from disturbed areas. This has been said, the requirements by the state of Alabama in designing and implementing the BMPs can be utilized for the study region in future years, as they were adequate enough about 1990 to control erosion and sediment yield within the state of Alabama.

Performance of BMPs may be affected by change in climatic variables over time. While increase in rainfall depth may result in shorter residence time and high runoff volume that can bypass a BMP, increases in temperature and CO_2 concentrations may accelerate vegetation growth and as a result increase the effectiveness of BMPs like vegetative filter strips. On the other hand, an increase in rainfall and runoff intensity may produce higher sediment loads that existing BMPs may not be able to mitigate. Assessing changes in BMP effectiveness and water quality due to climate change are significant issues that regulators, watershed managers, and stakeholders are facing. As rainfall erosivity is a key driving factor in erosion and sediment yield, quantifying potential future change in rainfall erosivity enable designers to adequately design BMPs for sediment yield as a non-point source pollutant. For example, structures like sediment ponds with minimal sediment inflow should continue to function effectively for years without any significant maintenance, but excessive sediment yield due to increase in rainfall erosivity may exceed their capacity or substantially decrease their effective operating lifetime.

7.5 Conclusion

This study investigated potential changes in future rainfall erosivity due to climate change in the new River basin of the southern Appalachian region for the time period 2010-2099 and for greenhouse gas emission scenarios B1, A1B, and A1FI of the CCSM model. Results showed that for all three scenarios, the rainfall erosivity will increase with similar monthly distribution within a year. The greatest increase in R-factor is related to the A1FI and the least is from the B1 scenario. A study by Nearing (2001) projected a 25-50% average increase in annual rainfall erosivity for East Tennessee from 2000-2019 to 2080-2099, and results from this study are consistent with his findings, suggesting a 7-49 % increase in annual rainfall erosivity from 2010 to 2099 based on different emission scenarios. The projected mean annual erosivity (R factor) shows a 49%, 28%, and 7% increase in comparison to the historic period (1959-1999), under the A1FI, A1B, and B1 scenarios, respectively.

Projected erosivities found by this study suggest that by about 1990 the annual rainfall erosivity in the study region was about the same as what is currently experienced by northern to central Alabama. The results from this study can widely be used to assess the potential future change in soil erosion in this area, and to evaluate the extent of future effectiveness of current BMP in reducing soil erosion and sediment delivery from coal mining sites located at the study area. The same method and technique is applicable for other regions of interest.

Summary

The primary focus of this research entails surface-water hydrology, erosion, and sediment transport on low-compaction steep sloped reclaimed surface coal surfaces, and the interaction of those processes with climate change. Establishment of native forest covers on these reclaimed slopes has recently become a priority and a US Department of Interior Office of Surface Mining directive focus of interest. The traditional method of using excessive compaction to achieve a more stable slope with a lower rate of erosion has previously been an obstacle to this native forest growth, due to low chance of root penetration. Consequently, a lower level of compaction in Forestry Reclamation Approach (FRA) has been introduced in the reclamation process, but there is not much information about the effect of this approach on the hydrology, erosion and sediment yield from the sites reclaimed using this method. To address this problem, three different active coal mine sites in the Appalachian region of East Tennessee were monitored during a 14-month period for hydrograph parameters, erosion rate, and sediment delivery.

The first study (Chapter 4) in this research addressed a significant lack of scientific information about the effects of FRA technique on the hydrology of steep sloped reclaimed surfaces, specifically addressing lack of a good representative curve number (CN) value. This study estimated CN values for low-compaction steep-sloped reclaimed surfaces by using natural precipitation-runoff data and utilizing both a standard technique and the asymptotic method as described by Hawkins (1993). Results showed that the differences due to spatial variation in rainfall and use of different reclaimed material between the original CN average values estimated for three different study sites were not statistically significant. Both asymptotic methods – that based on Hawkins (1993) and its modified version which uses I_{30} instead of P − suggest a standard asymptotic behavior for the study sites, with P-independent CN values around 58.5~60. Determining a CN value for low

compaction reclaimed surfaces is important, as it can be used to estimate runoff for adequate design of on-site retention basins and other BMPs for sediment erosion control.

The second study (Chapter 5) focused on erosion and sediment delivery on low-compaction reclaimed sites. This study found that erodibility on bare, loose spoils on steep slopes greater than 20% is highly susceptible to rill development, where during periods of rill development erodibilities (K factors) were estimated to range between 0.2 to 0.5 $t \cdot ha \cdot h \cdot (ha \cdot MJ \cdot mm)^{-1}$. Once rills apparently stabilized on these sites, estimated K factors were below 0.12 $t \cdot ha \cdot h \cdot (ha \cdot MJ \cdot mm)^{-1}$, with a median of 0.06 $t \cdot ha \cdot h \cdot (ha \cdot MJ \cdot mm)^{-1}$. Sediment yields from erosion were similarly impacted by rill development, averaging 391 $t \cdot ha^{-1}$ during the entire monitoring period for all three sites. In contrast to other studies that measured little or no runoff on low-gradient slopes with loose spoils, this study measured runoff sufficient to form rills. Coarse and fine sediments both erode from these steep sites, and the D_{50} estimates ranged from 0.06 to 2.67 mm during the study period. The above information provides valuable model input data for SEDCAD™, the model commonly used in the United States to plan BMPs to mitigate impacts from probable hydrological consequences, and generally supports surface coal mining reclamation practices.

The third study (Chapter 6) in this research investigated performance of the SEDCAD model on reclaimed mine lands. This study illustrated the importance of selecting CN and K factors that reflect site conditions. SEDCAD performed reasonably well for reclaimed surface coal mining sites considering the general predictive capabilities of sediment yield models based on RUSLE, but it tended to overestimate sediment yields. It was also relatively sensitive to CN selection. This study provided SEDCAD users critical information of interpretation of model outputs for designing runoff and sediment control structures on reclaimed surface mining sites.

The fourth study (Chapter 7) in this research investigated potential changes in future rainfall erosivity due to climate change in the New River basin of the southern Appalachian region for the time period 2010-2099 and for the greenhouse gas emission scenarios B1, A1B, and A1FI of the CCSM model. Results showed that for all three scenarios, the rainfall erosivity will increase with almost the same monthly distribution within a year. The largest increase was related to A1FI and the smallest was from the B1 scenario. Consistent with previous studies that projected a 25-50% average increase in annual rainfall erosivity for East Tennessee from 2000-2019 to 2080-2099, this study found a 7 – 49 % increase in annual rainfall erosivity from 2010 to 2099 based on the different emission scenarios. The projected mean annual erosivity (R factor) showed 49%, 28%, and 7% increases in comparison to the historic period (1959-1999), under A1FI, A1B, and B1 scenarios, respectively. Erosivities projected by this study suggest that by the late 2080's or early 2090's the annual rainfall erosivity at study region will probably be the same as what is currently experienced by southern to central regions in the state of Alabama. The results from this study can widely be used to assess potential future change in erosion and sediment yield from this area, and to evaluate future effectiveness of current BMPs in reducing soil erosion and sediment delivery from coal mining sites located at study region. The same method and technique is applicable for other regions of interest.

References

Allen M.R., and Ingram W. J. (2002). Constraints on future changes in climate and the hydrologic cycle, *Nature*, 419: 224 – 232.

Angel P., Davis V., Burger J., Graves D., Zipper C. (2005). The Appalachian regional reforestation initiative. *Forest Reclamation Advisory #1*. U.S. Office of Surface Mining.

Angel P., Graves D.H., Barton C., Warner R.C., Conrad P.W., Sweigard R.J., Agouridis C. (2006). Surface mine reforestation research: evaluation of tree response to low compaction reclamation techniques. R.I. Barnhisel (ed.) *Proc. 7th International Conference on Acid Rock Drainage.* St. Louis, Missouri. Published by ASMR.

Angel P., Barton C., Warner R., Agouridis C., Taylor T., Hall S. (2007). Hydrologic characteristics, tree growth, and natural regeneration on three loose-graded surface mine spoil types in Kentucky. Presentation at the *Mid-Atlantic Stream Restoration Conference*, Rocky Gap Lodge, Cumberland, MD, November 2007. http://www.canaanvi.org/canaanvi_web/events_ed.aspx?collection=cvi_workshops&id=140 accessed December 15, 2007.

Barfield B.J., Warner R.C., and Haan C.T. (1981). Applied hydrology and sedimentology for distributed areas. Oklahoma Technical Press, Stillwater, Oklahoma.

Barfield B.J., Barnhisel R.I., Powell J.L., Hirschi M.C., Moore I.D. (1983). Erodibilities and eroded size distribution of western Kentucky mine spoil and reconstructed topsoil. IMMR Final Report No. G1115211 and CRIS Project NO.907-15-2.

Barfield B.J., Barnhisel R.I., Powell J.L., Hirschi M.C., and Moore I.D. (1984). Erodibilities and eroded size distribution of western Kentucky mine spoil and reconstructed topsoil. *Proc., Symposium on surface mining, hydrology, sedimentology, and reclamation*. College of engineering, University of Kentucky, Lexington, KY, 179-189.

Barton C., Agouridis C., Warner R., Bidelspach D., Angel P., Jennings G., Marchant J., Osborne R. (2007). Recreating a Headwater Stream System on a Head-of-Hollow Fill. *Mid-Atlantic Stream Restoration Conference*, Rocky Gap Lodge, Cumberland, MD, November 2007. http://www.canaanvi.org/canaanvi_web/events_ed.aspx?collection=cvi_workshops&id=140 accessed December 15, 2007.

Berger C., Schulze M., Rieke-Zapp D., Schlunegger F. (2010). Rill development and soil erosion: a laboratory study of slope and rainfall. *Earth Surface Process and Landform* 35: 1456-1467.

Bonta JV. (2000). Impact of coal surface mining and reclamation on suspended sediment in three Ohio watersheds. *The American Water Resources Association* 36, 4: 869-887.

Brown L.C., Foster G.R. (1987). Storm erosivity using idealized intensity distributions. *Transaction of the ASAE,* 30: 379-386.

Burger J., Graves D., Angel P., Davis V., Zipper C. (2005). The Forestry Reclamation Approach. U.S. Office of Surface Mining, Forest Reclamation Advisory No. 2. Available at: http:// arri.osmre.gov/fra.htm.

Camorani G., Castellarin A., and Brath A. (2005). Effects of land-use changes on the hydrologic response of reclamation systems. *Physics and Chemistry of the Earth,* 30(4), 561–574.

Carey W.P., (1984). Effects of resource development on water quality in the Big South Fork National River and Recreational Area, Tennessee and Kentucky. Conference Proceeding Paper, *Water for Resource Development*, 624-628.

Carroll C., Merton I., Burger P. (2000). Impact of vegetative cover and slope on runoff, erosion, and water quality for field plots on a range of soil and spoil materials on central Queensland coal mines. *Journal of Soil Research,* 38: 313-27.

Cerda A. (2001). Effects of rock fragment on soil infiltration, inter-rill runoff and erosion. *European Journal of Soil Science,* 52: 1-10.

Curtis W.R. (1971). Strip mining, erosion and sedimentation. *Transaction of ASAE,* 14: 434-436.

Curtis W.R, Superfesky M.J. (1977). Erosion of surface mine spoils. *Proceeding of 32nd annual meeting of the soil conservation society of America*, 154-158.

Dickens P.S., Tschantz B.A., Minear R.A. (1985). Sediment yield and water quality from a steep-slope surface mine spoil. *Transactions of the ASAE,* 28: 1838-1845.

Diodato N., and Bellocchi G. (2009). Assessing and modeling changes in rainfall erosivity at different climate scales. *J. of Earth Surface Process,* 34: 969–980.

Edmunds W.E. (2002). Coal in Pennsylvania. *Pennsylvania geological survey,* 4: 1-27.

Elhakeem, M. and Papanicolaou A.N. (2009). Estimation of the Runoff Curve Number via Direct Rainfall Simulator Measurements in the State of Iowa, USA. *Water Resources Management* 23 (12):2455–2473.

Espigares T., Moreno de las Heras M., Nicolau J.M. (2011). Performance of vegetation in reclaimed slopes affected by soil erosion. *Restoration Ecology,* 19: 35-44.

Favis-Mortlock D., Boardman J. (1995). Nonlinear responses of soil erosion to climate change: a modeling study on the UK South Downs. *CATENA*, 25(1–4): 365–387.

Favis-Mortlock D.T., Savabi M.R. (1996). Shifts in rates and spatial distributions of soil erosion and deposition under climate change. In: Anderson, M.G., Brooks, S.M. (Eds.), Advances in Hillslope Processes. Wiley, Chichester, UK, 529 – 560.

Fields-Johnson C., Zipper C.E., Burger J.A., Evans D.M. (2009). First-year response of mixed hardwoods and improved American Chestnuts to compaction and hydroseed treatments on remained mine land. Proceedings on Revitalizing the Environment: Proven Solutions and Innovative Approaches. *American Society of Mining and Reclamation,* 1: 20-34.

Foltz R.B., Rhee H., Elliot W.J. (2008). Modeling changes in rill erosion and critical shear stress on native-surface roads. *Hydrological Processes,* 22: 4783-4788.

Foster G.R., Lane L.J. (1983). Erosion by concentrated flow in farm fields. *Proceedings, D. B. Simons Symposium on Erosion and Sedimentation,* Colorado State University; Ft. Collins; CO; 9.56-9.82.

Fox J.F. (2009). Identification of sediment sources in forested watersheds with surface coal mining disturbance using carbon and nitrogen isotopes. *JAWRA* 45: 1273-1289.

Gardner E.S. (2006). Cumberland Plateau – national heritage corridor feasibility study. Retrieved March 1, 2007, from the Tennessee Department of Environmental Conservation Alliance for the Cumberland's website, http://www.tdec.net/recreation/cumberlandplateau.pdf

Gilley J.E., Gee G.W., Bauer A., Willis W.O., Young R.A. (1977). Runoff and erosion characteristics of surfaced-mined sites in western North Dakota. *Transactions of ASAE,* 20: 697-700.

Govers G. (1987). Spatial and temporal variability in rill development processes at the Huldenberg experimental site. *Elsevier Science,* IDS No. J4089, ISSN: 0341-8162.

Graves D.H., Ringe J.M., Pelkki M.H., Sweigard R.J., and Warner R.C. (2000). High value tree reclamation research. *Environmental Issues and Management of Waste in Energy and Mineral Production.* Taylor & Francis, Balkema, Rotterdam, 413–421.

Guebert M.D., Gardner T.W. (2001). Macropore flow on a reclaimed surface mine: infiltration and hillslope hydrology. *Geomorphol* 39: 151-169.

Haan C.T., Barfield B.J., Hayes J.C. (1994). *Design Hydrology and Sedimentology for Small Catchments*. Academic Press: San Diego, CA; 672.

Hansen J.W., Ines A.M.V. (2005). Stochastic disaggregation of monthly rainfall data for crop simulation studies. *Agricultural and Forest Meteorology,* 131: 233–246.

Hahn D.T., Moldenhauer W.C., Roth C.B. (1985). Slope Gradient Effect on Erosion of Reclaimed Soil. *Transction of ASAE,* 28: 805-808.

Hancock G.R., Crawter D., Fityus S.G., Chandler J.A., Wells T. (2002). The measurement and modeling of rill erosion at angle of repose slopes in mine spoil. *Earth Surface Processes and Landforms,* 33: 1006-1020.

Hancock G.R., Willgoose G.R. (2004). An experimental and computer simulation study of erosion on a mine tailings dam wall. *Earth Surface Processes and Landforms*, 29: 457–475.

Harms T.E., Chanasyk D.S. (2000). Plot and small-watershed scale runoff from two reclaimed surface-mined watersheds in Alberta. *Hydrological Processes* 14: 1327-1339.

Hartley D.M. (1982). Runoff and erosion response of reclaimed surfaces. *Journal of Hydraulic Engineering*, 110: 1181-1199.

Hawkins R.H. (1973). Improved prediction of storm runoff in mountain watersheds. *J. Irrigation and Drainage*, 99(4), 519–523.

Hawkins R.H. (1993). Asymptotic determination of runoff curve numbers from data. *J. Irrigation and Drainage*, 119(2), 334–345.

Hawkins R.H., Woodward D.E., and Jiang R. (2002). Runoff curve number method: Examination of the initial abstraction ratio. *Second Federal Interagency Hydrologic Modeling Conference*, USGS, Las Vegas, NV., 40-51.

Hawkins R.H., Ward T.J., Woodward D.E., and Van Mullem J. A. (2009). *Curve Number Hydrology- State of the Practice*, 1st Ed., ASCE, Reston, Viginia.

Hegerl G.C., Zwiers F.W., Stott P.A., Kharin V.V. (2004). Detectability of anthropogenic changes in annual temperatures and precipitation extremes. *Journal of Climate* 17: 3683–3700.

Holtz R.D., Kovacs W.D. (1981). *An Introduction to Geotechnical Engineering*. Prentice Hall, ISBN-10: 0134843940.

Hoomehr S., Schwartz J.S., Wright W.C., and Drumm E.C. (2010). Surface erosion and sediment yields on steep-sloped coal mining reclamation sites in the Appalachian region. *Proc., World Water & Environmental Resources Congress*, ASCE/EWRI, Providence, RI., May 16-20, 1881-1892. DOI: 10.1061/41114(371)197.

Hoomehr, S., Schwartz, J.S., Yoder, S.C., Wright, W.C., and Drumm, E.C. (2012 a). "Curve numbers for hydrology on low-compaction, steep-sloped reclaimed mine lands in southern Appalachian region." *ASCE Journal of Hydrologic Engineering*.

Hoomehr, S., Schwartz, J.S., Yoder, S.C., Wright, W.C., and Drumm, E.C. (2012 b). "Erodibility factors for low-compaction steep-sloped reclaimed surface mine lands in southern Appalachian region." *Hydrological Processes*.

IEA. (2010). Key World Energy Statistics. *IEA Publication website*, http:// www.iea.org/textbase/nppdf/free/2010/key_stats_2010.pdf.

Intergovernmental Panel on Climate Change (IPCC), 2007. Climate Change, (2007). The physical science basis. Solomon S. et al. (Eds.), Contribution of Working Group I to the Fourth Assessment Report of the Intergovernmental Panel on Climate Change, Cambridge University Press, Cambridge, UK.

Jean J.S., Koe-Fe A., Kaimin S., Chao-Chi H. (2000). Stone cover and slope factors influencing hillside surface runoff and infiltration: laboratory investigation. *Hydrological Processes* 14: 1829–49.

Jeldes I., Hoomehr S., Wright W.C., Schwartz J.S., Lane D., Drumm E.C. (2010). Stability and erosion on steep slopes constructed by the forest reclamation approach. *Joint 27th Annual American Society of Mining and Reclamation and 4th Annual Appalachian Regional Reforestation Initiative*. Barnhisel R (ed). ASMR: Pittsburgh, New York; 470-482.

Johns T.C., Carnell R.E., Crossley J.F., Gregory J.M., Mitchell J.F.B., Senior C.A.,Tett S.F.B., and Wood R.A. (1997). The second Hadley Centre coupled ocean-atmosphere GCM: model description, spin up and validation. *Climate Dynamics*. 13, 103-134.

Katz R.W. 1996. The use of stochastic models to generate climate change scenarios. *Climate Change*, 32: 237-255.

Massey M.P. (2008). Use of the AnnAGNPS pollutant loading model for prediction of sediment yields in a mountainous Cumberland Plateau region: correlations with the stream bed sediment characteristics. *A Thesis Presented for the Master of Science Degree*, The University of Tennessee, Knoxville.

Mavromatis T., and Jones P.D. 1998. Evaluation of HadCM2 and direct use of daily GCM data in impact assessment studies. *Climate Change*, 41: 583-614.

McFarlane N.A., Boer G.J., Blanchet J.P., and Lazare M. (1992). The Canadian climate center second-generation general circulation model and its equilibrium climate. Journal of Climate, 5: 1013-1044.

McIntosh J.E., Barnhisel R.I. (1993). Erodibility and sediment yield by natural rainfall from reconstructed mine spoils. *Journal of soil science* 156: 118-126.

McKenzie G.D., Studlick J.R.J. (1979). Erodibility of surface-mine spoil banks in southeastern Ohio: An approximation. *Soil Water Conservation*, 34: 187-190.

Meadows M.E., and Blandford G.E. (1983). *Improved methods and guidelines for modeling stormwater runoff from surface coal mined lands*, Water resources research institute, University of Kentucky, Lexington, KY, 147.

Mearns L.O., Rosenzweig C., Goldberg R. (1997). Mean and variance change in climate scenarios: methods, agricultural applications, and measures of uncertainty. Climate Change, 35: 367–396.

Meyer L.D., Harmon W.C. (1989). How side slope length and steepness affect side slope erosion. *Transaction of ASAE,* 32: 639-644.

Mitchell J.K., Moldenhauer W.C., Gustavson D.D. (1983). Erodibility of selected reclaimed surface mined soils. *Transaction of ASAE,* 26: 1413-1417.

Mutchler C.K., Carter C.E. (1983). Soil erodibility variation during the year. *Transaction of ASAE,* 26: 1102- 1108.

Nearing M.A., Dear-Ascough L., and Laflen J. M. (1990). Sensitivity analysis of the WEPP hillslope erosion model. *Transaction of ASAE,* 33(3): 839–849.

Nearing M.A, Norton L.D., Bulgakov D.A., Larionov G.A., West L.T., Dontsova K. (1997). Hydraulics and erosion in eroding rills. *Water Resources Research,* 33: 865-876.

Nearing M.A. (2001). Potential changes in rainfall erosivity in the US with climate change during the 21st century. *Journal of Soil Water Conservation,* 56 (3): 29–232.

Nearing M.A., Jetten V., Baffaut C., Cerdan O., Couturier A., Hernandez M., Le Bissonnais Y., Nichols M.H., Nunes J.P., Renschler C.S., Souchere V., Van Ost, K., (2005). Modeling response of soil erosion and runoff to changes in precipitation and cover. *Catena,* 61: 131–154.

NEH-4 (1964, reprinted in 1985), National Engineering Handbook, Section 4, Hydrology. US Dept. of Agriculture, Soil Conservation Service, US Govt. Printing Office, Washington, DC.

Nicks A.D., Gander G.A., (1994). CLIGEN: a weather generator for climate inputs to water resource and other models. *Proceedings of the 5th International Conference on Computers in Agriculture, American Society of Agricultural Engineers,* St. Joseph, Michigan, pp. 3–94.

Nicolau J.M. (2002). Runoff generation and routing on artificial slopes in a Mediterranean–continental environment: the Teruel coalfield, Spain. *Hydrological Processes,* 16: 631-647.

NOAA: http://www4.ncdc.noaa.gov/cgi-win/wwcgi.dll?wwDI~StnSrch~StnID~20018515#DAF

NPS. (2007). Geology and history of the Cumberland Plateau. *Big South Fork National River and Recreation Area.* http://www.nps.gov/biso/planyourvisit/upload/webgeo.pdf

Overton D.E. (1980). Simulation of effects of contour coal strip mining on stormwater runoff and pollutant yields. *Symposium on Surface Mining Hydrology, Sedimentology and Reclamation,* 13: 100-124.

Palmer M.A., Bernhardt E.S., Schlesinger W.H., Eshleman1 K.N., Foufoula-Georgiou E., Hendryx M.S., Lemly A.D., Likens G.E., Loucks O.L., Power M.E., White P.S., Wilcock P.R. (2010). Mountaintop Mining Consequences. *Journal of Science,* 327: 148.

Pinson W.T., Yoder D.C., Buchanan J.R., Wright W.C., and Wilkerson J.B. (2003). Design and evaluation of an improved flow divider for sampling runoff plots. *Journal of Applied Engineering in Agriculture,* 20(4): 433-437.

Pruski F.F., Nearing M.A., (2002). Runoff and soil-loss responses to changes in precipitation: a computer simulation study. Journal of Soil Water Conservation, 57 (1): 7–16.

Rallison R.E. (1980). Origin and evolution of the SCS runoff equation. *Proceeding of ASCE Symposium on Watershed Management,* Boise, Idaho, ID, July 21-23, 1980, 912-924.

Renard K.G., McCool D.K., Cooley, K.R., Mutchler C.K, and Foster G.R. (1993). Rainfall - runoff erosivity factor (R). Chapter 2. *In* Renard, Foster, and Weesies (eds), " Predicting soil erosion by water – A guide to conservation planning with the Revised Universal Soil Loss Equation, RUSLE", Publication ARS. U.S. Department of Agriculture, Washington, DC.

Renard K.G., Freidmund J.R. (1994). Using monthly precipitation data to estimate the R-factor in the revised USLE. *Journal of Hydrology,* 157: 287–306.

Renard K.G., Foster G.R., Weesies G.A, McCool D.K., Yoder D.C. (1997). Predicting Soil Erosion by Water: A Guide to Conservation Planning with the Revised Universal Soil Loss Equation. U.S. Department of Agriculture, Agricultural Handbook No. 703. U.S. Government Printing Office, Washington, D.C.

Renard K.G., Foster G.R., Weesies G.A. (1997). RUSLE-Revised Universal Soil Loss Equation. *Soil and Water Conservation,* 49: 213-220.

Ritter J.B. and Gardner T.W. (1991). Runoff curve numbers for reclaimed surface mines in Pennsylvania. *Journal of Irrigation and Drainage Engineering,* 117(5): 656–666.

Romkens M.J.M. (1985). The soil erodibility factor: A perspective. El-Swaify S.A., Moldenhauer W.C., and Lo A., (eds.). *Soil Erosion and Conservation*, 445-461. Soil Water Conservation Society. Ankeny, Iowa.

Sauerborn P., Klein A., Botschek J., and Skowronek A. 1999. Future rainfall erosivity derived from large-scale climate models: Methods and scenarios for a humid region. *Geoderma,* 93(3-4): 269-276.

Savabi M., Stockle C. (2001). Modeling the possible impact of increased CO_2 and temperature on soil water balance, crop yield and soil erosion. *Environmental Modeling and Software,* 16(7): 631-640. DOI: 10.1016/S1364-8152(01)00038-X

Schneider L.E., and McCuen R.H. (2005). Statistical guidelines for curve number generation. *Journal of Irrigation and Drainage Engineering,*131(3): 282–290.

Schroeder S.A. (1987). Runoff curve number estimations for reshaped fine-textured spoils. *Journal of Reclamation and Revegetation Research,* 6(2): 129–136.

Semenov M.A., and Barrow E. 1997. Use of a stochastic weather generator in the development of climate change scenarios. *Climate Change*, 35: 397-414.

Sheridan G.J., So H.B., Loch R.J., Pochnee C., Walker C.M. (2000). Use of laboratory-scale rill and inter-rill erodibility measurements for the prediction of hillslope-scale erosion on rehabilitated coal mine soils and overburdens. *Australian Journal of Soil Science,* 38: 285-297.

Shukla M.K., Lal R., Underwood J., Ebinger M. (2004). Physical and hydrological characteristics of reclaimed minesoils in southeastern Ohio. *Soil Science Society of America Journal,* 68: 1352–1359.

Smets T., Poesen J., Bochet E. (2008). Impact of plot length on the effectiveness of different soil- surface covers in reducing runoff and soil loss by water. *Progress in Physical Geography,* 32: 654–677.

SWCS. (1993). RUSLE© User's guide; revised universal soil loss equation, version 1.03. *Soil and Water Conservation Society*: Ankeny, IA; 164.

Sweigard R., Burger J., Zipper C., Skousen J., Barton C., Angel P. (2007). Low compaction grading to enhance reforestation success on coal surface mines. *ARRI Forest Reclamation Advisory*, 3: 6-12.

Sweigard R.J., Kumar D. (2010). Field investigation of best practices for steep slope mine reclamation employing the forestry reclamation approach. *Bridging Reclamation, Science and the Community*, Barnhisel R.I. (ed). ASMR: Lexington, KY; 1258-1273.

Taylor P.B. (1995). Hydrologic assessment, SEDCAD model validation, and infiltration basin performance for the Appalachian coal region in Kentucky. M.S. Thesis, University of Kentucky.

Taylor T.J., Agouridis C.T., Warner R.C., Barton C.D. (2009). Runoff curve numbers for loose-dumped spoil in the Cumberland Plateau of eastern Kentucky. *International Journal of Mining, Reclamation and Environment*, 23: 103-120.

Thomas W.R., Pelkki M.H., Ringe J.M. (1999). Native high value tree reclamation on surface mined spoils in eastern Kentucky. *Proceedings, 12th central hardwood forest conference,* Stringe J.W., Loftis D.L. (eds). USDA: Lexington, KY; 100-120.

Tisseuil C., Vrac M., Lek S., and Wadec A. J. (2010). Statistical downscaling of river flows. *Journal of Hydrology*, 385: 279–291.

Torbert J.L., Burger J.A. (1994). Influence of grading intensity on ground cover establishment, erosion, and tree establishment on steep slopes. *Proceedings, International Land Reclamation and Mine Drainage Conference and the Third International Conference on the Abatement of Acidic Drainage*, USDOI Bureau of Mines: Philadelphia, PA; 226-231.

Torri D., Sfalanga M., Chisci G. (1997). Threshold conditions for incipient rilling. *Catena Supplement,* 8: 97-105.

Toy T.J., Foster G.R., Renard K.G. (1999). RUSLE for mining, construction and reclamation lands. *Journal of Soil and Water Conservation,* 54: 462-467.

U.S. Dept. of the Interior. (1977). Surface mining reclamation and enforcement provisions. *Federal Register,* 42: 62685-62688.

USGS. (2003). The Sedimentary Appalachians. *U.S. Geological Survey website,* http://3dparks.wr.usgs.gov/nyc/valleyandridge/sedimentaryapp.htm

U.S. Soil Conservation Service. (1985). National Engineering Handbook, Section 4, Hydrology. U.S. Government Print. Office, Washington, DC.

Warner R.C., Schwab P.J., Marshall D.J. (1998). SEDCAD™ 4, Design Manual and User's Guide. Civil Software Design: Lexington, KY; 126.

Wilby R.L., Wigley T.M.L. (1997). Downscaling general circulation model output: a review of methods and limitations. *Progress in Physical Geography,* 21: 530-548.

Wilks D.S., Wilby R.L. (1999). The weather generation game: a review of stochastic weather models. *Progress in Physical Geography,* 23: 329-357.

West T.O., Wali M.K. (1999). A model for estimating sediment yield from surface-mined lands. *International Journal of Surface Mining, Reclamation and Environment,* 13: 103-109.

Wilks, D.S. (1992). Adapting stochastic weather generation algorithms for climate change studies. *Climate Change,* 22: 67 – 84.

Wilks D.S., (1999). Multisite downscaling of daily precipitation with a stochastic weather generator. *Climate Research.* 11: 125–136.

Williams J., Nearing M.A., Nicks A., and Skidmore E., Valentine C., King K. and Savabi R. (1996). Using soil erosion models for global change studies. *Journal of Soil Water Conservation.* 51: 381–385.

Wischmeier W.H. and Smith D.D. (1965). Predicting rainfall-erosion losses from cropland east of the Mountains-Guide for selection of practices for soil and water conservation. *Agricultural Handbook,* 282: 152-164.

Wischmeier W.H. and Mannering J.V. (1969). Relation of soil properties to its erodibility. *Soil Science Society of America Proceedings,* 33: 131-137.

Wischmeier W.H., Smith D.D. (1978). Predicting rainfall erosion losses. *USDA Agriculture Handbook*: 537.

Wu C.C. (2001). Surface-cover subfactor for gravel-rich surfaces. *Proceedings of the International Symposium on Soil Erosion Research for the 21st Century*, Ascough JC, Flanagan DC (eds). ASAE: St. Joseph, MI; 521-524.

Wu Y.Q., Zheng Q.H., Zhang Y.G., Liu B.Y., Cheng H., Wang Y.Z. (2008). Development of gullies and sediment production in the black soil region of northeastern China. *Journal of Geomorphology*, 101, 683–691.

Yang D., Kanae S., Oki T., Koike T., Musiake K. (2003). Global potential soil erosion with reference to land use and climate changes. *Journal of Hydrological Processes*, 17: 2913–2928.

Yao C., Lei T., Elliot W.J., McCool D.K., Zhao J., Chen S. (2008). Critical conditions for rill initiation. *ASABE,* 51: 107-114.

Yoder D.C., Buchanan J.R., Honea G.S., Staley B.F., Wilkerson J.B., and Yoder R.E. (1999). The Tennessee fluid level indicator. *Applied Engineering in Agriculture,* 15(1): 49-52.

Yu B. (2002). Using CLIGEN to generate RUSLE climate inputs. *Transaction of ASAE*, 45: 993–1001.

Yu B. (2003). An assessment of uncalibrated CLIGEN in Australia. *Agricultural Forest Meteorology*. 119, 131–148.

Zhang G.H., Nearing M.A., Liu B.Y. (2005). Potential effects of climate change on rainfall erosivity in the Yellow River basin of China. *Transaction of ASAE,* 48: 511–517.

Zhang G.H., Liu Y., Han Y., Zhang X.C. (2009). Sediment Transport and Soil Detachment on Steep Slopes: Transport Capacity Estimation. *Soil Science Society of America Journal*, 73: 1291-1297.

Zhang X.C., Nearing M.A., Garbrecht J.D., Steiner J.L. (2004). Downscaling monthly forecasts to simulate impacts of climate change on soil erosion and wheat production. *Soil Science Society,* 68: 1376–1385.

Zhang X.C. (2005). Spatial downscaling of global climate model output for site-specific assessment of crop production and soil erosion. *Agricultural Forest Meteorology*, 135: 215–229.

Zhang X.C. (2007). A comparison of explicit and implicit spatial downscaling of GCM output for soil erosion and crop production assessments. *Climate Change*, 84: 337–363.

Zhang Y.G., Wu Y.Q., Liu B.Y., Zheng Q.H., Yin J.Y. (2007). Characteristics and factors controlling the development of ephemeral gullies in cultivated catchments of black soil region, Northeast China. *Soil and Tillage Research*, 96: 28–41.

Zhang Y.G., Nearing M.A., Zhang X.C., Xie Y., Wei H. (2010). Projected rainfall erosivity changes under climate change from multi-model and multi-scenario projections in Northeast China. *Journal of Hydrology*. 384: 97–106.

Appendix A

Statistical Tests

Curve Number

The Matched Pairs report shows a Tukey mean-difference plot, summary statistics, and the results of the paired t-test. The Difference plot shows differences by means for CNs estimated at study sites. The mean difference is shown as the horizontal line, with the 95% confidence interval above and below shown as dotted lines. If the confidence region includes zero, then the means are not significantly different at the 0.05 level. In this study the difference were not significant.

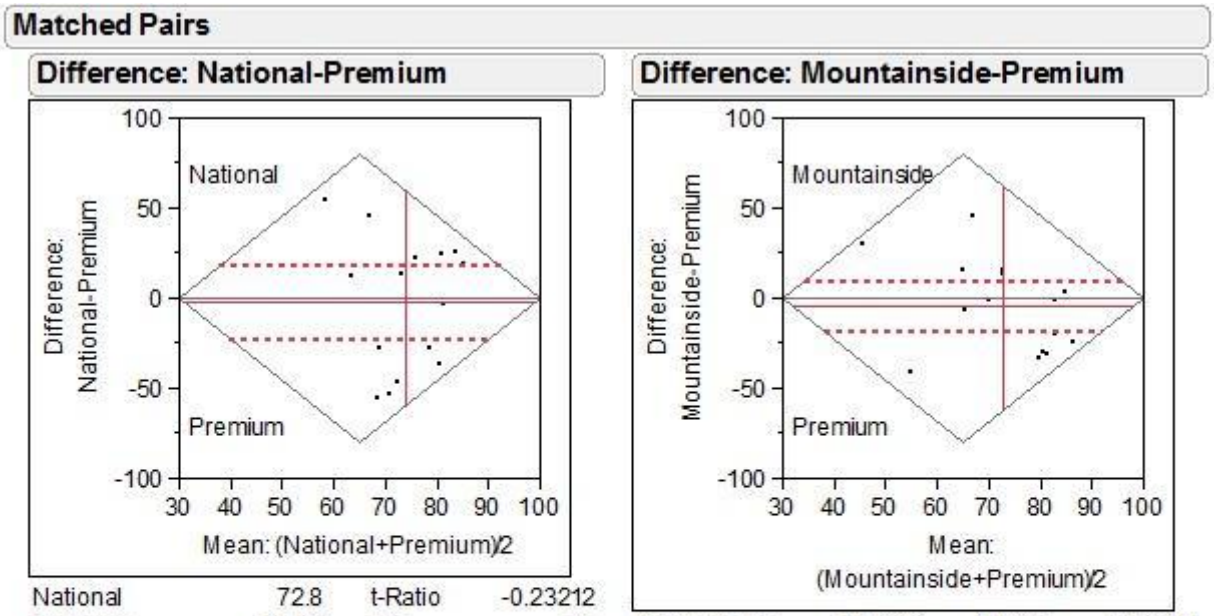

National	72.8	t-Ratio	-0.23212
Premium	74.98	DF	14
Mean Difference	-2.18	Prob > |t|	0.8198
Std Error	9.39182	Prob > t	0.5901
Upper 95%	17.9635	Prob < t	0.4099
Lower 95%	-22.323		
N	15		
Correlation	-0.6854		

Mountainside	70.5533	t-Ratio	-0.67334
Premium	74.98	DF	14
Mean Difference	-4.4267	Prob > |t|	0.5117
Std Error	6.57417	Prob > t	0.7442
Upper 95%	9.67352	Prob < t	0.2558
Lower 95%	-18.527		
N	15		
Correlation	-0.0871		

Matched Pairs

Difference: Mountainside-National

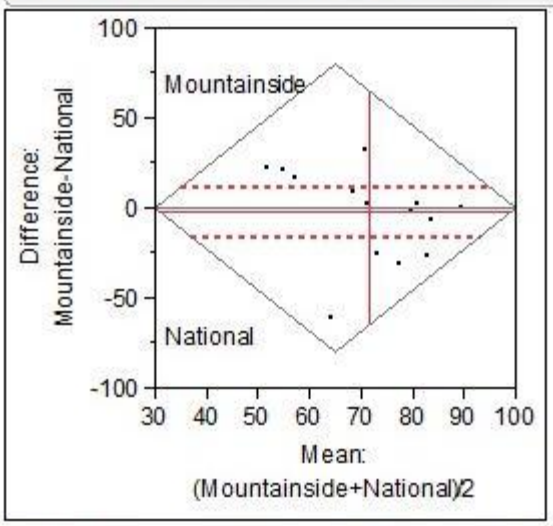

Mountainside	70.5533	t-Ratio	-0.35348
National	72.8	DF	14
Mean Difference	-2.2467	Prob > |t|	0.7290
Std Error	6.35592	Prob > t	0.6355
Upper 95%	11.3854	Prob < t	0.3645
Lower 95%	-15.879		
N	15		
Correlation	-0.1036		

Erosion Rates

The Matched Pairs report shows a Tukey mean-difference plot, summary statistics, and the results of the paired t-test. The Difference plot shows differences by means for erosion rates estimated for study sites. The mean difference is shown as the horizontal line, with the 95% confidence interval above and below shown as dotted lines. If the confidence region includes zero, then the means are not significantly different at the 0.05 level. In this study the difference were not significant.

Matched Pairs

Difference: Premium-National

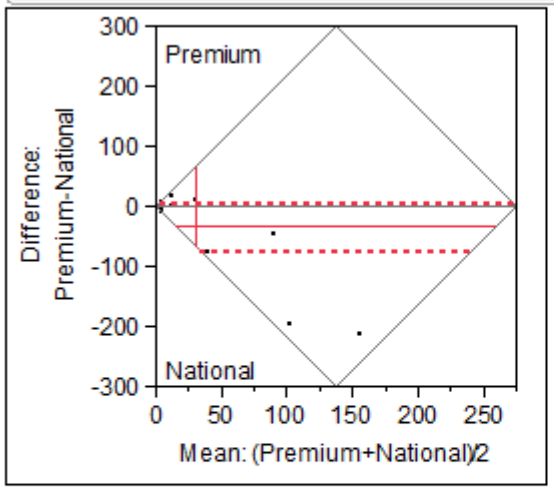

Premium	13.8813	t-Ratio	-1.80221
National	47.9913	DF	14
Mean Difference	-34.11	Prob > |t|	0.0931
Std Error	18.9268	Prob > t	0.9535
Upper 95%	6.48385	Prob < t	0.0465*
Lower 95%	-74.704		
N	15		
Correlation	0.53172		

Difference: Mountainside-National

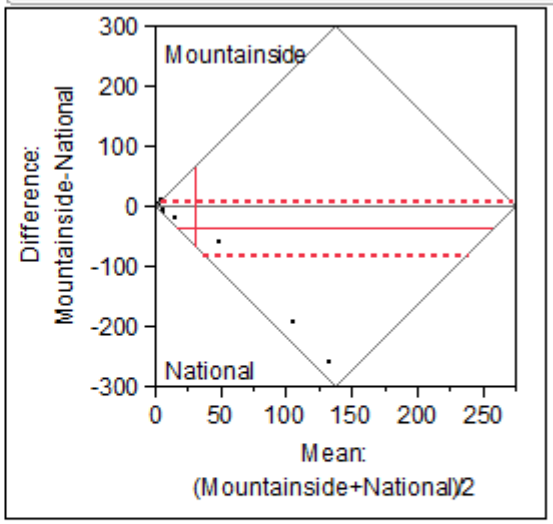

Mountainside	12.136	t-Ratio	-1.74459
National	47.9913	DF	14
Mean Difference	-35.855	Prob > |t|	0.1030
Std Error	20.5523	Prob > t	0.9485
Upper 95%	8.2249	Prob < t	0.0515
Lower 95%	-79.936		
N	15		
Correlation	0.26338		

Matched Pairs

Difference: Mountainside-Premium

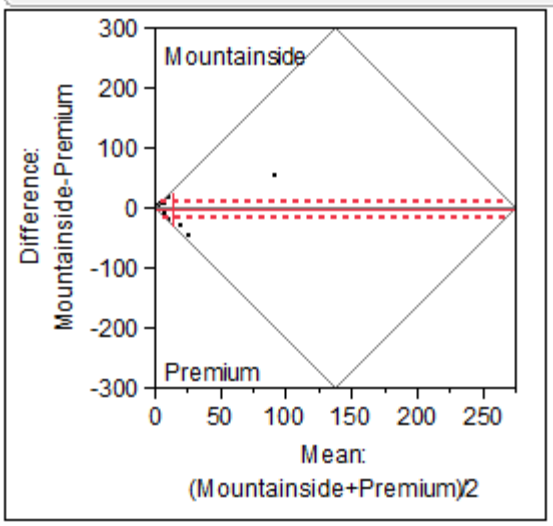

Mountainside	12.136	t-Ratio	-0.31145
Premium	13.8813	DF	14
Mean Difference	-1.7453	Prob > |t|	0.7601
Std Error	5.60399	Prob > t	0.6200
Upper 95%	10.274	Prob < t	0.3800
Lower 95%	-13.765		
N	15		
Correlation	0.68345		

Vita

Siavash Hoomehr was born and raised in Shiraz, Iran. He received a Bachelor‘s degree in civil engineering from Shiraz University in 2003. He earned his Master’s degree in civil engineering from University of Tehran in February 2007. He later attended the University of Tennessee – Knoxville where he graduated with a PhD in civil engineering and a Master of Science degree in Statistics, in May of 2012.